A platform for next-generation cancer therapies: multi-targeted non-viral vectors for site-specific gene delivery and expression

A Thesis
SUBMITTED TO THE FACULTY OF
UNIVERSITY OF MINNESOTA
BY

Maroof Mohammad Adil

IN PARTIAL FULFILLMENT OF THE REQUIREMENTS
FOR THE DEGREE OF
DOCTOR OF PHILOSOPHY

Efrosini Kokkoli

December 2013

Acknowledgements

I thank my advisor Prof. Efrosini Kokkoli for helping me get to this point in my career. I am especially grateful for her support of my interest in genetic technologies, and for her encouragement of my creativity and pursuit of independent projects. I would also like to thank Prof. Ben Hackel, Prof. Yiannis Kaznessis and Prof. Scott McIvor for being on my committee and for all their career-related advice over the past years. I am especially thankful to Prof. McIvor for his insight and many enlightening discussions. In addition, I owe it to Prof. Robert Langer and Prof. Yoon Yeo for introducing me to the field of controlled therapeutic delivery systems.

Chapter 3 presents previously published work, originally cited as: Adil, M.; Belur, L.; Pearce, T. R.; Levine, R. M.; Tisdale, A. W.; Sorenson, B. S.; McIvor, R. S.; Kokkoli, E. PR_b functionalized stealth liposomes for targeted delivery to metastatic colon cancer. *Biomater. Sci.* **2013**, *1*, 393–401 (Reproduced by permission of The Royal Society of Chemistry). T. R. Pearce imaged the liposome formulations using CryoTEM, R. M. Levine developed the DNA quantification assay, and A. W. Tisdale provided preliminary data. I am thankful to members of Prof. McIvor's group for help with in vivo experiments, especially L. Belur and B. S. Sorensen for the tumor development, liposome injections, and bioluminescence imaging.

The members of the Kokkoli group, both past and present, have been a great source of help. Also, life in lab and in the office would have been quite dull without them. Thanks to Nicole, Rachel, Matt, Tim, Frankie, Carolyn, Kamlesh, Ajay, and Brett for making the last few years memorable. Rachel, thank you for all of your support both in and out of lab, and of course for all your wonderful artwork. I am quite grateful to the undergraduate students, Kyle Huston and Zach Erdman, for help in lab. Zach has been very reliable over the past couple of

years, and progress would have been much slower without his creativity and diligence.

I am grateful to the Kaznessis and Hu groups for the use of their equipment. Members of the Kaznessis group, Dr. Katherine Volzing and Dr. Juan Borrero have been instrumental in discussions regarding the development of the new thereapeutic plasmid presented here. Dr. Huong Le and Kathryn Johnson in the Hu group have also provided much support in the plasmid development front. Kat, Juan and Kathryn, thank you for teaching me many of the molecular biology skills that I am now very fond of using. Dr. Michelle Gleason, thank you for all the uplifting and scientifically motivating coffee breaks, and your support during the thesis writing process.

This would not have been possible without the support of my friends and family. I had the opportunity to make lifelong friends in college. George, Huanan, Antone, Christian, Silvana, Cathlene, and the rest of my brothers at ZBT: I would like to thank you for the amazing reunions we have had over the past few years. In Minnesota, I have been lucky to be part of a very talented and social Department, which has allowed me to meet many amazing people over the last 6 years. Kat, Samia, Mazar, Ian, Kathryn, David, and Elizabeth: you all have made my time in Minnesota quite enjoyable. I realize that many of you have lived with me at 321 over the past four years, and it has truly been my pleasure to get to know you better. Kat, thank you very much for being a great source of support and motivation, both academically and otherwise. Much of my interest in academia stems from conversations with you. And of course, Penny and Pheona, thank you for your company and all your moral support. Lastly, I would like to thank my family for their continuing support from across the world.

Abstract

Advances in genetics have empowered gene therapy as a cancer treatment, however there are many challenges to delivering genes specifically to target disease sites. Presented here is the development of a new non-viral gene delivery vehicle, consisting of branched polyethyleneimine (bPEI) condensed plasmid DNA polyplexes encapsulated within a PR_b functionalized stealth liposome, for the delivery of genes specifically to $\alpha_5\beta_1$ integrin overexpressing cancer cells. This new transfection agent mediated higher gene expression than non-targeted stealth liposomes and unencapsulated polyplexes in tissue culture. In a liver-metastatic colorectal cancer mouse model, PR_b functionalized stealth liposomes outperformed non-targeted stealth liposomes and was able to specifically transfect the tumor site while avoiding healthy tissues. In addition, a comparative investigation of the transfection mechanism of PR_b functionalized nanoparticles, DOTAP/DOPE lipoplexes, bPEI polyplexes and stealth liposomes was carried out in DLD-1 cells. Results demonstrated that PR_b functionalized nanoparticles were optimally balanced for the transfection of DLD-1 cells with high colloidal stability, fast integrin mediated internalization kinetics, caveolae mediated uptake and endosomal escape. To further increase the specificity of gene expression in cancer tissue, a new therapeutic plasmid DNA (pNF-κB-DTA) was developed with expression of Diphtheria toxin fragment-A (DTA) gene regulated by the transcriptional activity of NF-κB, which is a transcription factor upregulated in cancer. The multi-targeted gene delivery system formed by encapsulating pNF-κB-DTA/bPEI polyplexes in PR_b functionalized stealth liposomes showed more specific gene expression in cancer cells versus healthy cells compared to either individually targeted system. Transfecting cancer cells using the multi-targeted gene delivery system resulted in a dose-dependent reduction of cellular protein expression and a dose-dependent increase in cytotoxicity. Our therapeutic delivery system specifically eradicated on average 70% of a variety of cancer cells while minimally affecting healthy cells. Moving forward, the modular nature of our non-viral delivery vehicle design can facilitate

targeting novel pairs of extracellular receptors and upregulated transcription factors for applications beyond cancer gene therapy.

Table of Contents

List of Tables

List of Figures

List of abbreviations/notations

CAG: CMV enhancer/chicken beta-actin promoter/chicken beta-globin intron sequence

CMV: Cytomegalovirus

DLS: Dynamic light scattering

DOPC: 1,2-dioleoyl-*sn*-glycero-3-phosphocholine

DOPE: 1,2-dioleoyl-*sn*-glycero-3-phosphoethanolamine

DOTAP: 1,2-dioleoyl-3-trimethylammonium-propane

DPPC: 1,2-dipalmitoyl-*sn*-glycero-3-phosphocholine

DTA: Diptheria toxin fragment-A

DMEM: Dulbecco's Modified Eagle Medium

MPS: Macrophagocyte system

N/P: Amine to phosphate ratio

NF-κB: Nuclear factor kappa B

PBS: Phosphate buffered saline

PEG: Polyethyleneglycol

RGD: Arginine-Glycine-Aspartate

PEI: Polyethyleneimine

pLL: Poly-L-Lysine

Chapter 1. Introduction

Cancer continues to be a major health problem worldwide. While early detection and prevention measures have improved cancer survival rates, cancers that avoid detection until later stages are still associated with a high mortality rate. According to a CDC report in 2010, half of the colorectal cancer cases and a third of the breast cancer cases were only detected at later stages, when treatment is more difficult, despite the availability of screening tests.[1] 40% of breast cancers progress to later stages before detection because of unsuccessful screening.[2] In the US, one in every two men and one in every three women will be diagnosed with cancer over their lifetime according to the American cancer society's annual cancer report for 2013. The report also estimates that in 2013, more than 1.6 million new cases of cancer will be diagnosed in the US alone. While the push for better screening techniques continues, we also require better therapeutic strategies to address cancers, especially those that continue to avoid early detection.

Recent advances in genetics have made gene therapy an increasingly viable treatment for diseases like cancer. As our molecular and genetic understanding of cancer grows, we are poised to move away from traditional non-specific forms of cancer treatment, such as chemotherapy and radiation therapy, that are associated with harmful side-effects, and specifically target the root causes of cancer. Genetic therapies can be designed such that therapeutic gene expression is promoted by factors prevalent only at diseased sites, thereby facilitating a target specific therapeutic effect. Exploring the versatile nature of genes can therefore aid in the development of novel therapeutic strategies. However, although oncology and genetics have taught us how to specifically attack cancer cells, a major challenge is to deliver gene based therapeutics to their target sites. Genes administered into the living body face many challenges before therapeutics success. These include surviving the body's defense mechanism by avoiding detection and elimination by the macrophage system

(MPS), recognition of and uptake into target cells, and successful endosomal escape and nuclear localization.[3] We need efficient gene delivery vehicles that can successfully navigate these barriers and transport genes to their sites of action.

Currently, genes can be delivered using viral and non-viral vectors.[3,4] Although non-viral vectors are not as efficient as viral vectors in terms of transfection, they are often more attractive because they are safer, more tunable and easier to build.[5,6] However, most non-viral vectors are trumped by many of the in vivo delivery challenges listed above. Stealth, or polyethyleneglycol incorporated (PEGylated), liposomes given their history of successfully solving many such problems for traditional chemotherapeutics,[7] can be a potential starting point for next generation gene delivery vehicles. In addition, the process of self-assembly that generates these liposomes is highly tunable and can incorporate biomimetic amphiphiles with unique functionalities. The applications of neutral stealth liposomes, such as those used to improve delivery of chemotherapeutics, remain as yet vastly unexplored as gene delivery vectors. Consequently, the method of transfection mediated by such transfection agents is also poorly understood. The development and characterization of targeted stealth liposomes as delivery vehicles for novel therapeutic genes may be instrumental in advancing gene therapy.

1.1 Scope

This thesis presents a modular integration of tunable biomimetic amphiphiles and versatile genetic components. Much of the present work has been made possible by the vast amount of knowledge gathered on liposomes as self-assembled chemotherapy delivery vehicles, and the recent advances in genetic technology. Targeted neutral stealth liposomes, which have been extensively used in drug delivery, have been combined here with plasmid DNA/polymer complexes (polyplexes) to create a new gene delivery system. The transfection mechanism of this new transfection agent was extensively investigated in vitro. Furthermore, a novel transcriptionally targeted therapeutic plasmid was developed to increase specificity of gene expression in cancer tissue, and encapsulated within a

targeted stealth liposome to generate a multi-targeted gene delivery system. The following sections briefly introduce the three chapters that comprise this thesis.

1.1.1 PR_b functionalized stealth liposomes for targeted delivery to metastatic colon cancer

Chapter 3 presents a new approach in which we fully encapsulate polymer condensed DNA into neutral stealth liposomes; thus, the DNA compaction and transfection properties of cationic polymers are combined with the colloidal stability of the stealth liposome. To date, there has been a minimal amount of work reported on encapsulating polyplexes into a stealth liposome and characterizing the system. This void in the literature is most likely due to two factors. First there is the difficulty of encapsulating a large, condensed plasmid DNA particle into the limited internal volume of a 100-200 nm liposome. Second, the proximity in size of unencapsulated polyplexes and polyplex containing liposomes presents a challenge in their separation and the quantification of total DNA in the final preparation. Chapter 3 presents a polyplex encapsulated liposome formulation procedure that addresses each of these challenges.

In order to further increase the specificity of such a delivery system, various targeting moieties can be incorporated into the basic carrier. Targeted liposomes have been previously used in the delivery of payloads to various disease sites including tumors.[8–10] However, the benefits of targeting remain controversial. Although targeted liposomes reduce non-specific delivery compared to the free therapeutic, there remains considerable room for improvement. When administered in vivo, targeted delivery vehicles often accumulate at significant levels in healthy tissues,[9,11–13] potentially causing undesirable toxic side effects. Identification of an optimal receptor-ligand pair that allows the delivery vehicle to interact with diseased cells expressing high levels of the receptor, and not with healthy cells expressing the receptor at a lower concentration, can lead to improved specificities of therapeutic delivery. $\alpha_5\beta_1$ integrin is a promising target that has been shown to be overexpressed on both cancer cells as well as on cancer vasculature, and associated with increased tumorigenicity, malignancy and tumor cell invasiveness.[14,15] In addition, $\alpha_5\beta_1$ displays elevated expression

levels on certain primary cell lines, while its expression is downregulated during development.[16] Our group has previously designed a targeting peptide PR_b based on fibronectin, the native binding ligand for $\alpha_5\beta_1$ integrin. PR_b was engineered by combining the RGD binding site and the PHSRN synergy site,[17] as this combination of sites is specific for binding to $\alpha_5\beta_1$.[17,18] PR_b has outperformed both fibronectin and RGD in terms of binding cells expressing the $\alpha_5\beta_1$ integrin.[17] Subsequently, a hydrophobic lipid tail was linked to the PR_b peptide to generate a peptide amphiphile. Taking advantage of the tunability of the self-assembly process, the PR_b amphiphile was mixed with an appropriate combination of other lipids to generate a self-assembled targeted stealth liposome. PR_b functionalized nanoparticles previously formulated in our group have shown increased in vitro delivery of model payloads when compared to non-targeted vehicles[19–21]. In Chapter 3, the potential of the PR_b functionalized stealth liposome as a new transfection agent is investigated in vitro, and for the first time its functionality is tested in vivo.

1.1.2 Investigating transfection mechanism

In general, in order to design efficient transfection agents without sacrificing stability and delivery specificity, it is necessary to better understand their mode of action in vitro. Currently, transfection mechanism of targeted PEGylated systems and how it differs from those of conventional unmodified transfection agents is not well understood. Researchers investigating the characteristics and transfection mechanisms of these agents often disagree and provide no consensus on the mode of their transfection.[3,22,23] It is apparent that different transfection agents have a range of effectiveness across different cell lines, but reasons behind the differential activity are not clear. One of the factors that may play an important role in determining transfection efficiency is the internalization pathway utilized by these transfection agents.[24] There have been several major pathways implicated so far in the cellular uptake of transfection agents, however there is no consensus on which is the most effective. [23,25,26] More work is therefore needed to characterize these vectors. In Chapter 4, the transfection mechanisms of several different transfection agents are investigated; with a focus

on understanding targeted PEGylated systems compared to commonly used cationic polymer condensed DNA complexes (polyplexes) and cationic lipid condensed DNA complexes (lipoplexes). Specifically, we studied how plasmid DNA delivered using DOTAP/DOPE based lipoplexes, branched polyethyleneimine (bPEI) based polyplexes, stealth liposomes encapsulating bPEI polyplexes and PR_b peptide functionalized stealth liposomes encapsulating bPEI polyplexes (presented in Chapter 3) transfect DLD-1 human colorectal cancer cells. To this end, flow cytometry and confocal microscopy was used to dissect the transfection mechanisms of these different transfection agents. Also, carefully selected chemical inhibitors previously shown to successfully inhibit their respective routes [27,28], were used to identify the major internalization routes preferred by each of the transfection agents. Finally, combined observations from the transfection and DNA uptake levels, internalization rate kinetics, intracellular colocalization, and inhibition of endocytosis facilitated in deciphering the transfection mechanisms of the different agents investigated.

1.1.3 Increasing cancer-specific gene expression

While PEGylation and incorporation of targeting ligands can improve delivery efficiency compared to traditional delivery of free therapeutics, these modified delivery systems continue to experience significant non-specific uptake by the macrophage system (MPS) when administered in vivo.[29] Also, many widely investigated cancer cell or cancer vasculature receptor targets such as integrins,[30] the endothelial growth factor receptor [31] and fibroblast growth factor receptor[32] are appreciably expressed in healthy tissues and vasculature.[33–35] These issues can lead to the same non-specific side effects that targeted therapy aims to avoid, and therefore call for further levels of control to minimize off-target delivery effects. Gene therapy can help solve the problem of non-specific delivery by combining transcriptional and extracellular receptor targeting. Transcriptional targeting has been widely investigated and shown to improve specific delivery to the target tissues.[36,37] Generally, transcriptional targeting involves delivering a gene under the control of a tissue specific promoter – allowing gene expression

in target tissues while avoiding healthy tissues. Multi-targeting by combining receptor targeting and transcriptional targeting has been shown before to effectively increase the specificity of a viral gene delivery system,[38–40] however it has not yet been sufficiently investigated in a non-viral delivery system before.[41]

NF-κB is a well-characterized family of transcription factors that is upregulated in a variety of diseases including cancer[42] and that is known to mediate resistance to chemotherapy and radiation therapy.[43] Inhibition of NF-κB activity has been shown to improve cancer therapy by reducing NF-κB mediated chemotherapy resistance.[44] However, its transcriptional activity has never been used as a therapeutic target before. Given the central role played by NF-κB as a transcription factor controlling a variety of cancer progression pathways, we hypothesized its upregulated activity would be sufficient to mediate a therapeutic response specifically in cancer cells. In Chapter 5, we present the development of a multi-functional therapeutic system wherein a NF-κB responsive transcriptionally targeted plasmid was condensed with bPEI and encapsulated in a PR_b functionalized stealth liposome. The increased transcriptional activity of NF-κB in cancer tissue was used to mediate therapeutic gene expression specifically in cancer cells. Also, targeting the transcriptional activity of a single upregulated transcription may improve control and outcome predictability compared to conventional transcriptional targeting that utilizes entire promoter sequences of upregulated genes. This idea is further discussed in Chapter 5. In addition, to address the problem of low gene expression mediated by most transcriptional targeting, the highly potent diphtheria toxin fragment-A (DTA) was chosen as the protein product of gene expression. DTA consists of only the catalytic fragment of diphtheria toxin and lacks a cell-penetrating domain, minimizing any bystander cell killing effect at off-target sites. A few molecules of DTA can be enough to result in cell death through inhibition of protein expression[45] and DTA-encoding plasmids have been previously used to successfully kill cancer cells.[36,46] By targeting two well-recognized cancer markers, $\alpha_5\beta_1$ integrin and upregulated NF-κB transcriptional activity, a general, modular platform for cancer-specific transfection agents was created.

1.2 Organization of thesis

In this thesis, the development of a new stealth liposome based transfection agent targeted to cancer tissue is presented. To start off, Chapter 2 presents useful background information to introduce topics presented in the subsequent chapters. Following, in Chapter 3, the challenges in formulating a liposomal gene delivery system are outlined, and steps taken to overcome them are presented. The optimization and characterization of gene delivery efficiency both in in vitro tissue culture as well as in a metastatic tumor mouse model is then discussed. Subsequently, the transfection mechanism of the newly formulated transfection agent is investigated in Chapter 4, and compared to the mechanisms of other commonly used non-viral transfection agents. Observations discussed in this chapter can help improve the design of transfection agents in general. In Chapter 5, the development of a new transcriptionally targeted therapeutic plasmid is presented. The newly developed plasmid was encapsulated in the transfection agent formulated in Chapter 3, thereby creating a new multi-targeted gene delivery vector. The multi-targeted system was tested for improvements in specificity of gene expression in cancer cells. Also, the therapeutic effect mediated by the multi-targeted system was investigated using a variety of techniques in multiple cancer cell lines. The results presented in Chapters 3-5 can advance liposomal gene delivery and aid in the development of more specific gene delivery vectors.

Chapter 2. Background

In this section, background information is provided on several key topics that are vital to the discussion that follows in subsequent chapters. The development of liposome technology and its application in cancer treatment is discussed. The benefits of incorporating polyethyleneglycol (PEG) and targeting ligands on the surface of delivery vehicles are also presented, with a focus on targeting $\alpha_5\beta_1$ integrin. Subsequently the basis of gene therapy is presented with an emphasis on transcriptional targeting using the upregulated transcriptional activity of NF-κB. This is followed by a discussion of the need for gene delivery vehicles, a brief history of their development and the state and functional properties of commonly used transfection agents. This chapter concludes with a discussion of the various cell internalization routes involved in the uptake of transfection agents.

2.1 Liposome technology

Liposomes are bilayered lipid vesicles often consisting of synthetic derivatives of naturally occurring lipids. Hydrophilic payloads can be encapsulated within the aqueous vesicle core and hydrophobic payloads are embedded in the lipid bilayer. Liposomes were suggested as a carrier for small molecule drugs shortly after their development in the early 1960's,[47] and was first approved by the Federal Drug Administration for clinical use in the mid 1990's. Therapeutic encapsulated liposomes circulate in the blood for a longer time, and release the payload at a slower rate resulting in lower peak levels of drug in the bloodstream.[48,49] Free drug may be cleared from the bloodstream with half-lives as low as 5 min, while liposome encapsulated drugs have half lives in the order of 30 to 60 min. Prolonged presence of drugs in the bloodstream can increase its therapeutic effect, and this phenomenon is further discussed in section 2.1.2a below.

In addition to a longer clearance time, a more favorable tissue distribution of liposome encapsulated therapeutics compared to freely administered

therapeutics also contributes to fewer toxic side effects. The relative bulkiness of the liposomes prevents extravasation into non-cancerous tissue, but allows passage into tumor tissue (section 2.1.1a Passive targeting and the EPR effect). Briefly, tumor endothelium has wider fenestrations compared to normal tissue allowing bigger particles such as liposomes to pass through and is a prospective passive target for cancer treatment. Through this effect, liposomes protect some normal tissues from being subjected to potentially toxic cancer therapeutics. Liposome encapsulation has been experimentally and clinically proven to reduce toxic side effects of therapeutics.[50,51]

2.1.1 Self assembly and the formation of liposomes

Liposomes are prepared from a variety of amphiphilic lipids or lipid mixtures, the most commonly used being phospholipids. Phospholipids, like all other amphiphilic compounds, consist of a polar head group and a hydrophobic tail group. In an aqueous environment, these amphiphilic molecules self-assemble into various structures through a hydrophobic effect that maximizes the entropy of the surrounding water molecules.[52] The final self-assembled structure formed by such amphiphilic compounds in an aqueous environment primarily depends on the shape of the individual molecules; the final shape of the self-assembled structure can therefore be controlled by using differently shaped monomers. Cylindrical double tailed amphiphilic molecules that have been shown to form lipid bilayers can assemble into bilayered vesicles, liposomes. The general structure of such a phospholipid, 1,2 Dipalmitoyl-sn-Glycero-3-Phosphocholine (DPPC), is shown in Fig. 1.

Tuning the original lipid mixture can control the properties of the liposome formed; thus it is important to monitor the lipid ratios used to ensure success of the liposome in its intended application. In addition to the basic requirement of cylindrical molecules, constituent lipids should be chosen based on phase transition temperature and effect on overall permeability, fluidity and stability of the liposome. Liposomes undergo a phase transition at temperatures higher than a critical temperature T_c where the membrane becomes fluid like with increased permeability and reduced mechanical strength. For in vivo applications, this is

undesirable as it can lead to liposome degradation or leakage of therapeutic loads.[7] Based on these criteria, our group commonly uses lipids such as DPPC and cholesterol. DPPC is the main liposome-forming lipid, while cholesterol is used as a strengthening agent. It has been shown that incorporation of cholesterol in greater than 33% inhibits phase transition, and reduces fluidity and permeability of the liposome membrane.[53]

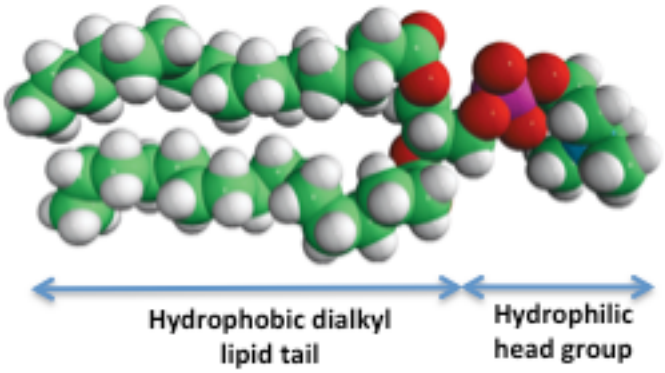

Figure 1. 1,2 Dipalmitoyl-sn-Glycero-3-Phosphocholine (DPPC).
Color codes for the different atoms are: Carbon (green), Hydrogen (white), Phosphorus (purple) and Oxygen (red). [Adapted from Avantipolar lipids]

Depending on the method of preparation of liposomes a variety of vesicle structures can result. The most common of these are multilamellar vesicles (MLV), small unilamellar vesicles (SUV) and large unilamellar vesicles (LUV). Depending on the particular application that the liposomes are intended for, one of these formulations may hold an advantage over the others.[7] Multilamellar vesicles are large and possess a low internal aqueous fraction, as the lamellar lipids take up most of the space. SUVs and LUVs both have a single outer lipid shell, the amount of internal aqueous cores being different as a result of their different sizes. For the encapsulation of aqueous loads the unilamellar vesicles are more desirable, while multilamellar vesicles are more useful for hydrophobic loads. The liposome size is a crucial factor determining in vivo fate of the delivery system. Liu et al. showed tumor accumulation is highest for liposomes in the range 100-200nm.[54] Below 100nm, liposomes are preferentially taken up in the liver, and much beyond this size accumulation in the spleen starts increasing.

Good therapeutic delivery systems need to evade capture in the liver, spleen and the rest of the MPS while specifically reaching the target tissue.[54]

Although liposomal drug encapsulation showed early promise, there remained some unaddressed concerns. The exposed outer surface of these “bare” liposomes make them vulnerable to unfavorable interactions with serum proteins called opsonins. This opsonization process attracts macrophages and encourages phagocytosis of bound liposomes. Detection and elimination by the macrophage system (MPS) constitute key steps in the body’s defense mechanism against unwanted foreign invaders. Intercalation of plasma proteins on the liposome surface also destabilizes the lipid bilayer causing the liposomes to break apart and release the encapsulated material.[55,56] Both opsonization and destabilization remove the liposomes from the blood stream, making them unavailable for the target tissue. In order to make liposomal drug delivery a success, new strategies were needed to increase liposome circulation lifetime in the blood by increasing their stability and decreasing their interactions with plasma proteins.

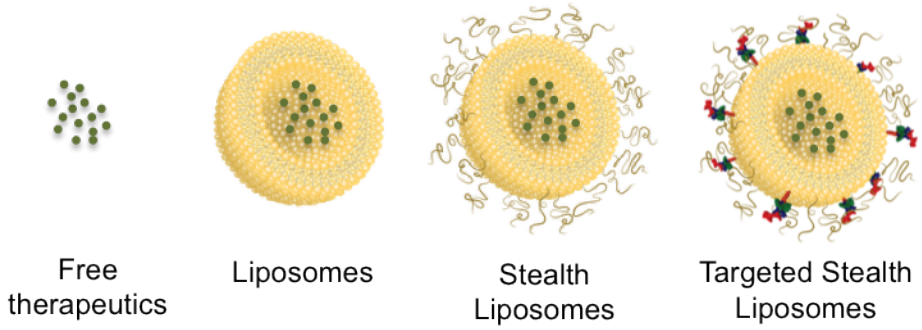

Figure 2. Evolution of liposomes as therapeutic delivery vehicles
[Liposome images credited to R. Levine].

2.1.2 Stealth liposomes

The evolution of liposomes as drug delivery vehicles is depicted in Fig. 2. Incorporation of polyethyleneglycol (PEG) on the surface of liposomes was suggested as a means to inhibit MPS clearance. The PEG layer on the liposome surface is believed to provide a steric barrier against protein adsorption,[57,58] and

thereby increased the liposome blood circulation lifetime to a half life of greater than 5 h compared to 30 min for conventional liposomes.[59,60] The term “Stealth liposomes” was coined to describe these long circulating PEGylated liposomes. Stealth liposomes are believed to be more successful than conventional bare liposomes due to its increased circulation lifetime, which in turn has been correlated to increased accumulation in the tumor tissue.[61] The increased circulation lifetime of drug encapsulated liposomes is especially beneficial for those drugs that require prolonged exposure for increased efficiency.[62,63] As discussed below, an increased circulation lifetime of stealth liposomes makes them better suited to enhanced permeation and retention (EPR) mediated tumor accumulation.

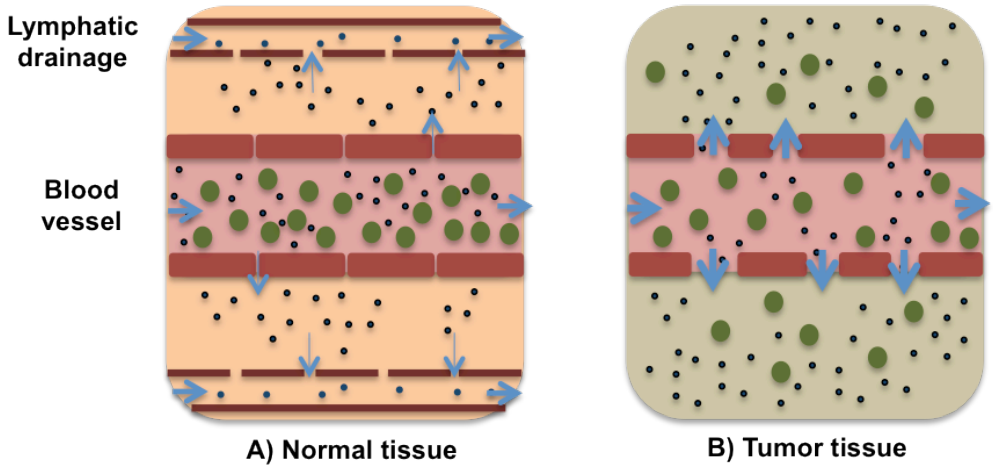

Figure 3. Enhanced permeation and retention effect.
In healthy tissues (A), normal fenestrations allow only smaller particles to escape the vasculature. Any left over particles in the tissues are then efficiently cleared out by the lymphatic drainage system. However, in tumor tissue (B), irregular blood vessel architecture with large fenestration enables large particles 100-200nm in diameter to escape into tissues. In addition, lack of proper lymphatic drainage results in prolonged tissue retention. Therapeutic delivery systems can use this effect to passively accumulate in tumor tissue.

2.1.2a Passive targeting and the EPR effect

Particle escape from the circulation occurs at locations in the vasculature with wider gaps or fenestrations, or with inflammation-induced abnormal endothelial barriers. Tumor vasculature is often characterized by a highly irregular

architecture with large fenestrations in the endothelial layer, increased vessel tortuosity and abnormally heterogeneous vessel density,[64] and is therefore associated with enhanced permeability, as depicted pictorially in Fig. 3. Several studies demonstrated that 100-200nm sized liposomes can successfully extravasate into tumors in experimental animals and humans.[7,54,65] In addition tumor tissue has high fluid retention due to the lack of lymphatic drainage; hence any liposomes that extravasate out from the vasculature into the tumor are retained. Together, this enhanced permeability and retention (EPR) effect in tumor tissues form the basis of the passive targeting of liposomes. The EPR effect can cause increased accumulation in the tumor tissue, but it is a slow process that can occur over days.[66] For this reason, long circulation lifetime is a crucial requirement for successful delivery. To improve the rate of tumor delivery of passively targeted stealth liposomes, active targeting strategies were required.

2.1.3 Actively targeted delivery

In the nineteenth century Paul Ehrlich first presented the concept of a magic bullet, a system to deliver therapeutic loads only to the specific diseased area while sparing the rest of the body. Two of the ways this could be achieved is by using site-specific or site-triggered delivery systems. Site-specific drug delivery involves the incorporation of targeting moieties on the surface of delivery vehicles, enabling these vehicles to selectively bind to target cells. Site-triggered delivery is designed to initiate payload release from delivery vehicles upon encountering conditions that prevail only in the target tissue such as temperature, pH or the presence of a particular enzyme. In this section we will primarily discuss the former of these two targeting strategies. The idea behind site-specific delivery revolves around two major concepts – identification of a good target and selection of a corresponding targeting ligand, and each of these is discussed in some detail below.

2.1.3a Identification of optimal targets- $\alpha_5\beta_1$ integrin

Cancer tissue is often distinguished from healthy tissue by the relative expression levels of molecules on the cell surface. Such a situation is illustrated in Fig. 4. A good cancer-specific target needs to be expressed at a higher level in cancer

tissue relative to healthy tissue and be accessible from the blood circulation. Cell adhesion molecules (CAMs) are a class of cell surface receptors that have been shown to be involved in many diseases including cancer.[67–70] Integrins, a subgroup of CAMs, are transmembrane glycoproteins involved in a wide range of cell adhesion interactions, and exist as non-covalent heterodimers of α and β polypeptide chains. There have been 18 α subunits and 8 β subunits identified so far in mammalian cells, and these can heterodimerize into at least 20 different integrins.[71] Out of these, $\alpha_5\beta_1$ integrin is one of the promising targets that has been shown to be overexpressed on both cancer cells as well as on cancer vasculature, and minimally expressed on normal healthy tissues, and associated with increased tumorigenicity, malignancy and tumor cell invasiveness.[14,15] In addition, $\alpha_5\beta_1$ is also expressed on certain primary cell lines, but its expression is downregulated during development.[16] $\alpha_5\beta_1$ integrin has therefore been widely investigated for the cancer-specific delivery of both chemotherapeutics and genes.

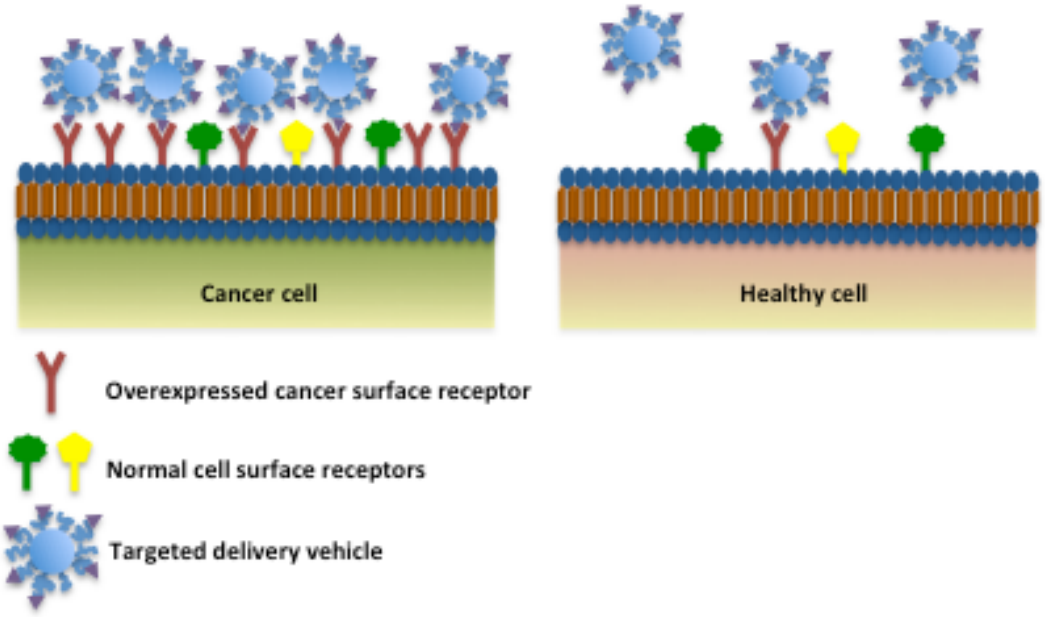

Figure 4. The concept of receptor targeted delivery.
Cancer cells often overexpress certain receptor molecules on their surface compared to healthy cells. Designing therapeutic delivery systems to recognize these surface markers can ensure specificity of delivery to cancer cells.

2.1.3b Identification of efficient targeting ligands – PR_b peptide

Targeting ligands, like in vivo targets, need to fulfill certain criteria to ensure efficient targeted therapeutic delivery. Primarily, we need these targeting ligands to be able to bind the in vivo targets with specificity and high affinity. In addition, these ligands need to be biocompatible, non immunogenic and demonstrate in vivo stability. Peptides can potentially meet many of these criteria and have therefore been investigated as targeting ligands for therapeutic delivery to various disease sites.[10]

Peptides consisting of the Arginine-Glycine-Aspartate (RGD) sequence are known to be potent ligands for integrin receptors.[72] RGD forms the active binding site in fibronectin, which is a native binding protein for integrins (Fig. 5A). RGD based peptide sequences have been previously shown to inhibit cancer progression.[73,74] Although high doses of RGD were initially required to achieve a therapeutic effect, numerous developments in RGD based targeting have since lowered the required dosage.[75–77] Liposomes functionalized with RGD analogs were shown to successfully prevent metastasis in an experiment mouse model of lung cancer.[78]

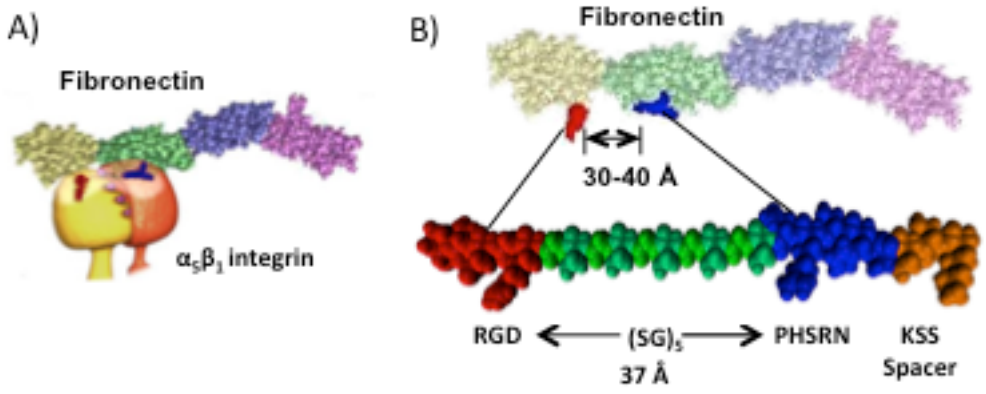

Figure 5. Design of PR_b.
(A) The fibronectin protein, part of which is shown here, specifically binds $\alpha_5\beta_1$ integrin through an RGD binding domain (red) and a PHSRN synergy site (blue) [Adapted from Tirrel et al.]. [79] (B) A fibronectin mimetic peptide amphiphile, PR_b, was created by artificially joining the RGD binding site and the PHSRN synergy site through a linker (SG_5) that mimics the natural linking sequence in fibronectin in terms of both length as well as hydrophobicity. A KSS spacer was included to extend the PR_b peptide away from an anchoring surface.

Despite these initial victories of the RGD sequence, its binding affinity for integrins is lower than fibronectin, and it binds a range of integrins without specificity for any one receptor.[80,81] A synergistic amino acid sequence found in fibronectin, Pro-His-Ser-Arg-Asn (PHSRN), was found to be important in mediating strong cell adhesion.[82] Subsequently, many peptides were designed linking the RGD binding domain to the synergy PHSRN site, but none of these fibronectin mimetic peptides were able to attain the same cell binding properties as fibronectin. A few years back our group hypothesized that in order to achieve the same binding properties as fibronectin, the peptide region linking the RGD and PHSRN sites should mimic the native linker region in fibronectin in both length as well as hydrophobicity.[83] Based on these criteria a peptide with the sequence KSSPHSRNSGSGSGSGSGRGDSP was designed (Fig. 5B), with five repeats of Serine-Glycine (SG) linking RGD to PHSRN and a Lysine-Serine-Serine (KSS) spacer at the amine terminus. This new sequence, named PR_b, was able to preferentially bind to $\alpha_5\beta_1$ integrin,[17,18] and was found to outperform other RGD based sequences as well as native fibronectin in terms of cell adhesion.[17] As depicted in Fig. 6, a C-16 dialkyl lipid group was attached to the N-terminus of the PR_b peptide to generate a biomimetic peptide amphiphile which, in combination with other lipids and cholesterol, could self-assemble into targeted liposomes.[17,19] PR_b functionalized vehicles previously formulated in our group have shown increased in vitro delivery of model payloads when compared to non-targeted vehicles.[19–21] In Chapter 3, we investigate the potential of the PR_b functionalized stealth liposome as a new transfection agent in vitro, and for the first time test its functionality in vivo.

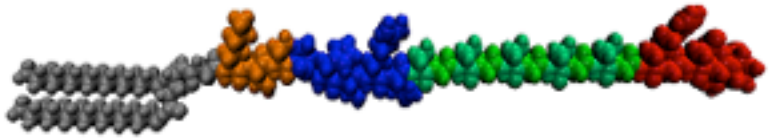

Figure 6. PR_b peptide amphiphile
A C-16 dialykl lipid group was attached to the N terminus of the PR_b peptide to generate an amphiphile.

2.2 Gene therapy

The genetic code regulates the behavior of all cells, and therefore of entire organisms. All the information to propagate and maintain life lies in the specific sequence of nucleotides that make up genes. Given the recent technological advances in the biomedical field and increased knowledge about the human genome, we now know the genetic basis of many diseases, and can target these deficit genes as a means to cure disease. Basically, gene therapy involves introduction of genetic material into a host cell with an end goal of achieving a therapeutic effect, often through the production of a therapeutic protein.

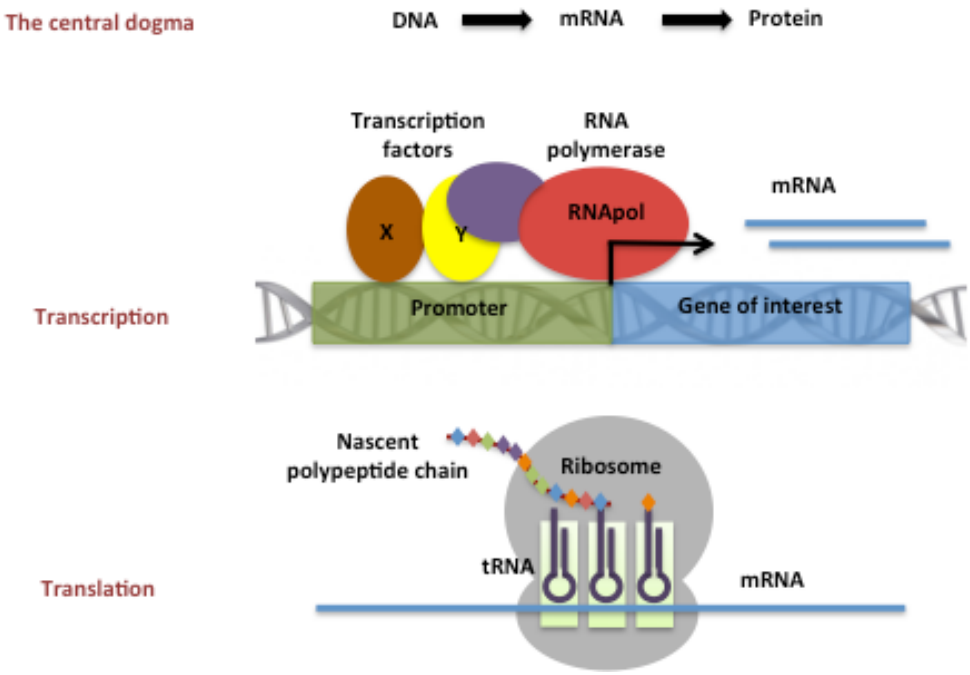

Figure 7. Basic concepts in gene expression

2.2.1 The central dogma

In mammalian cells, genes are decoded in the nucleus and used to synthesize messenger ribonucleic acid (mRNA) by a process called transcription.[84] As depicted in Fig. 7, transcription factors bind to the promoter region upstream of genes to be transcribed and recruit RNA polymerase. RNA polymerase then moves along the DNA strand and creates an mRNA molecule that matches the genetic code being transcribed. At the end of the transcription process, mRNA undergoes post-transcriptional modification and is transported out of the nucleus

into the cytoplasm where the message is translated into peptide sequences. In this process, ribosomes bind mRNA and recruit transfer-RNA (tRNA), which in turn forms a chain of amino acids based on the mRNA sequence. The polypeptide chains thus formed undergo further post-translational modification and possible combination with other polypeptide chains to form proteins. These proteins are designed to carry out a variety of functions and thus implement the instructions encoded in the genetic sequence.

2.2.2 Plasmid biology

In order to carry out a specific function in cells or tissues, genes encoding proteins with the appropriate functional properties can be artificially introduced

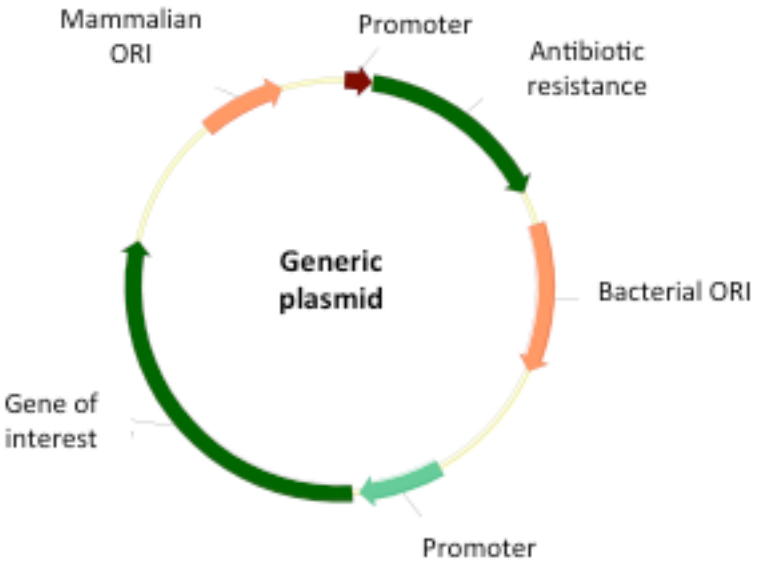

Figure 8. Common constituents of a generic expression plasmid

into a target cell. Plasmids, circular DNA of bacterial origin, are often used for such purposes. As depicted in Fig. 8, in general plasmids consist of a few basic functional genetic components, which include a bacterial origin of replication (ORI), an antibiotic resistance gene and its associated promoter, and finally at least one gene of interest and its associated promoter. The bacterial ORI and antibiotic resistance help in the proper amplification and production of the plasmid in bacterial cultures. In addition to these basic components listed here, plasmids may comprise additional components for further functions not

associated with basic maintenance. Often a mammalian ORI may be included to facilitate propagation of the plasmid in mammalian cells.

The promoter regions for the gene of interest can strongly influence the level of gene expression. Promoters vary in strength, and can be broadly classified as constitutive and tissue-specific. Constitutive promoters ubiquitously regulate gene expression. CMV or CAGS are examples of strong constitutive promoters that are commonly used in the design of many plasmids. In contrast, tissue-specific promoters, as the name suggests, are only active in certain target sites. This offers an opportunity to artificially regulate gene expression in a target-specific manner by introducing plasmids bearing a gene of interest under a target-specific promoter. This approach is termed transcriptional targeting.

2.2.3 Transcriptional targeting

The expression level of a single protein varies between tissues and can be regulated at the transcriptional or translational levels. Since gene therapy can often be used to transcriptionally control the expression level of a desired protein, this section aims to provide some background on transcriptional regulation. Transcriptional targeting utilizes promoters that are tissue specific or exogenously activated, and examples of each type have been reviewed extensively by Robson and Hirst.[85] In order to limit gene expression to a specific desired location, such as tumors, promoters that are specific to tumor tissue or tumor environment can be used.[85] Fig. 9 pictorially explains the concept of transcriptional targeting. Transcriptional targeting of genes can achieve a level of specificity unattainable by conventional small molecule therapeutics. Similar to extracellular targets and optimal targeting ligands discussed in Section 2.1.3, optimal tissue-specific promoters are also selected based on certain criteria. Promoters chosen for transcriptional targeting need to be sufficiently active to facilitate a therapeutic effect at the target site and should mediate minimal leaky expression elsewhere. Some transcriptionally targeted

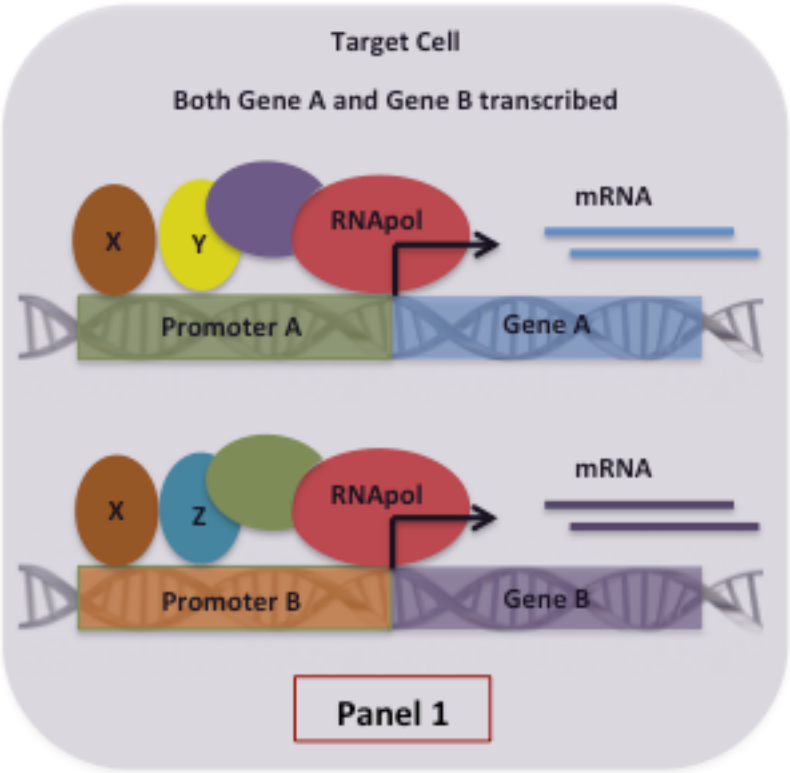
Target Cell
Both Gene A and Gene B transcribed
X
Y
RNApol
mRNA
Promoter A
Gene A
X
Z
RNApol
mRNA
Promoter B
Gene B
Panel 1

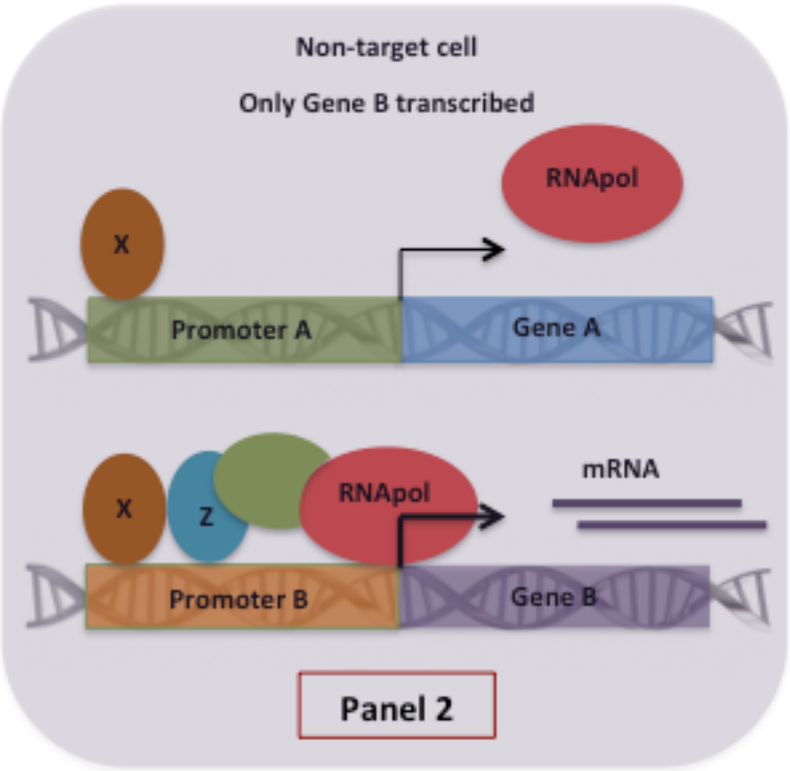
Non-target cell
Only Gene B transcribed
RNApol
X
Promoter A
Gene A
X
Z
RNApol
mRNA
Promoter B
Gene B
Panel 2

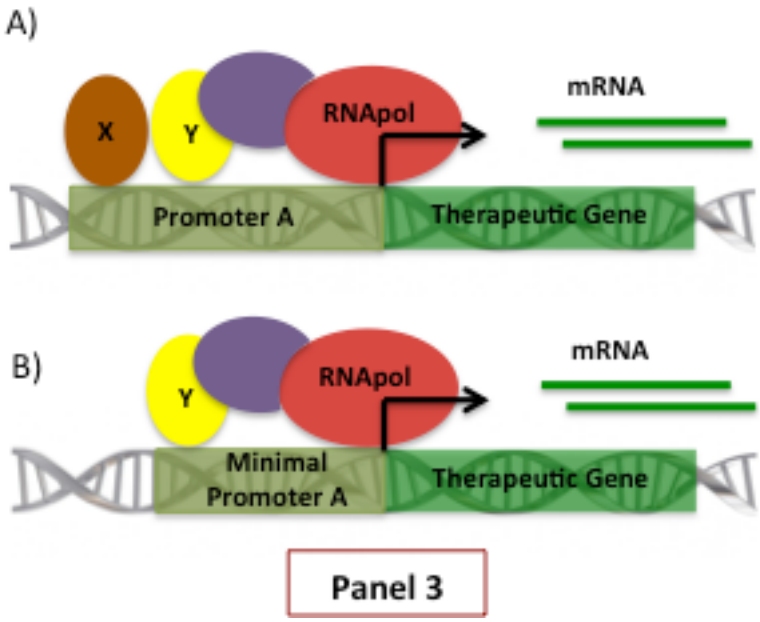

Figure 9. The concept of transcriptional targeting.
Panels 1 and 2 indicate two different cell lines with different active transcription factors resulting in differential levels of gene expression. In Panel 1, showing a target cell, transcription factors X, Y and Z are all active and can initiate transcription of both Gene A and Gene B. In Panel 2, showing a non-target cell, transcription factor Y is absent, and Gene A is not transcribed. In the design of a transcriptionally targeted therapeutic plasmid, shown in Panel 3, the promoter for Gene A can be used to drive the expression of a therapeutic gene in the target cell but not in the non-target cell (3A). Furthermore, the promoter region can be trimmed to a minimum sequence that is regulated by a single essential transcription factor (3B).

promoters that have been successfully used in tumor therapy include the Rad51 promoter for prostrate cancer,[36] H19 for bladder cancer,[86] and hTERT promoter for generic cancer.[37]

2.2.4 Transcription factors and NF-κB

Promoters, including target specific promoters, are regulated by transcription factors. These transcription factors are differentially active in different tissues. Consequently, there are several transcription factors that are specifically upregulated in cancer tissue and play a central role in disease progression. In fact, many oncogenes encode transcription factors and many oncogene-related signaling pathways converge on transcription factors. These transcription factors in turn regulate oncogene networks that propagate the disease state.

NF-κB is a well-characterized family of transcription factors that is upregulated in a variety of diseases including cancer.[42] These transcription factors consist of homo or heterodimers of at least five different proteins – RelA, RelB, cRel, NF-κB-1, NF-κB-2. Normal functions of NF-κB include negative feedback of its own activity, anti-apoptosis, proliferation and immunity.[42] In most healthy cells, most NF-κB is present as an inactive dimer form bound to inhibitors of NF-κB (IκBs) in the cytoplasm (Fig. 10).[42,87] However, in diseases such as cancer, various pathways result in the ubiquitination and subsequent degradation of IκBs, thus constitutively activating NF-κB and allowing it to translocate to the nucleus where it upregulates the transcription of many oncogenes.[42] NF-κB promotes tumorigenesis by stimulating cell proliferation, inhibiting apoptosis and encouraging metastasis and angiogenesis.[42] It has been implicated in many types of cancer including breast,[88,89] liver,[90] colon,[91,92] gastric,[93,94] lung,[44,95] and prostrate,[96] where it is often overexpressed in its activated form thus making it a desirable target for transcriptional targeting. A promoter activated specifically by NF-κB may therefore limit gene expression to the tumor tissue. NF-κB binding sequences in many promoters/enhancers have been well characterized.[97] From these and other NF-κB binding motifs, consensus sequences have been derived [98] that can be used in the construction of an NF-κB responsive promoter.

2.3 A brief history of gene delivery

An early method of gene delivery was the introduction of naked DNA into the system of interest. Although somewhat successful at in vitro cell transfection, this method performs rather poorly at in vivo situations. Naked DNA is cleared from circulation through enzymatic degradation and liver uptake within minutes, severely limiting chances of reaching the target tissue.[99,100] To improve the pharmacokinetics of DNA, it was recognized early on that some form of protective modifications needed to be made. Viral vectors are efficient DNA delivery agents, but these systems are immunogenic and are cleared rapidly from the circulation.[5] Fraley et al. and Wong et al. independently showed for the first time in 1980 that liposomes could be used to deliver DNA into cultured mammalian cells.[101,102]

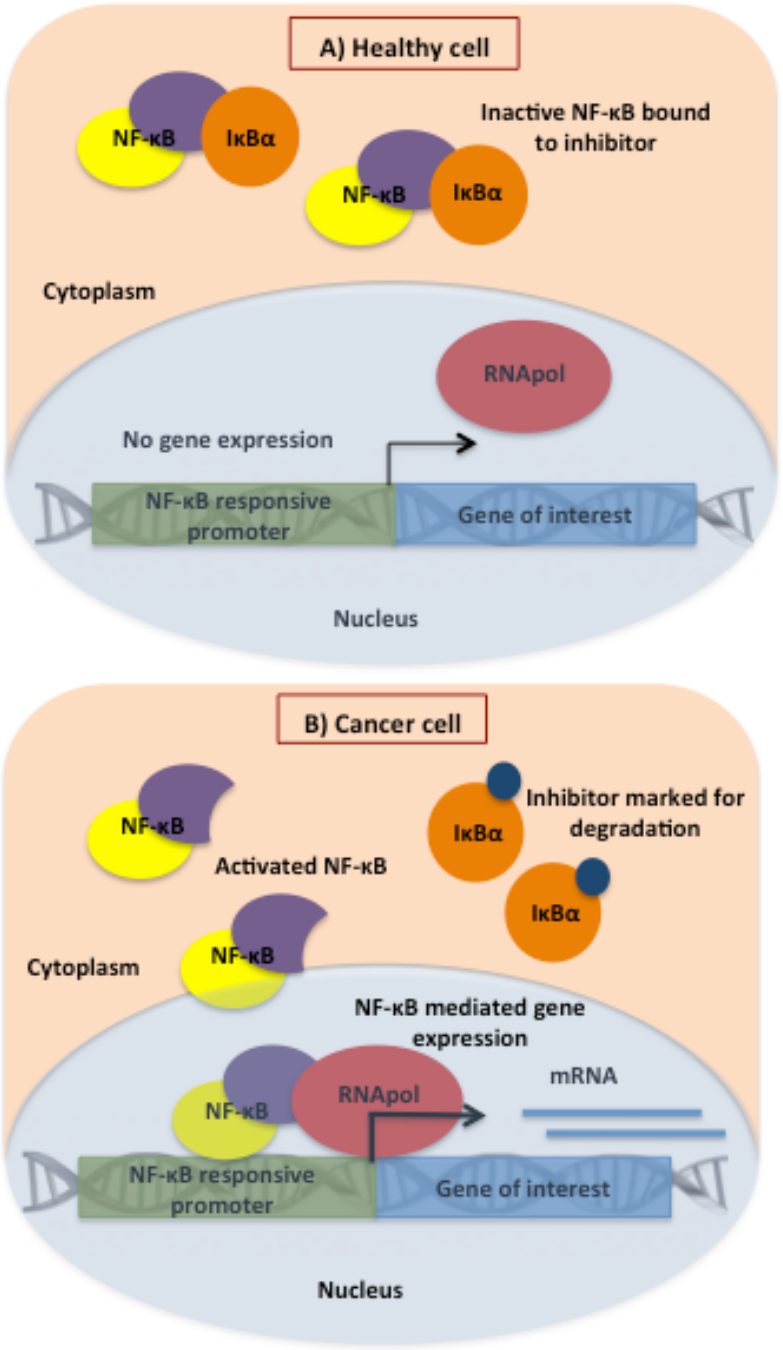

Figure 10. Transcriptional activity of NF-kB in cancer.

A) In healthy cells, most NF-κB remains bound to its inhibitor proteins such as IκBα in the cytoplasm and regulates minimal gene expression. B) In cancer cells, IκBα is marked for degradation and free NF-κB can translocate to the nucleus and initiate transcription.

Association with liposomes was suggested to improve the stability of DNA in transfection studies.

After brief modifications to the liposome formulation to increase transfection efficiency, the first in vivo liposomal gene delivery was done in liver cells.[103,104] A glycolipid targeting ligand was incorporated in the liposome to enable more efficient delivery to liver cells.[49] However, all these systems used anionic or neutral lipid compositions in making the liposomes, and were not very efficient in encapsulating the negatively charged DNA. Encapsulation of large DNA molecules into liposomes thus became an important technical difficulty in the use of liposomes for gene delivery. To address this problem, Felgner and coworkers first reported successful high efficiency DNA delivery in cationic liposomes.[105] The positively charged lipids interact directly with the negatively charged DNA forming lipid-DNA complexes, and have been shown to efficiently transfect cells both in vitro and in vivo.[106–109] Unfortunately, clinical trials performed with such lipid-DNA complexes failed to demonstrate any decisive clinical benefits.[110] Major drawbacks of these lipoplexes are the low in vivo stability and short half-life, and toxic side-effects both in vitro and in vivo.[111–113] Even hydrodynamic injections of naked DNA are sometimes preferred over these formulations in clinical trials.[114] Therefore, more work was needed for such systems to achieve their full potential. Specifically, it would be useful to concentrate the DNA into a smaller volume to allow the application of a higher dose in a stable form. One of the areas that has been extensively studied and can be applied to this cause is DNA condensation and association with stabilizing lipids.

2.3.1 DNA condensation

DNA condensation involves decreasing the volume occupied by a DNA molecule. In this process the molecule goes from being in a random coil to a more compact state where the volume fractions of solvent and DNA are comparable.[115] DNA condensation can protect DNA from DNA degrading enzymes, as well as help concentrate large amounts of DNA into small volumes to enable efficient encapsulation into carrier vesicles. Bloomfield lists the forces behind DNA condensation as the unfavorable effects from bending DNA and loss in entropy

from separation of DNA and solvent, and the favorable effects of coulombic interactions from oppositely charged ions and hydration force.[116] DNA condensation occurs through condensing or transfection agents, which work by increasing the condensation favorable forces and decreasing the unfavorable forces.

2.3.2 Common transfection agents

Most commonly used transfection agents consist of cationic lipids or cationic polymers, and modified versions of them. Polyethyleneimine (PEI) [117,118] for cationic polymers and dioleoyl trimethylammonium propane/ dioleoyl phosphatidylethanolamine (DOTAP/DOPE) [119] for cationic lipids are some of the most widely investigated transfection agents that can condense DNA into small particles and mediate efficient transfection in vitro. By varying the ratio of polymer or lipid to DNA during the condensation process, the net charge of the resulting particles can be controlled. Thus, in addition to protecting DNA from enzymatic degradation, the positive charge allows these particles to favorably interact with the negatively charged cell membrane and encourage internalization. Furthermore, PEI and DOTAP/DOPE each possess properties that allow them to escape the endosomal pathway following cell internalization.

PEI is known to escape endosomes through the proton sponge effect,[118] which is a consequence of structural configuration and protonation of its constituent amine groups. In PEI every third group is an amine, and at physiological pH only every fifth amine group is protonated. The amount of amines protonated increase as pH decreases: 45% of amines are protonated at pH 5 versus only 20% at pH 7.[118] The increase in protonation has two effects. First, there is increased charge repulsion, which can help release DNA from a compact structure. And second, as the name of this effect suggests, the increased positive charge attracts counterions into the endosomes and the resulting increase in osmolarity encourages an influx of water. This osmotic swelling ruptures the endosomes and releases the DNA into the cytosol. The transfection efficiency of PEI was tested in a range of cell lines and its success was attributed to the proton sponge effect.[120]

Cationic lipid-mediated transfection is strongly dependent on the mixtures of lipids used. Although cationic lipids such as DOTAP/DOPC can condense DNA into lamellar liquid crystalline closed packed structures and facilitate endosomal uptake, their transfection efficiencies are generally low due to their inability to escape the endosomes. DOPE, instead of DOPC, in the mixture with DOTAP and DNA can initiate a structural transition from lamellar to columnar inverted hexagonal phase that is amenable to fusion with anionic endosomal membranes.[121] The helper lipid DOPE can effectively lower the kinetic barrier to lipid fusion. The effective mixing of the cationic lipids and anionic endosomal lipids neutralizes electrostatic interactions, destabilizes the endosomal bilayer, and releases DNA from its initial compact structure into the cytosol outside.[121]

2.3.3 PEGylation and targeting of transfection agents

Despite possessing advantageous properties that can help mediate efficient gene expression in vitro, cationic lipid and cationic polymer based transfection agents suffer from several disadvantages in vivo.[122] PEI and DOTAP/DOPE have poor colloidal stability in serum, and have been shown to cause undesirable toxic side effects.[123,124] The interaction between these agents and cells is primarily mediated by electrostatics and can often lead to non-specific transfection at off target tissues. In addition, the high positive charge density of the resulting condensed DNA particles can form holes in transfected cells and increase membrane permeability thereby reducing cell viability.[125] One of the modifications suggested to address such challenges is the incorporation of PEG on the surface of these transfection agents. PEGylation can increase serum stability by reducing opsonization and can reduce non-specific cytotoxicity by shielding some of the excess surface positive charge. While the circulation half-life in blood after in vivo administration varies from a few minutes to 1 h for polymer or lipid condensed DNA particles, the inclusion of PEG on these particles increased half-life to over 6 h.[126] Thus PEGylated transfection agents enjoy some of the same benefits as stealth liposomes discussed in Section 2.1.2 above. Unfortunately, PEGylation reduces transfection efficiency of both cationic polymer and cationic lipid based systems,[127,128] by interfering with internalization into cells and endosome escape.

For cationic lipid based systems, the incorporation of PEG stabilizes the lamellar liquid crystalline phase, hinders fusion with the endosomal membrane and prevents subsequent DNA release.[128] The incorporation of targeting ligands on the surface of these PEGylated particles can increase internalization into target cells.[129,130] Ko and coworkers successfully increased gene delivery to the brain in an in vivo mouse model with a transferrin receptor targeted antibody on a PEGylated liposome encapsulated polyplex.[130] In order to design transfection agents with high transfection efficiencies without sacrificing stability and delivery specificity, it is necessary to better understand their mode of action in vitro. Currently, transfection mechanism of targeted PEGylated systems and how it differs from those of conventional unmodified transfection agents is poorly understood. Investigations of the characteristics and transfection mechanisms of these agents produce discordant results and offer no consensus on the mode of their transfection. [3,22,23] Experiments indicate that the efficiency of transfection agents is cell line dependent, but reasons behind the differential activity are not clear.[131] The internalization pathway utilized by these transfection agents may be one factor that plays a significant role in regulating transfection efficiency.[24]

2.3.4 Internalization routes of transfection agents and transfection mechanism

Sayed and Harashima recently proposed a useful classification of the various internalization routes based on their lipid-raft content, and present a useful review of their properties.[24] Lipid rafts are defined as dynamic, 10-200nm diameter heterogeneous sphingolipid and sterol rich regions on the cell membrane that can compartmentalize cellular processes.[132] Endocytic pathways can be classified as non-lipid raft mediated (clathrin mediated), mixed lipid mediated (phagocytosis and macropinocytosis), and lipid-raft mediated (caveolae, flotillin, Arf6, GRAF-1 and Rho-A mediated).

2.3.4a Clathrin mediated endocytosis

Clathrin mediated endocytosis (CME) is the most widely investigated endosomal uptake route. A clathrin coat, which consists of clathrin triskelion proteins recruited from the cytosol, is a distinguishing character of these internalizing

vesicles. Vesicles that undergo CME can be 200 nm or more in diameter, which is compatible with the diameters of most gene delivery vehicles. Clathrin coated vesicles fuse with early endosomes, where the acidification process starts. As the early endosomes mature into late endosomes the pH continues to drop, eventually followed by fusion with the lysosomal degradation compartments. Cargo internalized by CME will therefore eventually be degraded unless it can escape the endosomal route somewhere along the endosome maturation process. Both cationic polymer and cationic lipid mediated DNA internalization has been shown to progress through this route in specific cell lines.[23,133] The polyplexes and lipoplexes presented in these studies, using the proton sponge effect and endosomal fusion respectively, were able to effectively escape the endosomal pathway. However, studies in other cell lines by Rejman et al.[134] and Ur Rehman et al.[25] demonstrated that CME is not productive for transfection. Generally, in order to investigate the role of a particular endocytic route in the internalization of cargo, chemical inhibitors known to specifically block the appropriate route are used. Chlorpromazine is one of the most widely used inhibitors of CME.[131,135] However, it should be carefully implemented as high concentrations have been shown to be toxic to cells by membrane permeabilization and reactive metabolite formation.[136,137]

2.3.4b Phagocytosis

Phagocytosis is involved in the uptake of large particles > 500 nm in diameter.[138] Therefore most transfection agents designed for in vivo tumor delivery being smaller than this is not expected to be taken up by phagocytosis at the target site, although professional phagocytes patrolling the blood circulation may still take them up. Phagosomes consist of mixed lipid domains and their formation is dynamin-2 dependent. Inhibitors of dynamin, such as dynasore,[139] have therefore been suggested to block macropinocytosis. Similar to vesicles internalized by CME, phagosomes fuse with endosomes and continue the maturation process to late endosomes and lysosomes where their cargo is degraded. Particle shape has been shown to have a significant effect on phagocytosis, and is extensively reviewed by Hillaireau and Couvreur.[140]

2.3.4c Macropinocytosis

Macropinocytosis, like phagocytosis, occurs in mixed lipid domains at the cell membrane. It can internalize large sections of the cell membrane, and therein lies the potential for large volumes of material to be taken up non-specifically. Unlike phagocytosis and CME, macropinocytosis is dynamin-2 independent and is associated with an increased uptake of the fluid phase and associated fluid phase markers.[141,142] The fate of macropinosomes is cell line dependent – they mature parallel to endosomes in macrophages, HEK293 cells and COS-1 cells, while they are recycled back to the cell surface in A531 human carcinoma cells and HEP-G2 cells.[24,133] Macropinocytosis has been suggested as an advantageous uptake route for lipoplexes by some studies, [26,143] while others regard it as an inefficient process that leads to minimal transfection.[133] Sarkar and coworkers reported rottlerin to be a potent and specific inhibitor of macropinocytosis.[144] While other commonly used inhibitors of macropinocytosis, such as amiloride and amiloride related compounds, affect pathways other than their intended target, rottlerin at concentrations between 2-3 μM inhibited more than 80% of macropinocytosis and less than 25% of receptor mediated endocytosis in monocyte derived dendritic cells.[144]

2.3.4d Caveolae/lipid raft mediated endocytosis

Out of the lipid raft mediated endocytic processes, caveolar uptake is the most widely studied. Caveolar uptake is distinguishable from all the other lipid raft mediated uptake pathways by the involvement of caveolin-1 protein. The fate of cargo taken up through caveolae-mediated endocytosis is also cell line dependent. [24] In non-endothelial cells caveolar cargo is directed to acidic organelles for degradation, while in endothelial cells in vivo cargo may traverse a cell via transcytosis. Filipin III has been used on numerous occasions to specifically inhibit caveolar uptake.[131,134] In contrast to some of the other inhibitors of caveolar/lipid-raft mediated uptake such as methyl-β-cyclodextrin, filipin III can distinguish between caveolar/lipid raft mediated uptake and the other internalization routes.[145] While filipin III has been primarily used as an inhibitor of caveolar uptake by many researchers, recent evidence suggests that it may also

have an inhibitory effect on some of the other lipid raft mediated uptake pathways. Consequently, in this thesis, we consider filipin III to mostly block the caveolar mediated uptake route, with some possible inhibitory effects on the other lipid-raft mediated routes. It is unclear whether caveolar uptake confers any advantages to gene expression mediated by transfection agents. Wong and coworkers have shown that lipoplexes internalized via this route are degraded in the endolysosomal compartments.[146] Also, studies with dendrimers and chitosan nanoparticles as transfection agents reported similar fate.[147–149] In contrast, Rejman et al.[134] and Ur Rehman et al.[25] attributed successful transfection to caveolar-mediated endocytosis. It is apparent that such controversial viewpoints regarding the fate of internalized cargo exist for most of the internalization pathways and transfection agents discussed here.

Some of the other lipid raft mediated uptake pathways include flotillin, Arf6, GRAF-1 and Rho-A mediated routes. These pathways involve several players in common with intertwined roles, as extensively reviewed by Doherty and McMahon.[150] One of the few discernible criteria they have in common with each other, as well as with caveolar uptake, is the involvement of cholesterol. Unfortunately, they do not have specific chemical inhibitors as yet and are therefore hard to differentiate.[24] For these reasons, these pathways have been broadly referred to as lipid-raft mediated pathways in this thesis.

Chapter 3. PR_b functionalized stealth liposomes for targeted delivery to metastatic colon cancer

3.1 Summary

A gene delivery system was designed to carry a payload to integrin overexpressing cells. Branched-polyethyleneimine (bPEI) condensed plasmid DNA was encapsulated into targeted stealth liposomes, thereby combining the condensing and transfection properties of bPEI with the stealth and targeting properties of the liposomal carrier system. PR_b was used as a targeting ligand - a peptide we designed to bind specifically to the cancer cell surface marker $\alpha_5\beta_1$ integrin - and such a robust receptor-ligand interaction achieved higher specificity than what has been previously reported for targeted delivery systems. In the process of formulating the PR_b functionalized gene delivery vehicle, we developed a protocol to fully encapsulate condensed DNA in liposomes and accurately quantify the total DNA in the system. We demonstrate that compared to non-targeted stealth liposomes and non-encapsulated condensed DNA, the PR_b functionalized stealth liposomes mediated improved in vitro transfection specifically to colon cancer cells overexpressing the $\alpha_5\beta_1$ integrin. Furthermore, when administered in vivo to metastatic tumor bearing mice, PR_b functionalized stealth liposomes outperformed non-targeted liposomes and delivered genes specifically to the tumor site.

3.2 Introduction

Advances in genetics have made gene therapy an increasingly plausible method of disease treatment, and the search for better and more efficient gene delivery techniques continues. Free plasmid DNA faces many challenges in gene therapy in vivo: it is rapidly degraded by enzymes in the blood,[151] it is limited by low levels of cellular uptake and subsequently poor intracellular release, leading to low

transfection efficiencies.[152] Gene delivery vehicles can overcome these issues by protecting the plasmid DNA through compaction and improving the transfection efficiency through the use of agents that increase cellular uptake and intracellular release.

Both viral and non-viral methods have been used for delivery of therapeutic genes,[153–158] the latter being advantageous due to reduced immunogenicity, lower toxicity and ease of manufacture.[5,6] Non-viral vectors for DNA delivery include preparations containing cationic polymers and lipids.[119,159] Out of these, polyethyleneimine (PEI) has been widely investigated and has shown much promise as a transfection agent.[160–162] PEI condenses DNA into small particles and allows efficient DNA release in target cells by the “proton sponge effect” (Section 2.3.2).[118,163,164] However transfection by PEI alone has been shown to be toxic to cells.[123,152] To overcome this problem, PEI has been modified in various ways to reduce its toxicity and improve transfection efficiency and biocompatibility through conjugation to stabilizing polymers or lipids,[165–168] modifications of PEI linkages,[169,170] and inclusion of a targeting moiety to improve specificity of delivery.[171–173] PEI-DNA complexes have also been encapsulated in liposomes, or associated with liposomes to form lipopolyplexes,[130,174–176] and such association has been shown to increase the transfection efficiency of PEI-condensed DNA systems.[177]

Encapsulating payloads in liposomes holds several advantages over conventional administration of free therapeutics. Liposomes with diameters of 100-200 nm can specifically accumulate in tumor tissue by a passive targeting mechanism involving the enhanced permeability and retention (EPR) effect.[7,54] In addition, the steric effect of a polyethyleneglycol (PEG) brush layer on stealth liposomes helps to avoid detection by the macrophage system (MPS) and prolongs circulation lifetime.[57,58] Briefly, liposomes in this size range are able to permeate through the larger membrane fenestrations in tumor blood vessels into the tumor tissue. Liposomes much larger may non specifically accumulate in the spleen by a filtration mechanism, or be trapped in capillaries in the lung, while smaller particles can non specifically permeate into other tissues or experience

ineffective steric hindrance leading to a reduced circulation lifetime.[54,178,179] In order to further increase the specificity of the delivery system, various targeting moieties can be incorporated into the basic carrier system. Targeted liposomes have been used in the delivery of payloads to various disease sites including tumors.[8,9,180,181] However, the benefits of targeting remain controversial. Although targeted liposomes reduce non-specific delivery compared to the free drug, there remains considerable room for improvement. When administered in vivo, targeted delivery vehicles often accumulate to significant levels in healthy tissues, potentially causing undesirable toxic side effects.[9,11–13]

Identification of an optimal receptor-ligand pair that allows the delivery vehicle to interact with diseased cells expressing high levels of the receptor, and not to healthy cells expressing the receptor at a lower concentration, can lead to improved specificities of therapeutic delivery. $\alpha_5\beta_1$ integrin is a promising target that has been shown to be overexpressed on both cancer cells as well as on cancer vasculature, and minimally expressed on normal healthy tissues,[14,15,182] and associated with cancer-progression properties.[14,183,184] In addition, $\alpha_5\beta_1$ is also expressed on certain primary cell lines, but its expression is downregulated during development.[16] RGD is a peptide that binds integrins including $\alpha_5\beta_1$ integrin and is probably one of the most widely studied ligands in targeted drug delivery. [8,9,11–13] However, RGD targeted delivery systems do not reduce accumulation in healthy organs when administered *in vivo*.[9,11–13] Hence there is the need to develop better targeting systems capable of achieving increased in vivo specificity. Our group has previously designed a targeting peptide PR_b based on fibronectin, the native binding ligand for $\alpha_5\beta_1$ integrin by combining the RGD binding site and the PHSRN synergy site. This combination of sites is specific for binding to $\alpha_5\beta_1$.[17,18] PR_b has outperformed both fibronectin and RGD in terms of binding cells expressing the $\alpha_5\beta_1$ integrin.[17] PR_b functionalized vehicles previously formulated in our group have shown increased in vitro delivery of model payloads when compared to non-targeted vehicles.[19–21,185,186] In this study, we investigate the potential of the PR_b targeted liposomal system as a new transfection agent in vitro, and for the first time test its functionality in vivo.

To date, there has been a minimal amount of work reported on encapsulating condensed plasmid DNA into a targeted liposome and verifying specificity of the delivery vehicle. This is most likely due to two factors. First is the difficulty of encapsulating a large, condensed plasmid DNA particle into the limited internal volume of a 100-200 nm liposome. Second, the proximity in size of unencapsulated particles and condensed DNA containing liposomes presents a challenge in their separation and the quantification of total DNA in the final preparation. This chapter presents a DNA encapsulated liposome formulation procedure that addresses each of these challenges.

In this study we encapsulated condensed DNA into PR_b functionalized stealth liposomes. We subsequently purified the system and quantified total DNA to formulate a vehicle that delivers the desired DNA load specifically to cells bearing the $\alpha_5\beta_1$ integrin. We have investigated the ability of cationic polymers poly-L-lysine (pLL) and branched polyethyleneimine (bPEI) to condense DNA into small particles that can be encapsulated into a 200 nm liposome. We also tested the in vitro DNA transfection efficiency of these condensing agents in both liposomal and non-liposomal forms. We used the most efficient condensing system, bPEI in our case, to optimize the concentration of the PR_b targeting moiety on targeted stealth liposomes. We demonstrate the superior performance by the PR_b functionalized gene delivery system when compared to non-targeted liposomes, or unencapsulated condensed DNA, in terms of transfection efficiency and targeting specificity in vitro and in a metastatic tumor model in vivo.

3.3. Materials and Methods

3.3.1 DNA condensation

20 μg of plasmid pT2/Cal,[187] which encodes the firefly luciferase transgene, under transcriptional control of a chimeric CAGS promoter (CMV enhancer/chicken beta-actin promoter/chicken beta-globin intron sequence) was used in this study. An endotoxin-free stock solution of this plasmid was diluted to 125 μl in distilled water. The amine to phosphate (N/P) ratio of the DNA:polymer mixture was calculated as shown previously.[188] Calculated volumes of the

condensing agent 22.5 kDa pLL (Sigma Aldrich, Saint Louis, MO) or 25 kDa branched PEI (Sigma Aldrich, Saint Louis, MO) to achieve a particular N/P ratio were also diluted to 125 μl in distilled water. The condensing agent was then added rapidly to the DNA solution followed by rapid pipetting to allow quick mixing. The system was then vortexed at the lowest speed for 5 minutes and then incubated at room temperature for 30 min. DNA particle size was measured by dynamic light scattering (DLS) (Brookhaven Instruments Corporation) and zeta potential determined using the PALS zeta potential analyzer (Brookhaven Instruments Corporation).

3.3.2 DNA liposome formulation and characterization

1,2-dipalmitoyl–sn-glycero-3-phosphocholine (DPPC), 1,2-dipa- lmitoyl-*sn*-glycero-3-phosphoethanolamine-N-[methoxy (poly- ethylene glycol)-2000] (ammonium salt) (DPPE-PEG2000) and cholesterol were purchased from Avantipolar Lipids, Inc (Alabaster, AL). Non-targeted stealth liposomes were made with 55 mol% DPPC, 35% cholesterol and 5% DPPE-PEG2000. Targeted stealth liposomes were made with (55-x) % DPPC, 35% cholesterol, 5% DPPE-PEG2000 and x% PR_b peptide amphiphile, where x was varied between 1.5 and 9. The PR_b peptide was purchased from University of Minnesota Genomics Center (UMGC), and the peptide amphiphile was made as described previously.[17,189] All liposomes were made using the thin film hydration method,[190] where the mixture of lipids was deposited on the bottom of a 50 ml round bottom flask and dried under a stream of argon followed by overnight incubation in a vacuum oven. The films were then hydrated with a solution of condensed DNA in DI water and incubated at 45-50 °C in a water bath for 2 h. The resulting liposomes were extruded through 200 or 400 nm polycarbonate membranes (Avestin, Ottawa, Canada) 11 times with a handheld Liposofast extruder (Avestin, Ottawa, Canada). Liposomes were then purified by a 24 h dialysis through a 1000 kDa cellulose ester dialysis membrane (Spectrum Labs, Rancho Dominiguez, CA). Lipid concentration was measured using a phosphorus assay as described elsewhere (reagents from Sigma Aldrich).[191] PR_b concentration on the liposomes was determined by the BCA assay (Thermo Scientific, Waltham,

MA) following the manufacturer's protocol. The PR_b concentration is expressed as a mole percentage of total lipid. pT2/Cal plasmid DNA was condensed using initially pLL at a N/P ratio of 4 and with bPEI at a N/P ratio of 8 (choices justified in section 3.4.1), and encapsulated in liposomes functionalized with approximately 5 mol% PR_b (actual concentrations are shown in the figure captions) or in non-targeted stealth liposomes. The ZetaPALS Zeta Potential Analyzer (Brookhaven Instruments, Holtsville, NY) was used to determine both the zeta potential, and diameter (by dynamic light scattering; DLS) of the stealth liposomes that encapsulated bPEI condensed DNA at N/P ratio of 8. To further characterize the size and shape of stealth liposomes encapsulating condensed DNA, cryogenic transmission electron microscope (cryo-TEM) images were taken. Briefly, 4 µL of liposome samples dissolved in water were deposited onto a lacey formvar/carbon copper grid (Ted Pella) treated for 15 s with glow discharge and vitrified in liquid ethane by Vitrobot (Vitrobot parameters: 5 s blot time, -1 offset, 3 s wait time, 3 s relax time, 95% humidity). Following vitrification, the grid was transferred to a Tecnai G2 Spirit TWIN 20-120 kV/LaB6 Transmission Electron Microscope. Images were captured using an Eagle 2k CCD camera with an accelerating voltage of 120kV.

3.3.3 DNA quantification

Plasmid DNA was labeled with cy5 fluorescent dye using the Label IT cy5 DNA labeling kit (Mirus, Madison, WI) according to the manufacturer's protocol. 5% of the plasmid DNA used in the DNA condensation process was cy5 labeled. At the post hydration stage of liposome preparation, a DNA concentration standard curve was generated, which was used to quantify the total DNA in the system after the final purification step.

3.3.4 In vitro transfection

DLD-1 human colon carcinoma cells (ATCC, Manassas, VA) were cultured in T75 flasks using Dulbecco-modified Eagle Medium (DMEM) supplemented with 10% fetal bovine serum and penicillin-streptomycin to 70% confluence and then subcultured into white 96 well plates at 5000 cells/well 24 h prior to transfection. All cell culture reagents were purchased from the Invitrogen Supply Center,

University of Minnesota. On the day of transfection medium was replenished and DNA liposomes (liposomes containing 100 ng of condensed DNA) were added to wells in replicates of six and incubated at 37 °C for 40 h. Luciferase expression was then measured with the Luciferase Reporeter assay kit (Promega, Madison, WI) following the manufacturer's protocol. Luminescence measured from untreated cells was used as the background, and that measured from 100 ng of unencapsulated DNA condensed with either pLL or bPEI under the same conditions was used as control.

3.3.5 Effect of PR_b concentration on transfection

Different PR_b concentrations were used to prepare PR_b functionalized PEGylated liposomal films. Each of these films was hydrated using DNA condensed with bPEI at an N/P ratio of 8. DNA liposomes were then prepared and characterized as described above. DLD-1 cells subcultured in a white 96 well plate were transfected using 100 ng of liposomal DNA, and luciferase activity was assayed as described above in the in vitro transfection section.

3.3.6 Specificity of targeting

DLD-1 cells were seeded in a white 96 well plate at 5000 cells/well and cultured overnight. Cells were provided with fresh medium the next day and the plate was placed at 4 °C for 30 min to equilibrate before the addition of 4 μg of the GRGDSP peptide (UMGC) to each well. Following 30 min incubation at 4 °C, bPEI-DNA polyplexes encapsulated in PR_b functionalized stealth liposomes were added to each well. The plate was incubated at 37 °C and 5% CO_2 for a total of 32 h with the addition of 4 μg/well GRGDSP peptide every 8 h to maintain a high concentration of free peptide for the purposes of blocking integrin binding. As positive controls, the same liposomes were used without GRGDSP blocking. All wells received 100 ng DNA, as quantified by the cy5 quantification assay described above. At the end of the incubation period, luciferase expression was assayed as described above. To demonstrate the binding specificity of the PR_b peptide, a scrambled PR_b sequence (ScrPR_b, SGRSGSGSHGGDSGSS-KSSPNPR), was obtained from the UMGC, and used as an alternate targeting ligand on liposomes. DLD-1 cells plated at 5000 cells/well in a white 96 well plate

were transfected with PR_b or ScrPR_b functionalized stealth liposomes. In parallel, DLD-1 cells were first blocked with 16 μg/well free PRb peptide followed by transfection with either the PR_b or ScrPR_b targeted liposomes for 32 h at 37 ^{o}C in the presence of free PR_b added every 8 h. All wells received 100 ng of DNA encapsulated in liposomes as quantified by the cy5 quantification assay. At the end of this incubation period, luciferase expression was measured as described above.

3.3.7 Toxicity of encapsulated or free bPEI-DNA

DLD-1 cells were seeded overnight in a clear 96 well plate at 5000 cells/well. After a medium change the next morning, cells were treated with 100 ng/well bPEI-DNA encapsulated in PR_b functionalized stealth liposomes. For comparison, unencapsulated bPEI-DNA was delivered at 100 ng/well. Untreated cells were used as the control and medium alone was used as the background. After 40 h of incubation at 37 ^{o}C, 10 μl WST-1 reagent (Clontech, Mountain View, CA) was added to each well and incubated after a gentle shake at 37 ^{o}C for a further 2 h. Following incubation, the absorbance of the plate was read at 450 nm using a Spectramax Plus spectrophotometer (Molecular Devices, Sunnyvale, CA). Cell viability is reported as the sample absorbance signals as a percentage of the signals from the untreated cells.

3.3.8 Establishment of hepatic tumors

Female Balb/c mice were obtained from NIH (Frederick, MD) and maintained under specific pathogen-free conditions. All animals were treated according to the NIH Guidelines for Animal Care with approval of the IACUC of the University of Minnesota. Exponentially growing murine CT26 colon carcinoma cells (ATCC, Manassas, VA) were trypsinized, resuspended in Hanks balanced salt solution (HBSS), and 1 x 10^5 viable cells in a volume of 150 μl were injected intrasplenically into 4-6 week mice. Animals were administered an anesthetization cocktail consisting of ketamine HCl (8 mg/ml; Phoenix Scientific, St. Joseph, MO), acepromazine maleate (0.1 mg/ml; Phoenix Scientific), and butorphanol tartrate (0.01 mg/ml; Fort Dodge Animal Health, Overland Park, KS). A peritoneal incision was made, and cells were directly injected into the spleens

of recipient animals. Pressure was applied to the injection site for 3 min, and the animals were splenectomized. Cells injected into the spleen in this manner flow from the splenic vein into the portal vein and seed into the liver, thus confining tumor formation to the liver. The incision site was closed with staples, and the animals were allowed to recover.

3.3.9 In vivo liposomal gene delivery and luciferase imaging

Animals were injected with liposomal formulations at 2 weeks post-tumor injection, with tumor growth determined by measuring the abdominal girth of the animal. The three groups investigated were: tumor-bearing mice that received non-targeted stealth liposomes, tumor-bearing mice that received PR_b functionalized stealth liposomes, and healthy, non-tumor-bearing mice that received PR_b functionalized stealth liposomes. Four animals per group were injected intravenously via the lateral tail vein with liposomal formulations containing 700 ng of pT2/Cal plasmid DNA in a total volume of 0.5 ml. 24 h after liposomal injections, expression of luciferase was visualized by in vivo bioluminescence imaging using the Xenogen IVIS Imaging Sytem (Xenogen, Alameda, CA). Mice were anaesthetized using the cocktail described above, followed by an intraperitoneal injection of 100 μl luciferin (Promega) and the whole mouse was imaged for bioluminescence 5 min later. Mice were sacrificed, livers extracted, and imaged ex vivo in 100 μl PBS containing 100 μl luciferin. Luciferase expression is reported as photons emitted per second per cm^2.

3.4 Results and Discussion

3.4.1 Sizing and zeta potential of condensed DNA particles

Dynamic light scattering data of condensed DNA particle sizes formed at different amine to phosphate (N/P) ratios is presented in Fig. 11. The goal of these experiments was to identify the optimal N to P ratio to form small condensed

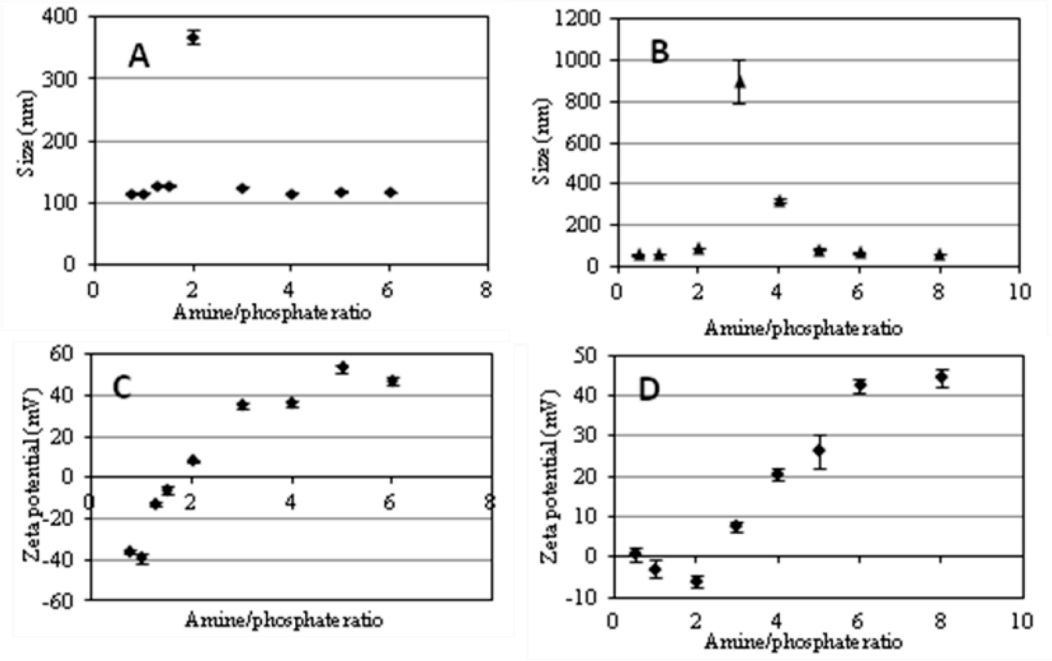

Figure 11. Characterization of polymer condensed DNA.
DLS size measurement of pLL (A) and bPEI (B) condensed DNA particles at different amine to phosphate ratios. Corresponding zeta potential charge measurements for pLL (C) and bPEI (D) condensed DNA particles. Values represent the mean ± SD (n =3).

DNA particles that can be efficiently encapsulated into a 200 nm liposome, and have a net positive charge for better transfection. pLL condensed DNA particles were approximately 100 nm for all the N/P ratios tested, except around 2, where large visible aggregates were formed resulting in the increased particle size (Fig. 11A). As others have suggested before,[192] this aggregation happens at N/P ratios that result in nearly charge neutral particles which experience no repulsion as they come together. This is verified by the zeta potential data presented in Fig. 11C where the net charge of the particles increases from negative to positive as the ratio of the positive polymer is increased and is seen to go through zero around an N/P ratio of 2. Similarly, for the bPEI condensed DNA particles, this aggregation effect was seen around an N /P ratio of 3, with particles sizes less than 100nm for other ratios away from this aggregation zone (Fig. 11B). The zeta potential of the particles at these same N/P ratios show similar trends to the pLL condensed DNA system, with a net neutral zone occurring around a ratio of 3 (Fig. 11D). Overall the bPEI particles were seen to be smaller than the pLL

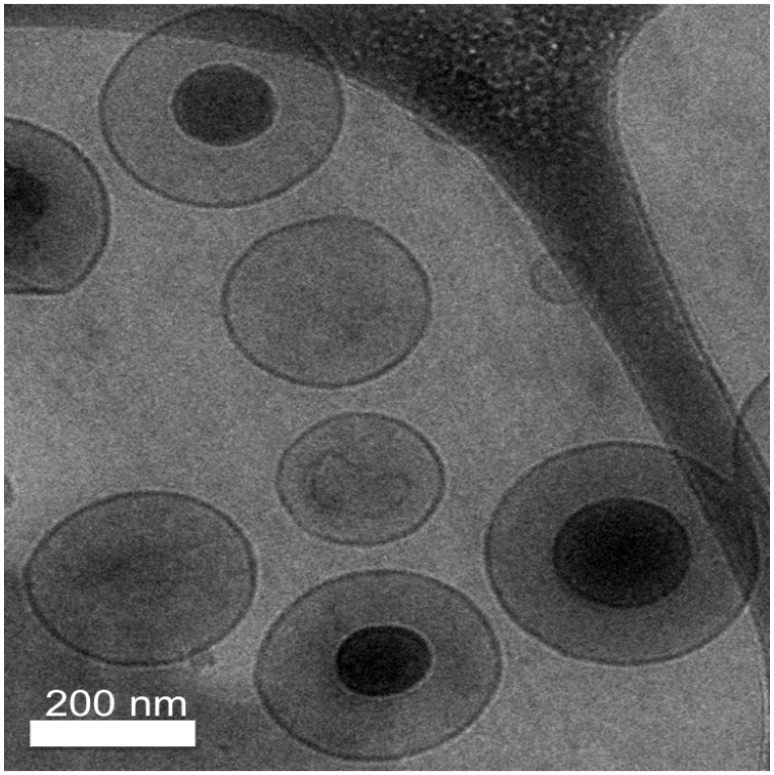

Figure 12. Cryo-TEM image of PR_b functionalized stealth liposomes encapsulating bPEI condensed DNA

condensed particles at N/P ratios away from the aggregation ratio. In order to obtain small positively charged particles to be encapsulated in liposomes, we chose an N/P ratio of 4 for the pLL condensed DNA and a ratio of 8 for the bPEI condensed DNA system.

3.4.2 Characterization of targeted and non-targeted stealth liposomes encapsulating condensed DNA

Unlike many previous gene delivery systems where polyplexes are complexed with anionic liposomes, we have encapsulated polyplexes into liposomes composed of neutral lipids. In this process, there is no active interaction between the polyplexes and the liposomes. Polyplexes in the aqueous phase are passively encapsulated into liposomes by a thin film lipid hydration process. 20 μmol lipid films were hydrated with 20 μg of cationic polymer-condensed DNA. After the purification step, where unencapsulated condensed DNA is removed,

an average concentration of about 5 μg/ml DNA, corresponding to a 40% concentration-based yield, is obtained in the final DNA-liposome formulation.

Three characteristic stealth liposomes each for PR_b functionalized and non-targeted formulations, containing bPEI condensed DNA at N/P 8 were analyzed. Measured sizes were 204 ± 6 nm with zeta potential of -15.3 ± 0.6 mV for the non-targeted stealth liposomes. The size of the PR_b functionalized stealth liposomes was 279 ± 51 nm and the zeta potential was -3.1 ± 1.8 mV. Although the bPEI-DNA complexes are positively charged, once encapsulated in stealth liposomes the system as a whole is close to neutral or slightly negative. The lipid bilayer and the PEG layer effectively shield the charge of the encapsulated DNA particles. In addition, cryo-TEM images of PR_b functionalized stealth liposomes encapsulating bPEI condensed DNA were taken and shown in Fig. 12. These images confirm the presence of approximately 100 nm sized condensed DNA particles within spherical stealth liposomes sized around 250 nm, correlating with the sizes measured using DLS.

3.4.3 Transfection efficiency of liposomes encapsulating pLL and bPEI condensed DNA

For both pLL and bPEI condensed DNA, the PR_b functionalized stealth liposomes mediated better transfection than the non- targeted liposomes (Fig. 13). However, when the targeted formulations are compared, the bPEI condensed system performed over an order of magnitude better in terms of transfection efficiency than the pLL condensed system. These results are consistent with previous studies reported in the literature showing that bPEI condensed DNA performs better than the pLL counterpart in different gene delivery systems.[161–163,193] Unencapsulated DNA particles condensed with either pLL or bPEI were both ineffective at transfecting DLD-1 cells to any appreciable extent under the same conditions. At the same time non-targeted stealth liposomes encapsulating the same amount of DNA failed to give a noticeable level of transfection. These results demonstrate the stealth properties of these non- targeted liposomes, as the PEG brush layer is preventing these liposomes from interacting with and delivering their payload to cells.

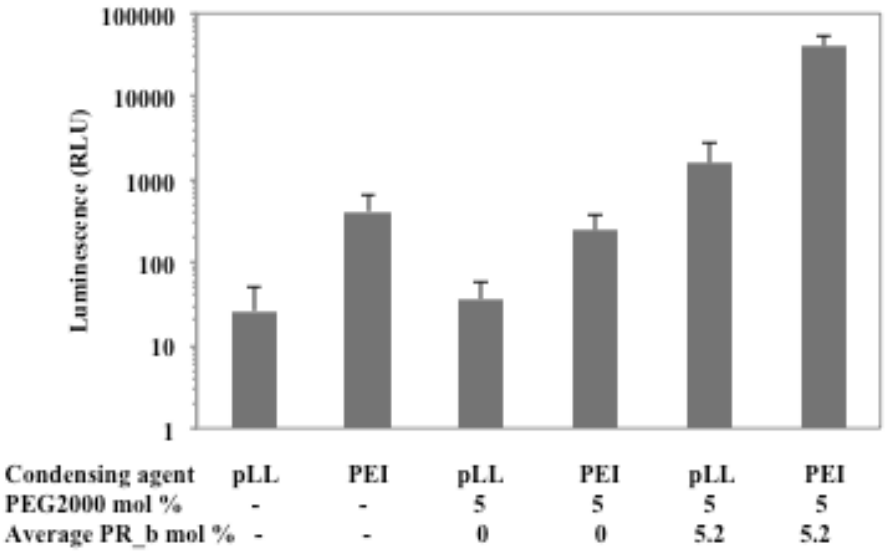

Figure 13. Transfection efficiency of liposome encapsulated and unencapsulated DNA condensed with bPEI or pLL
100 ng of DNA was delivered in different formulations to DLD-1 cells and incubated for 40 h at 37 ºC, after which luminescence was measured. The values represent mean ± standard error of two separate experiments (n=2), each done in replicates of six.

As our results show, transfection is successful when the PR_b targeting peptide is included on the stealth liposomes.

3.4.4 Effect of PR_b concentration on transfection

Having demonstrated the necessity of the PR_b peptide on our gene delivery vehicle, the PR_b concentration was optimized on stealth liposomes. As the concentration of the ligand is increased, an increase in the expression of luciferase in DLD-1 cells was observed (Fig. 14). At an average concentration of 1.5 mol% PR_b the transfection level of the targeted liposomes was only slightly higher than the non-targeted system. However at an average of 3 mol% a substantial difference was observed between transfection levels of non-targeted and targeted liposomes.

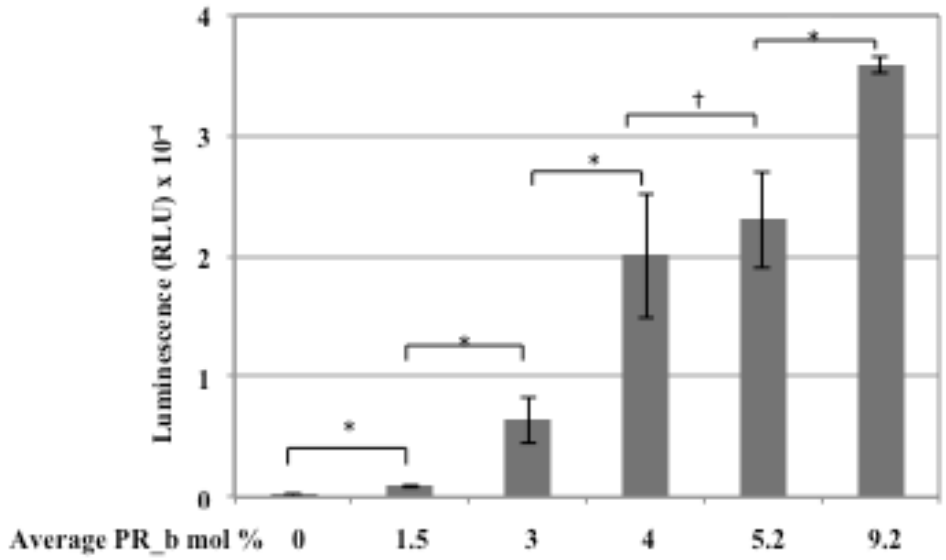

Figure 14. Effect of PR_b concentration on transfection efficiency.
100 ng of bPEI condensed DNA encapsulated in different stealth liposome formulations was delivered to DLD-1 cells and incubated for 40 h at 37 ºC, followed by luminescence measurement. The values represent mean ± standard error of three separate liposomal experiments (n =3), each done in replicates of six. Students t-test statistical analysis was performed and the statistical significance notated for the bracketed data. * indicates $p<0.005$; † indicates $p>0.5$ and no statistical significance.

Average concentrations of 4 and 5 mol% PR_b showed similar levels of transfection with no statistical difference between them, and both substantially higher than non-targeted liposomes. This increasing trend was maintained up to about 9 mol% PR_b, the highest concentration that we investigated. A similar trend with the PR_b concentration was seen in a previous study by our group delivering liposomes encapsulating a fluorescent dye to colorectal cancer cells,[19] where conventional liposomes functionalized with PR_b between 0.7 and 3.5 mol% and PEGylated liposomes with PR_b between 1.1 and 2.6 mol% were tested. One hypothesis that can explain the effect of ligand concentration is the requirement of a certain minimum number of receptor-ligand interactions for the delivery vehicle to remain at the cell surface long enough to be internalized through a receptor mediated pathway. This requirement further adds to the specificity of the delivery vehicle. Healthy tissues, which may have a lower number of integrin receptors, may not achieve the required number of integrin-

ligand interactions and therefore may not be transfected. Although the highest levels of transfection were obtained with 9 mol% PR_b, sufficiently high transfection levels were also observed at 4 and 5 mol % PR_b. Thus, for subsequent in vitro and in vivo work, liposomes were prepared with an average of 4 or 5 mol% PR_b concentration. We did not examine peptide concentrations higher than 9 mol%, as previous work in our group demonstrated that Langmuir-Blodgett bilayers of peptide amphiphiles mixed with PEGylated lipids remained well-mixed at molar concentrations less than 10 mol% and higher than 35 mol%, while between 10 and 35 mol% the peptide amphiphiles phase separated.[194]

3.4.5 Demonstrating specificity of targeting

The GRGDSP peptide is a known binding ligand for integrins, including the $\alpha_5\beta_1$ integrin. Blocking the integrin sites with an excess of free GRGDSP peptide would theoretically prevent the PR_b peptide from binding and thus hinder transfection. A 1000-fold excess of GRGDSP over the number of PR_b ligands on liposomes was used in these experiments, an average of 4 μg peptide per well in a 96 well plate. Additional GRGDSP was added every 8 h to maintain an excess of blocking peptide, as this schedule proved to be more effective at blocking integrin binding compared to a large initial dose. Fig. 15A shows that PR_b liposomes transfected unblocked cells at a level over an order of magnitude higher than the blocked liposomes. This experiment demonstrates the necessity of the integrin-PR_b interaction for successful transfection using the PR_b functionalized liposomal gene delivery vehicle. The results of these experiments are in agreement with our previously reported work where blocking experiments with peptides and antibodies demonstrated that PR_b is a specific ligand for the $\alpha_5\beta_1$ integrin,[19,186] with a dissociation constant of 76.3 ± 6.3 nM.[195] To further investigate the specificity of the PR_b sequence for $\alpha_5\beta_1$ integrin, a scrambled PR_b sequence (ScrPR_b) was designed as a negative control.

Fig.15B shows that in DLD-1 cells bPEI-DNA encapsulated in ScrPR_b functionalized stealth liposomes mediated minimal luciferase

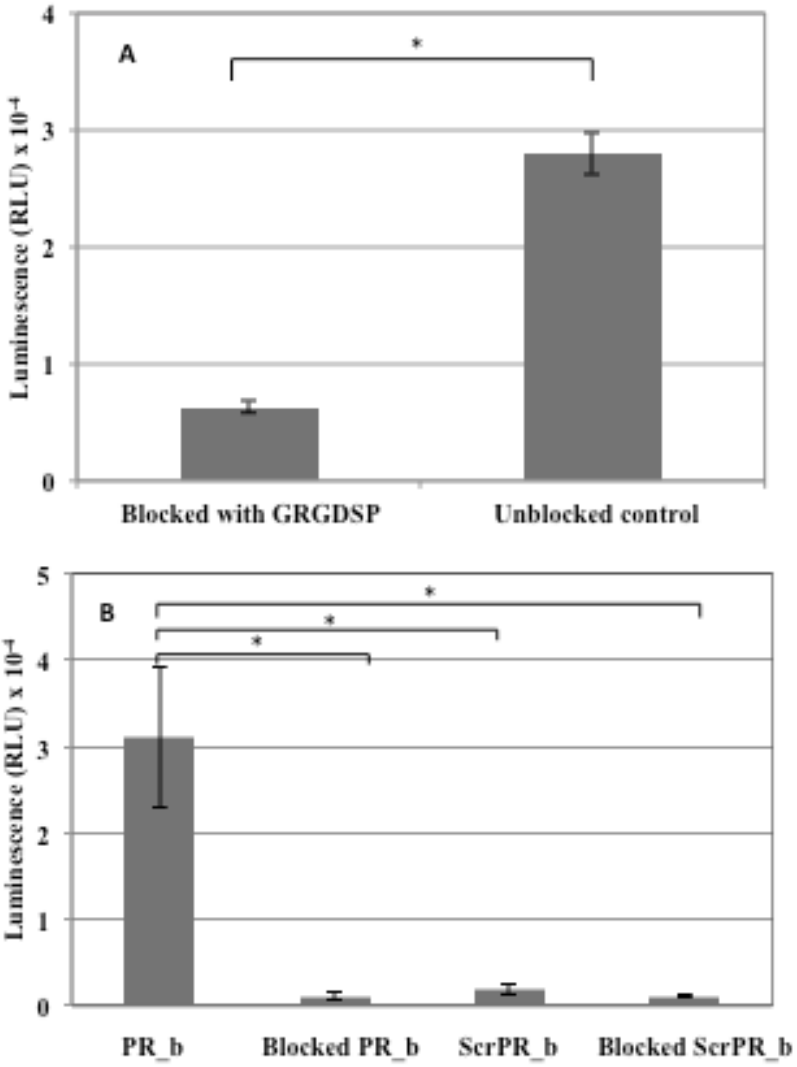

Figure 15. Demonstrating specificity of gene delivery
A) Delivery of bPEI condensed DNA encapsulated in PR_b functionalized PEGylated liposomes to either unblocked DLD-1 cells or DLD-1 cells with their surface integrins blocked by GRGDSP peptides free in solution. Cells were incubated with 100 ng of DNA loaded stealth liposomes functionalized with 5 mol% PEG2000 and 5.3, 4 and 4 mol % PR_b (for the three liposomal formulations tested) for 40 h at 37 ºC after which the luminescence was quantified. B) Delivery of bPEI condensed DNA encapsulated in PR_b functionalized or Scrambled PR_b functionalized PEGylated liposomes to either unblocked DLD-1 cells or DLD-1 cells with their surface integrins blocked by PR_b peptides free in solution. Cells were incubated with 100 ng of DNA loaded stealth liposomes functionalized with 5 mol% PEG2000 and 4.8, 6.1 and 5.9 mol% PR_b or 6.4, 5.4 and 5.9 mol% ScrPR_b for 40 h at 37 ^{0}C after which the luminescence was quantified. The values represent mean ± standard error of three separate liposomal experiments (n =3), each done in replicates of six. Students t-test statistical analysis was performed and the statistical significance notated for the bracketed data. * indicates $p<0.001$.

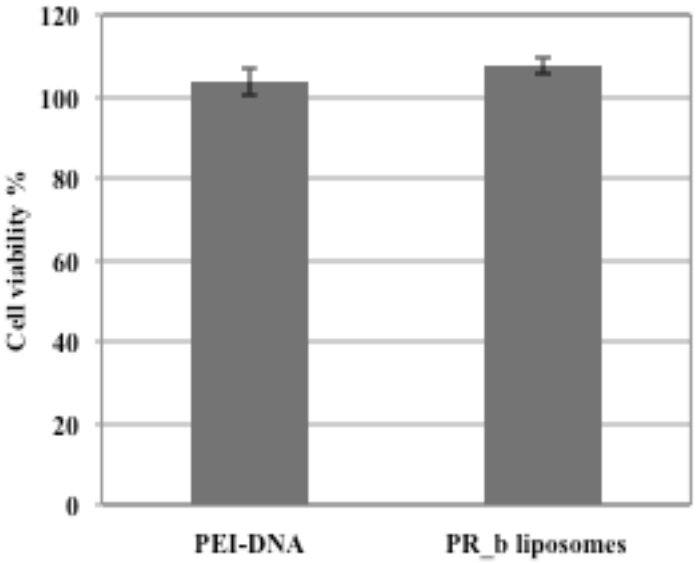

Figure 16. Effect of transfection agents on cell viability.
100% cell viability is representative of untreated cells. DLD-1 cells were treated with PR_b (3.9, 4.1 and 6.1 mol%) functionalized stealth liposomes (5 mol% PEG2000) encapsulating bPEI-DNA or free bPEI-DNA followed by WST-1 treatment and absorbance measurement. The values represent mean ± standard error of three separate liposomal experiments (n =3), each done in replicates of six.

expression when compared to PR_b functionalized stealth liposomes. Furthermore, blocking with the free PR_b peptide inhibited the interaction of PR_b functionalized liposomes with DLD-1 cells almost completely. These results, taken together with the GRGDSP-blocking experiments shown in Fig. 15A, demonstrate the need for a specific integrin-PR_b interaction for efficient transfection.

3.4.6 Cytotoxicity of transfection agents

Transfection subjects cells to high stress levels that scale with the amount of genetic material being introduced into the cells.[123] However, at the concentrations of DNA used in our experiments the PR_b targeted system is able to increase transfection efficiency without adversely affecting cell viability (Fig. 16). Previous studies have shown that the electrostatic method of intracellular DNA uptake maybe detrimental to cell viability.[125] For bPEI, the stronger the electrostatic attraction between the delivery vehicle and the cells, the higher the transfection level at the expense of cell viability. The non-electrostatic uptake of

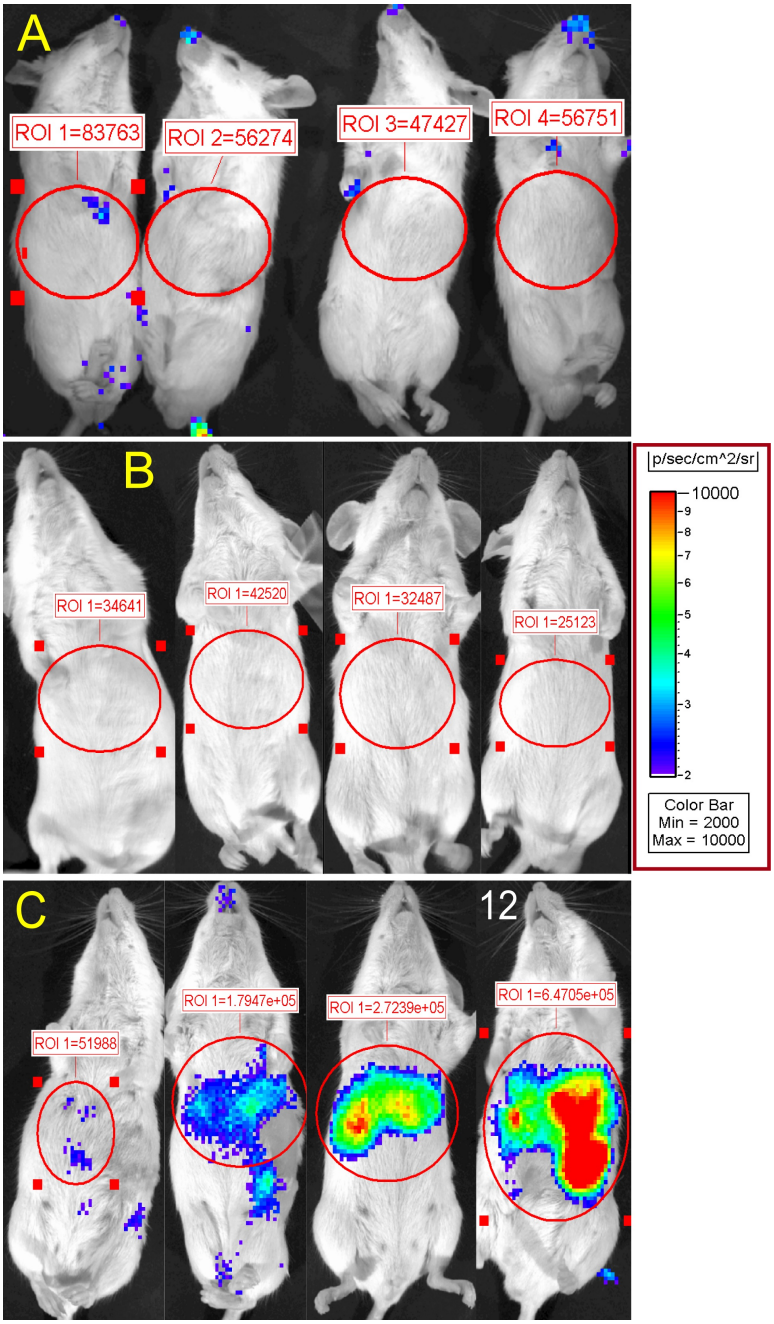

Figure 17. Bioluminescence from luciferase expression after in vivo administration 700 ng of bPEI-condensed DNA encapsulated in different stealth liposome formulations were injected into mice via tail vein. 24 h after liposome injection expression of luciferase was visualized by bioluminescence imaging. Total relative optical intensity (ROI) is shown for each image as measured in photons/second/cm^2 by the Xenogen IVIS Imaging System A) Non-targeted stealth liposomes, with 5 mol% PEG2000, delivered to CT26 tumor bearing mice. B) 3.3 mol% PR_b functionalized stealth liposomes (5 mol% PEG2000) delivered to healthy mice. C) 3.3 mol% PR_b and 5 mol% PEG2000 targeted stealth liposomes delivered to CT26 tumor bearing mice.

PR_b functionalized liposomes could be a reason for high cell viability concurrent with high transfection.

3.4.7 In vivo gene delivery

Non-targeted stealth liposomes injected into tumor-bearing mice (Fig. 17A) and PR_b functionalized stealth liposomes injected into healthy mice (Fig. 17B) showed minimal to no bioluminescent signal after one day. Considering that non-specific delivery to healthy organs continues to be a drawback for in vivo delivery vehicles,[196] the lack of luciferase expression in the healthy mice may indicate minimum levels of gene delivery to healthy tissues using the PR_b functionalized stealth liposomes. When these liposomes were administered to tumor-bearing mice, luciferase expression was seen preferentially in the region of the tumor, i.e., the liver (Fig. 17C). This metastatic tumor model has been designed to localize the tumor in the liver, and Fig. 18 (A, B) is an ex vivo image of the dissected abdomen from mouse 12 in Fig. 17C, clearly showing the presence of luciferase expressing tumor localized in the liver.

Our preliminary results are in contrast to previous studies targeting the integrins in vivo in which significant non-specific uptake in the liver was reported.[9,11,13,197] Ex vivo images of the liver are shown in Fig. 18C, and a closer inspection shows bioluminescence in the liver tissue originating from the tumor nodules, and minimal signal from the surrounding healthy liver tissue (Fig. 18D). The essence of targeted therapy is in the specificity of delivery - in the ability to differentiate between healthy organs and the diseased site. Figs. 17 and 18 show that PR_b functionalized stealth liposomes may have the potential to differentiate not only between healthy organs and tumor bearing organs, but also between tumor tissue and healthy tissue within the same organ. Our preliminary in vivo studies show that the PR_b functionalized stealth liposome warrants further investigation as an in vivo delivery vehicle for therapeutic payloads.

In addition, most in vivo studies report administration of anywhere from 5 to 50 μg of DNA per mouse.[156,187,198,199] A high dose combined with poor specificity can

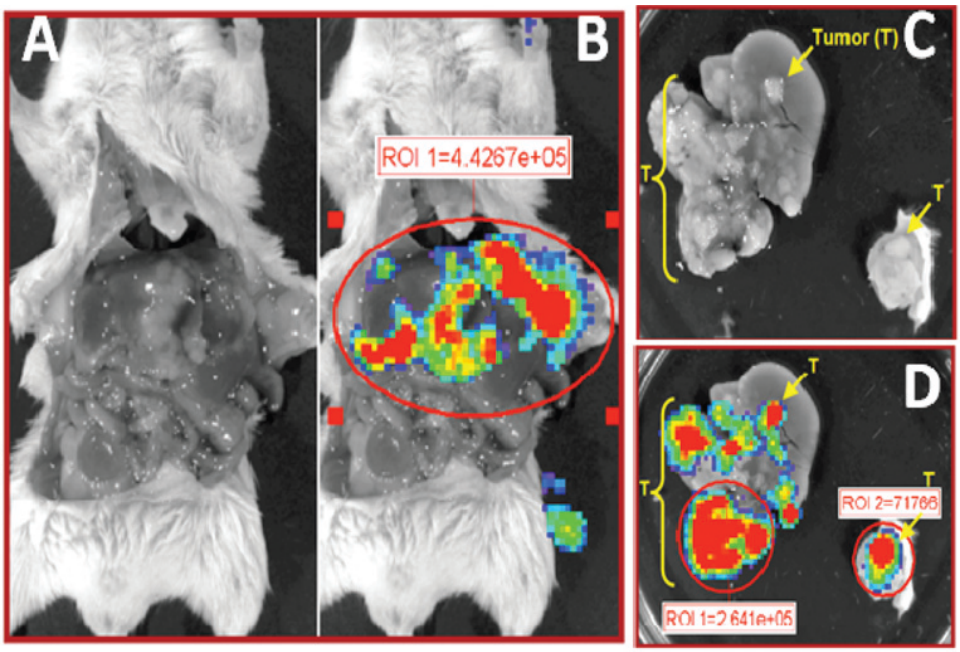

Figure 18. Ex vivo bioluminescence from luciferase expression
Images taken from abdominal dissection of mouse 12 shown in Fig. 17 after experimental endpoint. Total relative optical intensity (ROI) as measured in photons/second/cm^2 by the Xenogen IVIS Imaging Sytem is shown for each image. Lateral dissection showing tumor load on liver (A) with superimposed bioluminescence (B). Excised liver showing white tumor nodules (C) with superimposed bioluminescence (D).

result in significant undesirable accumulation of therapeutics in healthy tissues. In this paper we have demonstrated the in vitro specificity of the PR_b functionalized liposome, and shown in our in vivo work that we can potentially achieve gene expression specifically in the target site with less than 1 μg DNA injected per mouse. However, whether this expression level is enough to achieve a therapeutic effect still needs to be investigated.

3.5 Conclusion

We have designed and developed a gene delivery vehicle that encapsulates bPEI condensed DNA in PR_b functionalized stealth liposomes. The PR_b targeted vehicle is biocompatible, non-toxic, stable to aggregation, and specifically targets cells overexpressing $\alpha_5\beta_1$ integrin with the potential to differentiate between healthy and diseased tissue within the same organ. Many diseased cells including cancers often overexpress $\alpha_5\beta_1$ integrin, making the

PR_b functionalized stealth liposome a potentially effective therapeutic delivery agent that may specifically reach the diseased site while sparing healthy tissues.

Chapter 4. Transfection mechanisms of polyplexes, lipoplexes and stealth liposomes in $\alpha_5\beta_1$ integrin bearing DLD-1 colorectal cancer cells

4.1 Summary

Receptor targeted, PEGylated transfection agents can improve stability and delivery specificity of current cationic lipid and polymer based non-viral gene delivery vehicles, but their mode of transfection is poorly understood. We therefore investigated the transfection mechanisms of 1,2-dioleoyl-3-trimethylammonium-propane (DOTAP)/1,2-dioleoyl-*sn*-glycero-3-phosphoethanolamine (DOPE) lipoplexes, branched polyethylenimine (bPEI) polyplexes, and bPEI encapsulated in either PEGylated (stealth) non-targeted liposomes or PR_b peptide (targeted to $\alpha_5\beta_1$ integrin) functionalized stealth liposomes in DLD-1 colorectal cancer cells *in vitro* with gene expression assays, flow cytometry and confocal microscopy. DOTAP/DOPE and PR_b functionalized stealth liposomes mediated higher gene expression compared to non-targeted stealth liposomes and bPEI. However DOTAP/DOPE was internalized slowly leading to lower levels of DNA uptake. In contrast, despite high internalization of bPEI polyplexes, gene expression levels were low as DNA was unable to escape from the endosomes. Non-targeted stealth liposomes also mediated low gene expression due to low amounts of DNA internalized and slow internalization kinetics. PR_b functionalized stealth liposomes struck an optimal balance amongst these transfection agents with efficient transfection arising from fast integrin mediated internalization kinetics, high amounts of DNA uptake and endosomal escape. We found $\alpha_5\beta_1$ integrin to be a valuable target for gene delivery, and that the caveolar endocytic pathway may offer an advantage to receptor targeted PEGylated transfection agents in DLD-1 cells.

4.2 Introduction

Gene delivery vectors face many challenges when administered *in vivo*.[3,200] These include survival in blood circulation when systemically administered, recognition of and uptake into target cells, and successful endosomal escape and nuclear localization. Delivery vectors need to navigate past each of these barriers before successful gene expression. Current gene delivery vectors can be broadly classified as viral or non-viral vectors.[3,4] Although non-viral agents often have lower transfection efficiencies than viral vectors, they are safer, less immunogenic, more tunable and easier to build.[5,6] These advantages make non-viral vectors an attractive medium for gene delivery and much progress has been made in their development.[3] However, many of the current non-viral transfection agents that mediate gene expression *in vitro* are still ineffective *in vivo*.[30] For example, commonly used transfection agents based solely on cationic polymers like bPEI[117,118] and cationic lipid mixtures like DOTAP/DOPE[119] are unstable (prone to aggregation) under *in vivo* conditions and often toxic to healthy cells.[123,124] Surface modification with a polyethylene glycol (PEG) layer may be used to increase stability and lower non-specific toxicity, but it often reduces transfection efficiency by reducing internalization into cells and hampering endosomal release.[127,128] To increase transfection mediated by PEGylated systems, targeting moieties can be included on the nanoparticles to encourage specific receptor mediated uptake.[129,196] However, although incorporation of targeting ligands may be able to increase cell internalization, it does not necessarily mediate the same level of transfection as the non-PEGylated, non-targeted delivery systems.[201] In order to design transfection agents with high transfection efficiencies without sacrificing stability and delivery specificity, it is necessary to better understand their mode of action *in vitro*.

Currently, the transfection mechanism of targeted PEGylated systems and how it differs from those of conventional cationic polymer or lipid based transfection agents is poorly understood. Researchers investigating transfection mechanisms of these agents often disagree and provide no consensus on the mode of their transfection.[3,22,23] It is apparent that different transfection agents are effective in

different cell lines, but reasons behind the differential activity are not clear. One of the factors that may play an important role in determining transfection efficiency is the internalization pathway utilized by these transfection agents.[24] Clathrin mediated endocytosis, caveolar mediated endocytosis and macropinocytosis are major pathways that have been implicated so far in the cellular uptake of transfection agents; however, it is not clear if certain pathways are more effective than others.[23,25,26] More work is therefore needed to characterize these non-viral nanoparticles used for gene delivery.

In this study, the transfection mechanisms of several different transfection agents were investigated, with a focus on understanding targeted PEGylated systems compared to commonly used polyplexes and lipoplexes. Specifically, we studied how DOTAP/DOPE based lipoplexes, bPEI based polyplexes, stealth liposomes encapsulating bPEI condensed DNA and PR_b peptide functionalized stealth liposomes encapsulating bPEI condensed DNA[202] transfect DLD-1 human colorectal cancer cells. PR_b functionalized stealth liposomes is a transfection agent developed in our group, and was shown to have efficient transfection properties *in vitro* and *in vivo.*[202] The targeting ligand PR_b (with amino acid sequence KSSPHSRNSGSGSGSGSGRGDSP) is a fibronectin mimetic peptide designed to specifically bind to $\alpha_5\beta_1$ integrin with a binding affinity of 76.3 ± 6.3 nM [17,195] and has been successfully used to functionalize nanoparticles for a variety of targeted delivery applications.[20,21,185,203,204] PR_b functionalized nanoparticles were shown to outperform nanoparticles functionalized with other RGD based sequences at delivering payloads to $\alpha_5\beta_1$ integrin receptor bearing cells, and could also differentiate between cells that expressed different levels of the $\alpha_5\beta_1$ integrin receptor.[186] $\alpha_5\beta_1$ integrin is a well-known cancer marker that is overexpressed in cancer tissue and cancer vasculature[14,15] thereby making it a good target for cancer-specific gene delivery. Previous experiments showed that PR_b functionalized stealth liposomes targeted to $\alpha_5\beta_1$ integrin bearing cells can outperform non-targeted stealth liposomes as well as bPEI polyplexes.[202] One of our goals here is to identify reasons behind differences in transfection mediated by different agents. In addition, we also aim to investigate barriers to gene

expression faced by these different transfection agents and suggest potential design parameters to overcome them.

Flow cytometry and confocal microscopy were used to identify the transfection mechanisms of DOTAP/DOPE lipoplexes, bPEI polyplexes, stealth liposomes and PR_b functionalized stealth liposomes. Carefully selected chemical inhibitors for clathrin mediated endocytosis, caveolar mediated endocytosis and macropinocytosis, previously shown to successfully inhibit their respective routes,[27,28] were used to identify the major internalization routes preferred by each of the transfection agents. At the end, a combination of observations from the transfection and DNA uptake levels, internalization rate kinetics, intracellular colocalization and inhibition of endocytosis aided in understanding the mode of transfection of the different agents investigated. DOTAP/DOPE and PR_b functionalized stealth liposomes proved to be most efficient at gene expression. Non-targeted stealth liposomes suffered from poor uptake and slow internalization kinetics. Contrary to some previous studies,[117,118] bPEI failed to transfect due to its inability to escape acidic intracellular organelles. Our results implicate a combination of a caveolar and macropinocytosis mediated endocytic pathways as the uptake routes that may lead to successful gene expression following transfection of DLD-1 cells by targeting the $\alpha_5\beta_1$ integrin with PR_b peptide functionalized delivery nanoparticles. Overall, PR_b functionalized stealth liposomes, with high DNA uptake, fast integrin-mediated internalization and endosomal escape, demonstrated efficient gene expression in DLD-1 cells.

4.3 Materials and Methods

4.3.1 Formulation and characterization of transfection agents

25 kDa branched polyethylenimine (bPEI) (Sigma Aldrich, St Louis, MO) dissolved in distilled water was added to a solution of plasmid DNA in 10 mM Tris-HCl buffer for an amine to phosphate ratio (N/P) of 8. This ratio was deemed to be in the optimal charge ratio range as discussed previously, resulting in particles 63.5±0.6 nm in diameter and a zeta potential of 44.3±2.18 mV.[202] The mixture was rapidly pipetted, followed by vortexing at the slowest speed setting

for 5 min. The condensed DNA was then incubated at room temperature for 30 min before use.

1,2-dioleoyl-3-trimethylammonium-propane (DOTAP) and 1,2-dioleoyl-*sn*-glycero-3-phosphoethanolamine (DOPE) lipids (Avanti Polar Lipids Inc, Alabaster, AL) were mixed together at an equivalent molar ratio, and made into 100 nm liposomes using a thin film lipid water hydration process[190] followed by extrusion through 100 nm polycarbonate membranes in a Liposofast hand held extruder (Avestin, Ontario, CA). N/P ratios for lipid-DNA mixtures were calculated as previously described.[188] The DOTAP/DOPE liposomes were added to a plasmid DNA solution in 10 mM Tris-HCl and rapidly mixed by pipetting followed by vortexing at the slowest speed for 5 min. DNA was condensed at different N/P ratios to obtain particles that best matched the bPEI condensed DNA particles for charge (Fig. 19), and N/P of 6 proved optimal. The DOTAP/DOPE condensed DNA particles were incubated at room temperature for 30 min before use.

Lipids used in the formation of liposomes, 1,2-dipalmitoyl-sn-glycero-3-phosphocholine (DPPC), 1,2-dipalmitoyl-sn-glycero-3 phosphoethanolamine-N-[methoxy(polyethylene glycol)-2000] (ammonium salt) (DPPE-PEG2000) and cholesterol, were purchased from Avanti Polar Lipids, Inc (Alabaster, AL). The PR_b peptide (KSSPHSRNSGSGSGSGSGRGDSP) was purchased from the University of Minnesota Genomics Center (UMGC) and formed into an amphiphile by attaching a dialkyl C_{16} lipid tail to the amine-terminus of the peptide headgroup as previously described.[17] PR_b functionalized stealth liposomes and non-targeted stealth liposomes were made using a thin film lipid hydration method, which was previously shown to be the best liposome formulation method for the encapsulation of condensed DNA.[205] Briefly, a mixture of lipids containing x mol % PR_b peptide-amphiphiles, 5 mol % DPPE-PEG2000, (60-x) mol % DPPC and 35 mol % cholesterol were deposited in a 50 ml round bottom flask and dried under a stream of argon (x = 0 for non-targeted stealth liposomes and 5 for PR_b functionalized stealth liposomes). Plasmid DNA was labeled with Label IT cy5 fluorescent probe (Mirus, Madison, WI) according to the manufacturer's instructions. bPEI condensed DNA (including 5% or 25% cy5

labeled DNA) at an N/P ratio of 8 was then used to hydrate the lipid film for 2 h in a water bath held at 45 ^{o}C. Following this incubation, the hydrated liposomes were extruded through 400 nm polycarbonate membranes in a hand held Liposofast extruder (Avestin, Ontario, Canada) to obtain non-targeted stealth liposomes of 204 ± 6 nm and PR_b functionalized stealth liposomes 279 ± 51 nm in diameter. Liposomes were then dialyzed against water for 24 h in a 1000 kDa MWCO dialysis membrane (Spectrum labs, Rancho Dominguez, CA) with frequent water changes.

For all transfection agents, particle sizes and zeta potentials were measured with dynamic light scattering (DLS) on the ZetaPALS zeta potential analyzer (Brookhaven instruments, Holtsville, NY). For PR_b functionalized stealth liposomes, the lipid content was measured using a phosphorus assay[191] (reagents purchased from Sigma Aldrich). The PR_b peptide concentration was measured using a bicinchoninic acid (BCA) protein assay (Thermo Scientific, Waltham, MA) according to the manufacturer's instructions, and reported as a mol % of total lipids. The DNA concentration in the liposomes were measured using a cy5 fluorescence standard as described previously.[202,205]

4.3.2 Luciferase DNA transfection and luminescence measurement

DLD-1 human colorectal cancer cells (ATCC, Manassas, VA), grown to 70-80% confluence in T-75 flasks in Dulbecco's Modified Eagle Medium (DMEM) (Invitrogen supply center, University of Minnesota) supplemented with 10% fetal bovine serum and 10% of a 10,000 units/ml penicillin – 10 mg/ml streptomycin solution (Sigma Aldrich, St Louis, MO), were subcultured into white 96 well plates at 5,000 cells/well in 100 μl of medium. Medium was replenished the next day and 100 ng of 5% cy5 labeled pT2/Cal[187] DNA (a Firefly luciferase expression plasmid, gift from Prof. McIvor, University of Minnesota) were delivered per well with the different transfection agents. The transfection agents were incubated with the cells for 48 h at 37 °C and 5% CO_2. The non-targeted stealth and PR_b functionalized stealth liposomes used here contained 5% cy5 labeled condensed DNA for quantification of DNA encapsulation. Following incubation, cells were washed once with 200 μl phosphate buffered saline (PBS) and the Luciferase

reporter assay kit (Promega, Madison, WI) used according to the manufacturer's protocol. A luminescence plate reader (Biotek, Winooski, VT) was used to measure luminescence resulting from luciferase expression.

4.3.3 Evaluation of transfection efficiency with flow cytometry

DLD-1 cells were subcultured in clear 12 well plates at 100,000 cells/well in 1 ml of medium. Medium was replenished the next day and 1 μg of 5% cy5 labeled pmaxGFP plasmid DNA (gift from Prof. Hu, University of Minnesota) was delivered per well with the different transfection agents for 24 h at 37 °C and 5% CO_2. Non-targeted stealth liposomes and PR_b functionalized stealth liposomes used here contained 5 % cy5 labeled DNA. Cells were washed once with 1 ml PBS, medium was replenished and incubation continued for 24 h more. Cells were then harvested with TrypleE Express cell dissociation reagent (Invitrogen supply center, University of Minnesota), pelleted by centrifugation at 250 g for 5 min, resuspended in PBS and analyzed on a FACSCalibur flow cytometer (Masonic cancer center, University of Minnesota). Transfection efficiency is reported as the percentage of cells expressing GFP compared to the untransfected cells (% positive difference reported by the FCS express software).

4.3.4 Evaluation of DNA uptake and internalization kinetics with flow cytometry

DLD-1 cells were subcultured in clear 12 well plates at 100,000 cells/well in 1 ml of medium. Medium was replenished the next day and 1 μg of 25% cy5 labeled pT2/Cal DNA was delivered per well with the different transfection agents for 24 h at 37 °C and 5% CO_2. Cells were washed once with 1 ml cold PBS and harvested with TrypleE Express cell dissociation agent (Invitrogen supply center, University of Minnesota), pelleted by centrifugation at 250 g for 5 min. In order to remove any DNA still attached to the cell surface, cells were treated with 100 µl Trypsin and 0.5 ml of 0.5 mg/ml heparin sulfate solution (Sigma Aldrich, St Louis, MO) for 5 min. Following another PBS wash and recentrifugation, cells were resuspended in 1 ml cold PBS and analyzed using a FACSCalibur flow cytometer (Masonic cancer center, University of Minnesota). DNA uptake efficiency is reported as the percentage of cells with internalized DNA compared to untransfected cells (%

positive difference reported by the FCS express software). To measure internalization kinetics similar techniques were followed, but transfection agents were allowed to incubate with cells for a range of different times: 0.5, 1, 2, 6, 12 and 24 h.

4.3.5 Confocal microscopy

DLD-1 cells were subcultured on 20 mm fibronectin coated cover slips (Neuvitro, El Monte, CA) in a clear 12 well plate at 100,000 cells/well in 1 ml of medium. The following day, the fibronectin coverslips were transferred to a new well with fresh medium, and BacMam 2.0 Cell light early endosome GFP label (Life technologies, Grand Island, NY) added to the cells at 15 μl/well along with 5 mM sodium butyrate (Sigma Aldrich, St Louis, MO). 24 h later, 25% cy5 labeled DNA was transfected into cells using different transfection agents and incubated for 24 h at 37 °C and 5% CO_2. The wells were washed the following day with 1ml PBS and incubation continued for a further 24 h. 2 h before experimental endpoint, 15 μl of a 20 μM solution of Lysotracker Red DND-99 (Life technologies, Grand Island, NY) was added to cells in 1ml of medium for a final concentration of 300 nM. Cells were then washed in PBS and fixed by treating with freshly made 4 (w/v) % paraformaldehyde (Sigma Aldrich, St Louis, MO). Nuclei were labeled by adding 1 µl of Hoescht 33432 (Life Technologies, Grand Island, NY) in 1ml of PBS and incubating for 10 min at 37 °C and 5% CO_2. Fibronectin coverslips were then washed with PBS and mounted with Prolong gold antifade reagent (Invitrogen, University of Minnesota) on microscope slides and visualized with an Olympus upright confocal microscope (University imaging center, University of Minnesota). .

4.3.6 Cell viability after treatment with endocytic inhibitors

DLD-1 cells were subcultured in a clear 96 well plate at 5000 cells/well in 100 µl of medium. Medium was replenished the next day, and cells were treated with 5 µg/ml filipin III, 10 µg/ml chlorpromazine or 2 µM rottlerin at 37 °C and 5% CO_2. All inhibitors were purchased from Sigma Aldrich (St Louis, MO). 30 min later, 10 µl WST-1 reagent (Promega, Madison, WI) was added per well, and cell viability

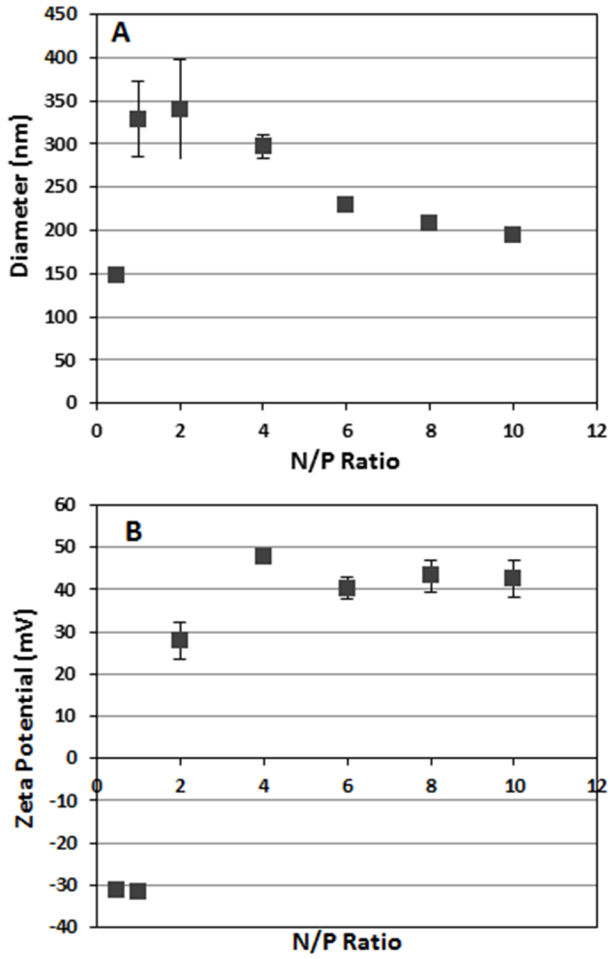

Figure 19. Characterization of DOTAP/DOPE condensed DNA.
A) Dynamic light scattering size measurement and B) corresponding zeta potential measurements for condensed pT2/Cal DNA particles at different amine (N) to phosphate (P) ratios. Data are presented as the mean ± standard error of three independent experiments (n=3), done in triplicate.

measured according to the manufacturer's protocol after a further 1h incubation at 37 °C and 5% CO_2.

4.3.7 Inhibition of endocytosis

DLD-1 cells were subcultured in a clear 6 well plate at 250,000 cells/well in 1ml of medium. Medium was replenished the next day and cells were incubated with 5 µg/ml filipin III, 10 µg/ml chlorpromazine or 2 µM rottlerin for 30 min at 37 °C and 5 % CO_2. All inhibitors were purchased from Sigma Aldrich (St Louis, MO). The concentrations of inhibitors used here are similar to levels previously shown to be effective (Section 2.3.4), and was verified for minimal cytotoxicity. Cells were

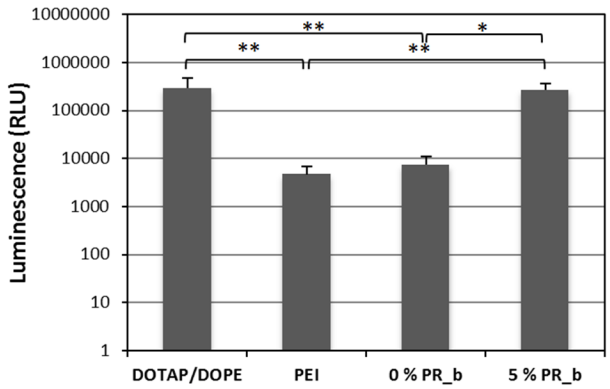

Figure 20. Comparison of luminescence from luciferase expression following transfection with different transfection agents.
DLD-1 cells were transfected with 100 ng of pT2/Cal plasmid DNA delivered using DOTAP/DOPE, bPEI, non-targeted stealth liposomes (0% PR_b) or 5 mol% PR_b functionalized stealth liposomes for 48 h followed by luminescence measurement. Data are presented as mean ± standard error of four independent experiments (n=4) done in triplicate. Student's t-test statistical analysis was performed, * indicates $p<0.01$ and ** $p<0.005$. If no symbol is displayed there is no statistical significance for that pair.

then incubated with 1 µg 25% cy5 labeled DNA/well delivered using different transfection agents for 1 h more under the same conditions. Cells were washed once with 1ml PBS and subsequent preparation and analyses were carried out using FACScalibur flow cytometer (Masonic cancer center, University of Minnesota) as described earlier for measuring DNA uptake (Section 4.3.4).

4.4 Results

4.4.1 Luciferase transfection in DLD-1 cells

We first investigated the ability of DOTAP/DOPE, bPEI, non-targeted stealth liposomes or PR_b functionalized stealth liposomes to transfect DLD-1 human colorectal cancer cells with a luciferase expressing plasmid pT2/Cal (Fig. 20).[187] Results show that PR_b functionalized stealth liposomes outperformed non-targeted stealth liposomes, demonstrating the need of the PR_b ligand for successful transfection using stealth liposomes. Also, PR_b functionalized stealth liposomes performed as well as DOTAP/DOPE lipoplexes in transfecting DLD-1 cells. DOTAP/DOPE, given its structural and functional similarity to Lipofectamine, 2,3-dioleyloxy-N-[2-(sperminecarboxamido)ethyl]-N,N-dimethyl-1-propanaminium/1,2-dioleoyl-sn-glycero-3-phosphoethanolamine

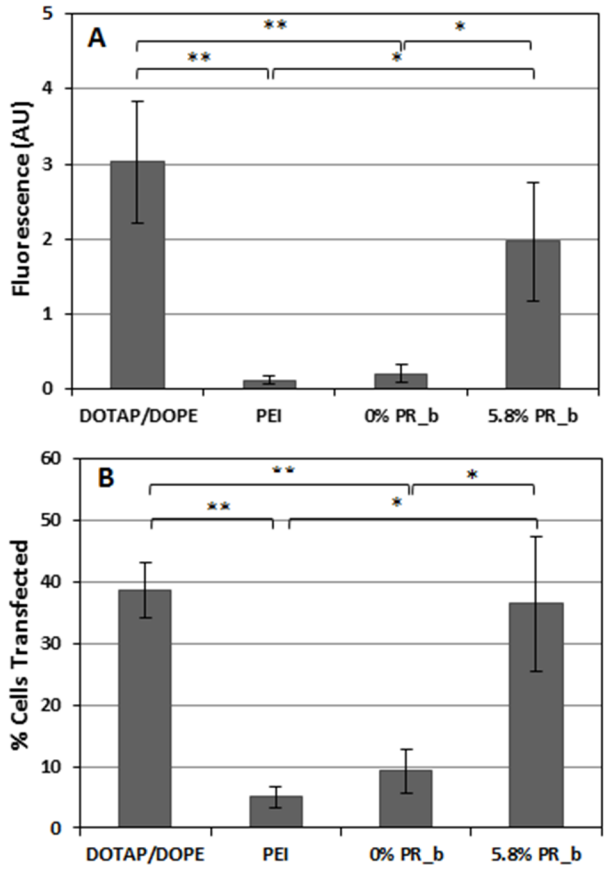

Figure 21. A) GFP expression levels and B) transfection efficiency following transfection with different agents.
DLD-1 colorectal cancer cells were transfected with 1 µg pmaxGFP DNA using DOTAP/DOPE, bPEI, non-targeted stealth liposomes (0% PR_b) or 5.8 mol% PR_b functionalized stealth liposomes for 24 h at 37 °C and 5% CO_2. GFP expression was quantified with flow cytometry after a further 24 h incubation. Transfection efficiency is reported as the percentage of cells expressing GFP compared to untransfected cells. Data are presented as mean ± standard error from four independent experiments (n=4) done in triplicate. Student's t-test was performed and bracketed data are statistically significant where * indicates $p<0.05$ and ** $p<0.01$.

(DOSPA/DOPE), is one of the gold standards of *in vitro* non-viral transfection agents. Therefore, these results show that PR_b functionalized stealth liposomes possess efficient transfection properties. Fig. 20 also demonstrates that DOTAP/DOPE mediates better transfection than bPEI. This is not surprising, as there are several instances where cationic lipid based transfection agents have been shown to outperform cationic polymer based system.[23,206] These results demonstrated the improvement in transfection of the bPEI after incorporating the bPEI polyplexes in a targeted delivery system such as the PR_b functionalized

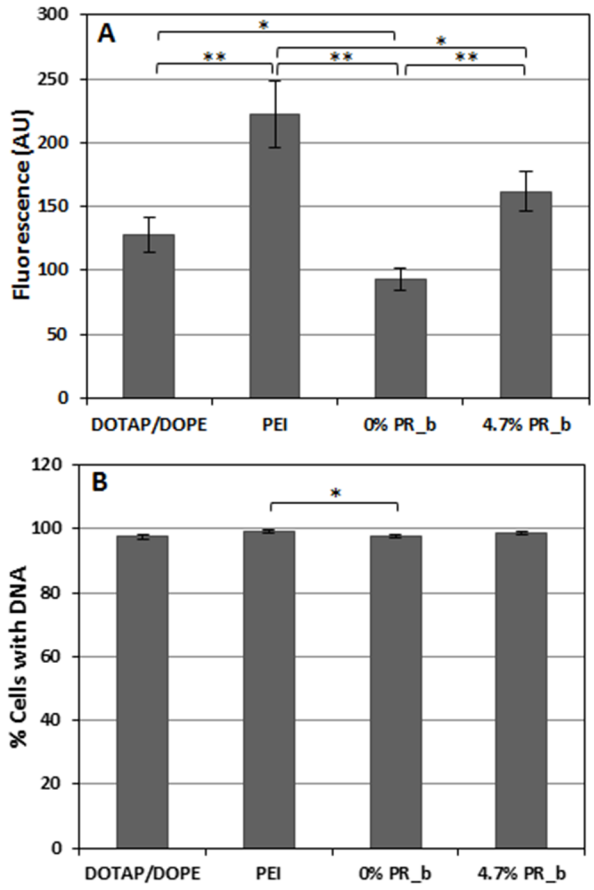

Figure 22. A) DNA internalization and B) percentage of cells with internalized DNA after transfection with different agents
DLD-1 colorectal cancer cells were transfected with 1 µg of 25% cy5 labeled pT2/Cal DNA using DOTAP/DOPE, bPEI, non-targeted stealth liposomes (0% PR_b) or 4.7 mol% PR_b functionalized stealth liposomes for 24 h at 37 °C and 5% CO_2. Cells were washed and the amount of DNA internalized was quantified using flow cytometry. Percentage of cells with internalized DNA is reported relative to untransfected cells. Data are presented as mean ± standard error from four independent experiments (n=4) done in triplicate. Student's t-test was performed and bracketed data are statistically significant where * indicates $p<0.05$ and ** $p<0.01$.

stealth liposomes. Next, we investigated the potential reasons behind the differences in gene expression mediated by these agents.

4.4.2 Flow cytometric analysis of transfection and DNA uptake

Flow cytometry was used to further investigate the transfection mechanisms of DOTAP/DOPE, bPEI, non-targeted stealth liposomes and PR_b functionalized stealth liposomes and to help understand the trends reported in Fig. 20. A green

	TFL	TFE	UPL	UPE	TFL/TFE	UPL/UPE	TFL/UPL
DOTAP/DOPE	3.03	38.6	128.0	97.5	0.0785	1.31	0.0237
PEI	0.12	5.1	222.7	99.1	0.0236	2.25	0.0005
Stealth liposomes	0.20	9.3	161.8	97.5	0.0216	1.66	0.0012
PR_b stealth liposomes	1.96	36.4	92.7	98.7	0.0539	0.94	0.0212

Table 1 Summary and further analysis of data from Fig. 21 and Fig. 22.
Abbreviations used - TFL : Transfection level (Figure 2A); TFE : Transfection efficiency (Figure 2B); UPL : Uptake level (Figure 3A); UPE : Uptake efficiency (Figure 3B).TFL/TFE represents amount of protein expressed per cell; UPL/UPE represents amount of DNA internalized per cell; TFL/UPL represents amount of protein expression per amount of DNA internalized.

fluorescent protein (GFP) expression plasmid, pmaxGFP, was used to transfect DLD-1 cells and GFP fluorescence was measured using flow cytometry (Fig. 21). Fig. 21A shows similar trends to the luciferase expression experiment, with DOTAP/DOPE and PR_b functionalized stealth liposomes both outperforming bPEI and non-targeted stealth liposomes. In addition, under these experimental conditions, PR_b functionalized stealth liposomes and DOTAP/DOPE transfected on average 36.4% and 38.6% of DLD-1 cells respectively, while bPEI and non-targeted stealth liposomes trailed behind transfecting 5% and 9% of DLD-1 cells (Fig. 21B).

To investigate whether the difference in transfection arose from a difference in DNA uptake, flow cytometry was used to measure cy5-labeled DNA uptake in DLD-1 cells after transfection with DOTAP/DOPE, bPEI, non-targeted stealth liposomes or PR_b functionalized stealth liposomes. Surprisingly, Fig. 22A shows that bPEI mediated better DNA uptake than any of the other transfection agents. Also, under these experimental conditions, all the transfection agents were able to internalize into most of the cells (Fig. 22B). Table 1 summarizes data from Figs. 21 and 22. Ratios of the different parameters measured were taken to represent various physical phenomena. For example, the level of transfection (Fig. 21A) divided by transfection efficiency (Fig. 21B) (TFL/TFE) represents total amount of protein produced per cell transfected. DOTAP/DOPE produced the highest amount of protein per cell, closely followed by PR_b functionalized liposomes, while bPEI and non-targeted stealth liposomes mediated protein production that was barely detectable. Given the similar DNA uptake efficiencies

(Fig. 22B) of the different agents, bPEI resulted in the highest amount of DNA uptake per cell that had internalized DNA (results from Fig. 22A/Fig. 22B: UPL/UPE). Although DOTAP/DOPE mediated lower DNA internalization (Fig. 22A), its high level of transfection (Fig. 21A) resulted in the highest ratio of protein produced to DNA uptake (TFL/UPL). PR_b functionalized stealth liposomes had a TFL/UPL ratio (protein produced per DNA uptake) similar to that of DOTAP/DOPE and 42 fold that of bPEI. Clearly, the differences in transfection levels are not because of differences in DNA uptake. We hypothesize that they may instead arise due to differences in the intracellular fate of these transfection agents.

4.4.3 Visualization of intracellular fate with confocal microscopy

To understand the intracellular fate of the transfection agents, cy5 labeled DNA (shown in red) delivered using DOTAP/DOPE, bPEI, non-targeted stealth liposomes or PR_b functionalized stealth liposomes was visualized using confocal microscopy in cells with Hoescht stained nuclei (shown in gray), GFP stained early endosomes (shown in blue) and lysotracker red labeled late endosomes or lysosomes (shown in green) (Fig. 23). The images were taken at 48 h after transfection, equivalent to when protein expression was measured in Figs. 20 and 21. For bPEI (Figs. 23C and 23D), the majority of the DNA (red) is seen in the late endosomes or lysosomes (green) as indicated by the yellow bodies. Thus, in DLD-1 cells, bPEI is not able to escape the endosomal pathway. This may explain why despite resulting in a large amount of internalized DNA (Fig. 22A) bPEI cannot mediate protein expression (Figs. 20 and 21A).

In contrast, there is a large amount of free DNA (red) for cells transfected with DOTAP/DOPE (Figs. 23A and 23B). There are several instances where free DNA is seen in the cytoplasm and in the nucleus (Fig. 23B) and some of the free DNA also appears in ensembles, a phenomenon absent for all the other transfection agents tested. The presence of the free DNA shows that DOTAP/DOPE is able to successfully escape the endosomal pathway, which explains the higher transfection seen (Figs. 20 and 21A). Therefore, the endosomal escape of DNA

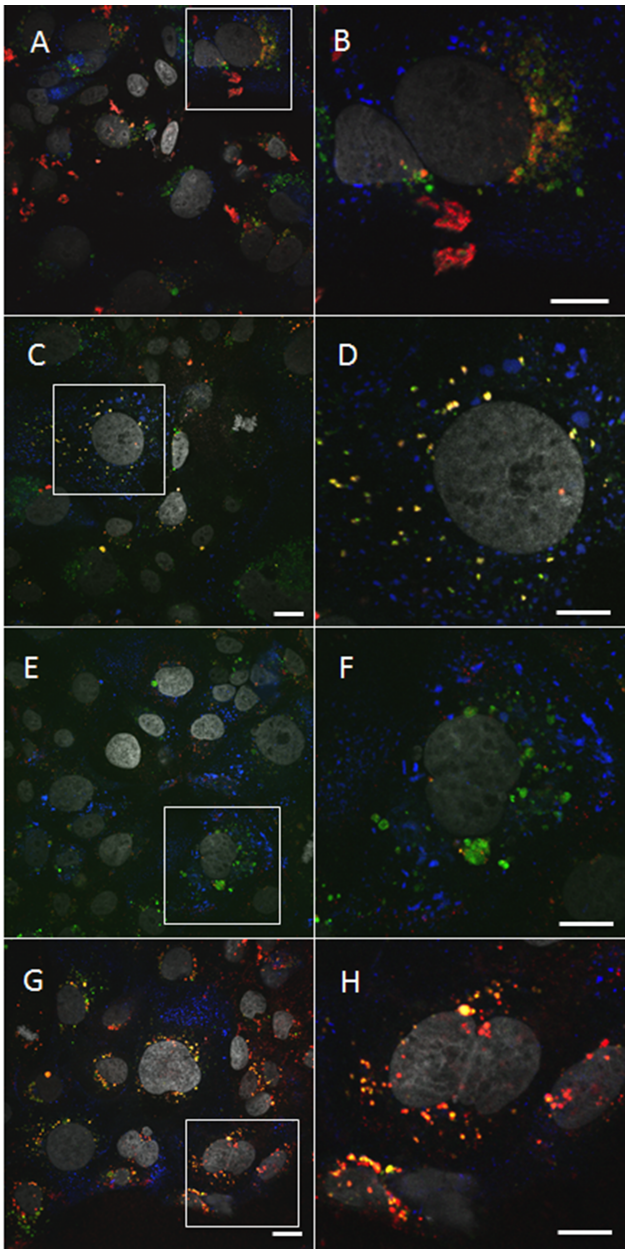

Figure 23. Intracellular distribution of internalized DNA after transfection with different agents.
DLD-1 human colorectal cancer cells were transfected with 1 µg of 25% cy5 labeled pT2/Cal DNA delivered using (A, B) DOTAP/DOPE, (C, D) bPEI, (E, F) non-targeted stealth liposomes or (G, H) 4.7 mol% PR_b functionalized stealth liposomes for 24 h at 37 °C and 5% CO_2. Following a further 24 h incubation, cells were imaged using confocal microscopy. Cy5 DNA is shown in red. Early endosomes (blue) were labeled with Cell light early endosomes-GFP, acidic organelles (green) were labeled with the Lysotracker Red and nuclei (gray) were labeled with Hoescht dye (color was removed to aid in interpretation). The specific combination of colors was chosen to aid in visual recognition of colocalization. Images shown here are representative of three independent

experiments (n=3) with panels B, D, F and H at original magnification and A, C, E, G zoomed out. Scale bar is 20 μm.

generated by DOTAP/DOPE through the hexagonal phase transition of its constituent lipids[121] appears to be quite effective in DLD-1 cells.

A small amount of the DNA delivered with non-targeted stealth liposomes was internalized, and much of it still remained relatively far from the nucleus once internalized (Figs. 23E and 23F). This indicates that the internalization or subsequent trafficking, or a combination of both, of the stealth liposomes may be a slower process compared to the other transfection agents. Also, DNA delivered with the non-targeted stealth liposomes appeared as punctuate dots much smaller than those associated with the other transfection agents. This may possibly be due to overall less DNA being internalized with stealth liposomes.

PR_b functionalized liposomes resulted in a higher amount of free red DNA seen inside the cell, and even in the nucleus in certain cases (Figs. 23G and 23H) compared to bPEI (Figs. 23C and 23D). These observations support the successful transfection that is mediated by PR_b functionalized stealth liposomes compared to bPEI. Taken together, the fact that PR_b functionalized stealth liposomes that encapsulate bPEI condensed DNA can successfully transfect DLD-1 cells, and that DNA can be visualized outside acidic compartments and in the nucleus, point to a favorable internalization route taken by these liposomes that allowed DNA to escape endosomes and enter the nucleus. However, much of the DNA internalized still appears sequestered in acidic organelles, which may mean that only part of the liposomes is internalized in a route favorable for transfection.

4.4.4 Internalization kinetics

Amount of DNA internalized into DLD-1 cells was measured over time after transfection with various transfection agents (Fig. 24). At all time points, bPEI and PR_b functionalized stealth liposomes mediated higher DNA internalization

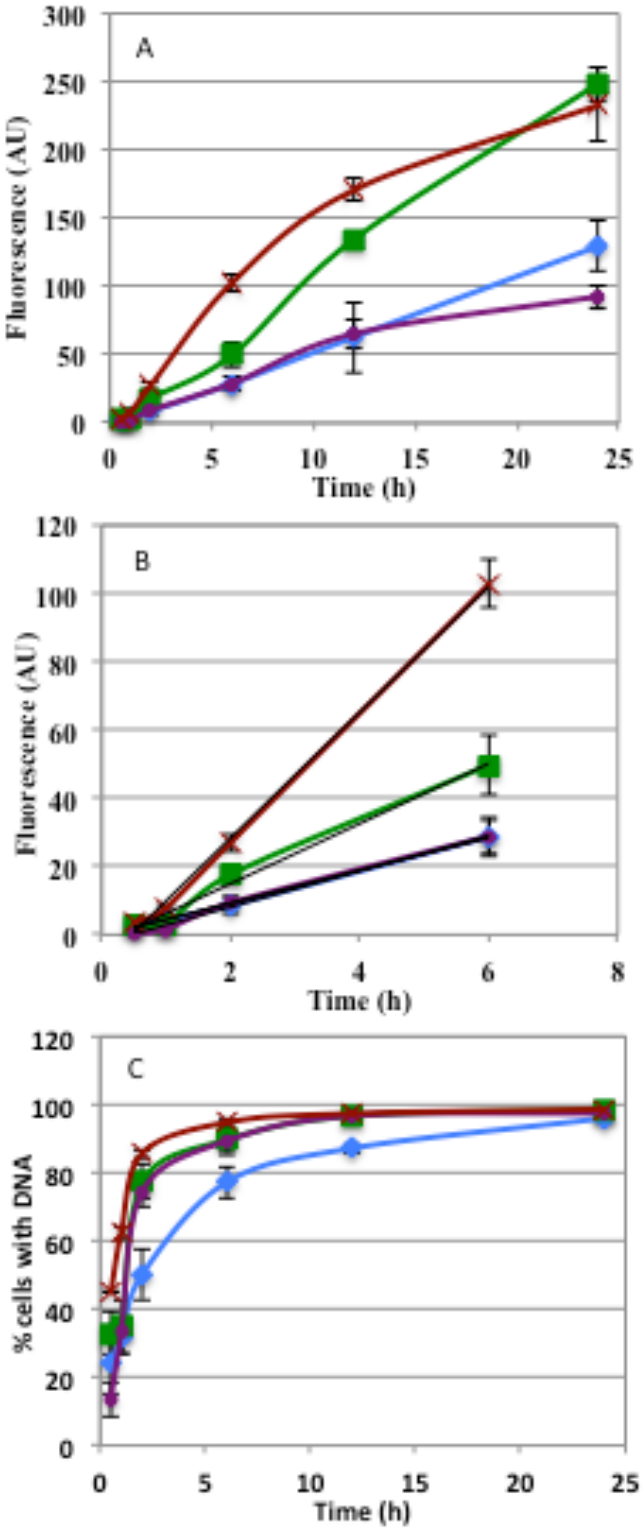

Figure 24. Kinetics of DNA internalization following transfection with different agents.

DLD-1 colorectal cancer cells were transfected with 1 µg 25% cy5 labeled DNA using DOTAP/DOPE (blue ◆), bPEI (green ■), stealth liposomes (purple •) or 4.7 mol% PR_b functionalized stealth liposomes (red x) for different times at 37 °C and 5% CO_2. Cells were washed and quantified using flow cytometry, (A,B) Total amount of DNA internalized, and C) Percentage of cells with internalized DNA reported as the percentage positive difference between transfected and untransfected cells. B) shows calculation of internalization rate kinetics from first 6 h of (A). Linear trendlines, shown in black, were fitted to the data points in Excel. The relative uptake rate of DNA for DOTAP/DOPE, bPEI, non-targeted stealth liposomes (0% PR_b) and 4.7 mol% PR_b functionalized stealth liposomes are 4.8x-0.3, 8.8x-2.6, 5.2x-2.3 and 18.4x-8.5 respectively, where x is time in h. DOTAP/DOPE and non-targeted stealth liposomes closely overlap at all the data points. Data are presented as mean ± standard error from three independent experiments (n=3) each done in triplicate.

compared to DOTAP/DOPE and stealth liposomes. PR_b functionalized stealth liposomes outperformed even bPEI at lower time points. However, at higher time points, 24h, the rate of uptake mediated by PR_b functionalized stealth liposomes was a little lower compared to bPEI (Fig. 24). This conforms to the higher amount of DNA uptake mediated by bPEI at 24 h seen in Fig. 22A. In contrast, the rate of uptake of DOTAP/DOPE and non-targeted stealth liposomes was maintained at a lower level throughout the duration of the experiment

4.4.5 Inhibition of endocytic pathways

To investigate whether different internalization routes was a potential reason for the heterogeneous behavior exhibited by the transfection agents, different endocytic pathways were blocked and the effect on DNA internalization was measured with flow cytometry (Fig. 25). We chemically inhibited three specific endocytic pathways previously implicated in the uptake of non-viral gene delivery vehicles: clathrin-mediated endocytosis, caveolae-mediated endocytosis and macropinocytosis. The concentrations of the different inhibitors used were on the same order of magnitude as used in previous experiments,[28,134] and their effect on cell viability was measured using a WST-1 metabolic assay (Fig. 26). Inhibitor concentrations and treatment times that showed minimum effect on cell viability were used in these experiments. Filipin III, which primarily blocks caveolae-mediated endocytosis, only affected the internalization of PR_b functionalized stealth liposomes decreasing it by 23.3 ± 3.6%. Chlorpromazine, which primarily blocks clathrin-mediated endocytosis, decreased DOTAP/DOPE and the non-targeted stealth liposome mediated DNA internalization by 56.3 ± 3.8 % and 24.4

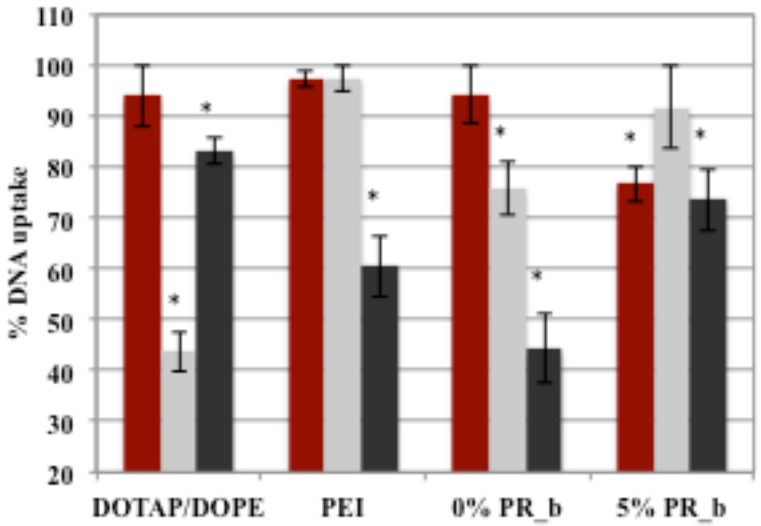

Figure 25. Effect of endocytic inhibitors on DNA internalization after transfection with different agents.
DLD-1 colorectal cancer cells were pretreated with different inhibitors for 30 min and transfected with 1 µg of 25% cy5 labeled pT2/Cal DNA using DOTAP/DOPE, bPEI, non-targeted stealth liposomes (0%) or 4.7 mol% PR_b functionalized stealth liposomes for 1 h at 37 °C and 5% CO_2. The different inhibitors used were filipin III (red ■), for caveolar-mediated endocytosis, chlorpromazine (gray ■), which blocks clathrin-mediated endocytosis and rottlerin (black ■) that inhibits macropinocytosis. Cells were washed and the amount of DNA internalized quantified using flow cytometry. Data are presented as mean ± standard error from three independent experiments (n=3) done in triplicate. Student's t-test was performed and symbols directly over bars represent significance compared to untreated samples: * $p<0.005$.

± 5.2%, while minimally affecting the PR_b functionalized stealth liposomes and bPEI. Rottlerin, which primarily inhibits macropinocytosis, decreased DNA internalization of all the transfection agents but affected the non-targeted stealth liposomes and bPEI more strongly, reducing DNA internalization by 55.7 ± 6.7% and 39.4 ± 6.1 % respectively.

4.5 Discussion

Results from experimental investigations into the effect of blocking endocytosis pathways are often confounded by a variety of factors, and caution is advised in their interpretation.[145,207] First of all, many chemical inhibitors are not specific to a single internalization pathway. Also, inhibiting certain endocytosis pathways can artificially upregulate other internalization routes that are not originally involved in transfection agent uptake. For these reasons, our inhibition experiments were

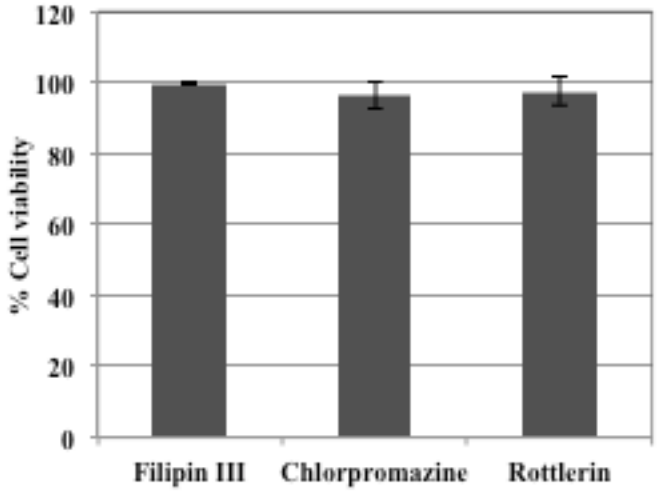

Figure 26. Cell viability after treatment with endocytic inhibitors.
DLD-1 cells were treated with 5 µg/ml filipin III, 10 µg/ml chlorpromazine or 2 µM rottlerin for 1.5 h at 37 °C and 5% CO_2 and cell viability was measured using the WST-1 metabolic assay. Data are shown as the mean ± standard error from three independent experiments (n=3) done in triplicate, and are presented as a percentage of viability of untreated cells.

designed to observe effects at short times and in the process minimize cell adaptation and upregulation of secondary uptake pathways.[145] The scope of these experiments was not to identify exact quantitative combinations of specific internalization pathways involved in the uptake of the different transfection agents, but to observe relative differences in the uptake of transfection agents after cells were treated with chemical inhibitors. Endocytic pathways can be classified as non-lipid raft mediated (clathrin mediated), mixed lipid mediated (phagocytosis and macropinocytosis), and lipid-raft mediated (caveolae, flotillin, Arf6, GRAF-1 and Rho-A mediated).[24] Phagocytosis is involved in the uptake of particles > 0.5 µm in diameter,[138] and was not investigated in this study as all our transfection agents were smaller in diameter at the time of transfection. Out of the rest, clathrin mediated, caveolae mediated and macropinocytosis have been previously implicated in the uptake of transfection agents;[23,26,27] in accordance, our results showed these pathways played different roles in the uptake of the different transfection agents tested in DLD-1 cells. The rest of the lipid-raft mediated endocytic pathways have intertwined roles and as yet lack specific chemical inhibitors,[150] and were not investigated in this study.

DOTAP/DOPE lipoplex mediated transfection was most successful after DNA internalization, leading to the highest protein production to DNA uptake ratio (Table 1). Lower amounts of DNA were internalized with DOTAP/DOPE (Fig. 22A) and this was further corroborated by slow internalization kinetics measured by flow cytometry (Fig. 24). Inhibition of endocytosis pathway blocking implicated mostly clathrin-mediated endocytosis and some macropinocytosis as pathways involved in DOTAP/DOPE mediated DNA uptake (Fig. 25). Also, DOTAP/DOPE has been previously demonstrated to be unstable in serum conditions, making them unsuitable for *in vivo* gene delivery.[119] In addition, DOTAP/DOPE lipoplexes mediate transfection in a non-specific manner, and is unable to differentiate between a specific set of target cells and off-target cells. In contrast, our previous studies have shown that PR_b functionalized nanoparticles can specifically transfect $\alpha_5\beta_1$ integrin bearing cells.[202] Fig. 20 shows that PR_b functionalized stealth liposomes can mediate the same level of transfection as DOTAP/DOPE in DLD-1 cells. In applications where gene expression is needed to be limited to cells bearing $\alpha_5\beta_1$ integrin, in cancer treatment for example, PR_b functionalized stealth liposomes is the better choice for a transfection agent.

bPEI has been previously shown to mediate transfection in cells, hypothesized to be facilitated by endosomal escape through a proton sponge effect.[117] However, the efficacy of the proton sponge effect has been the subject of debate.[164,208,209] Previous studies have presented situations where bPEI polyplexes are unable to escape endosomes, and that further modifications are necessary to improve transfection efficiency.[209,210] Our results demonstrate such a situation where bPEI polyplexes are stuck in organelles such as lysosomes as evident by their colocalization with the green organelles (Figs. 23C and 23D). Despite having better transfection properties compared to other polymers such as poly-L-lysine,[202] bPEI has a lot of room for improvement with regard to lysosomal escape in DLD-1 cells.

Macropinocytosis has been suggested as an uptake route that can help increase transfection in CHO cells by amphiphilic transfection agents and in NIH3T3 cells by high density octaarginine modified liposomes.[26,211] In our studies

macropinocytosis was found to be the primary pathway involved in the uptake of bPEI and non-targeted stealth liposomes (Fig. 25) but neither of these two transfection agents mediated a significant level of transfection in DLD-1 cells. Thus, macropinocytosis is not always conducive to gene transfection. These results can potentially be explained by the fact that different pathways are effective in the transfection of different cell lines.[131] Also, escape from macropinosomes is an inefficient process.[212] In accordance, non-targeted stealth liposomes and bPEI both appear as punctuate dots within the cells (Fig. 23). In addition, our internalization kinetics experiment shows that the rate of uptake of bPEI condensed DNA is almost twice as much as that of the non-targeted stealth liposomes (Fig. 24B). That implies that either macropinocytosis is proceeding at different rates for these transfection agents, or that one of the other lipid-raft mediated endocytic pathways is working in conjugation with macropinocytosis for bPEI uptake. In addition, the higher electrostatic binding of bPEI polyplexes to the cell membrane may also contribute to fast internalization kinetics. Consistent with the slow rate of uptake, most of the DNA delivered with the non-targeted stealth liposomes was seen further away from the nucleus in small punctate dots (Figs. 23E and 23F). Despite the slower uptake rate and peripheral DNA, there is no significant colocalization of the non-targeted stealth liposomes with early endosomes. This conforms to the idea that most non-targeted stealth liposomes are taken up in macropinosomes, which initially do not possess the Rab5 early endosome marker but acquire it during subsequent maturation.[213] Eventually macropinosomes merge with acidic lysosomal compartments.[213,214]

Our results implicated macropinocytosis and caveolar mediated endocytosis in the uptake of DNA encapsulated in PR_b functionalized stealth liposomes targeted to $\alpha_5\beta_1$ integrin (Fig. 25). PR_b functionalized stealth liposomes partly comprise of bPEI condensed DNA and stealth liposomes. The presence of the PR_b peptide can change the uptake route from predominantly macropinocytosis, as seen for bPEI and non-targeted stealth liposomes, to one with a stronger caveolar influence. While macropinocytosis is involved in DNA uptake, the results from bPEI and the non-targeted stealth liposomes transfection

suggest that this may not be an effective internalization route for gene expression in DLD-1 cells for certain transfection agents. Amongst all the transfection agents tested here, only PR_b functionalized stealth liposomes were internalized using caveolar pathway. In a previous study with polyplexes modified with the RGD peptide, which also binds integrins, it was shown that the targeted polyplexes internalized via a caveolar pathway.[215] In fact, it has been suggested that the caveolar uptake is the only productive internalization route for some transfection agents.[27] Caveolae mediated endocytosis may confer an advantage to internalized DNA. While caveosomes were initially thought to be non-acidic and non-digestive compartments,[216] recent evidence suggests that these organelles slowly merge with late endosomes over time.[217] This slower maturation process could potentially allow more time for internalized cargo to escape the endosomal pathway.[25] Additionally, caveolae have previously been implicated in the uptake of β_1 integrins.[218] In accordance, our results show that targeting $\alpha_5\beta_1$ integrin with the PR_b peptide functionalized stealth liposomes promotes cellular internalization mediated by caveolae.

We show that different transfection agents appear to be facing different barriers to gene expression. DOTAP/DOPE mediates good transfection when internalized, but suffers from a low uptake rate. Non-targeted stealth liposomes have poor transfection efficiency in part due to slow internalization kinetics. As discussed in the introduction section, the *in vivo* stability of transfection agents are often improved by addition of a PEG layer on the particle surface, at the expense of transfection efficiency. Our results show that an effective balance can be struck by using targeted stealth liposomes. PR_b functionalized stealth liposomes mediate fast internalization and have high transfection efficiency. In contrast to all the other transfection agents tested here, PR_b functionalized stealth liposomes are the only system that can mediate transfection in a specific target group of cells – namely, those bearing the $\alpha_5\beta_1$ integrin. The specificity of PR_b functionalized nanoparticles for the $\alpha_5\beta_1$ integrin has been extensively demonstrated before.[186,202] Unfortunately, bPEI, a key component in the design of the PR_b functionalized transfection agent, when used on its own failed to

efficiently escape endosomes in DLD-1 cells. PR_b functionalized stealth liposomes may therefore be improved further by encapsulating DNA condensed using a different cationic polymer with better endosomal release properties.

Our results support the notion that there is not a single transfection agent that is effective in all situations.[131] Also, transfection agents appear to not have a consistent mechanism of mediating gene expression across different cell lines. For example, bPEI, which has been claimed to be a stellar polymer based transfection agent in other cells,[117,118] failed to promote appreciable gene expression in DLD-1 cells. Macropinocytosis, which has been claimed to offer an advantage to transfection agents,[26] was ineffective at gene expression using bPEI and non-targeted stealth liposomes. Just as transfection agents themselves behave differently in different cell types, it appears that different endocytic pathways may have different fates also depending on the cell types.[131] This is likely the reason why there is not a consensus on a correlation between transfection agents and their preferred internalization pathways, and also why there is a discord regarding which pathways offer the best advantage for mediating gene expression. One way to generalize the behavior of transfection agents and predict outcomes of gene expression may be to study transfection mechanisms in a variety of different cell lines. Such information may enable us to decipher patterns in cell phenotypes and relate that to optimal transfection mechanisms within a group of cells.

4.6 Conclusion

We investigated the transfection mechanism of DOTAP/DOPE lipoplexes, bPEI polyplexes, non-targeted stealth liposomes and PR_b functionalized stealth liposomes in DLD-1 human colorectal cancer cells. The predominant form of endocytosis was clathrin mediated for DOTAP/DOPE, macropinocytosis for bPEI and non-targeted stealth liposomes and a combination of caveolar and macropinocytosis for PR_b targeted stealth liposomes. We discovered that bPEI may be ineffective in DLD-1 cells after internalization in macropinosomes and lysosomes. However, targeting to $\alpha_5\beta_1$ integrin using PR_b functionalized nanoparticles, thereby switching the internalization route to caveolar or lipid raft

mediated pathways, can salvage gene expression. PR_b functionalized stealth liposomes are rapidly taken up with fast integrin-mediated internalization kinetics, mediate efficient transfection in DLD-1 cells, and can potentially benefit from additional advantages of the caveolar uptake pathway.

Chapter 5. Increasing cancer-specific gene expression by targeting overexpressed $\alpha_5\beta_1$ integrin and upregulated transcriptional activity of NF-κB

5.1 Summary

We developed a modular multi-functional non-viral gene delivery system by targeting the overexpressed cancer surface receptor $\alpha_5\beta_1$ integrin and the upregulated transcriptional activity of the cancer resistance mediating transcription factor NF-κB, thereby introducing a new form of transcriptional targeting. NF-κB regulated therapy can improve specificity of gene expression in cancer tissue and also may offset NF-κB mediated cancer resistance. We delivered a luciferase gene under the control of an NF-κB responsive element (pNF-κB-Luc) encapsulated in a PR_b peptide functionalized stealth liposome that specifically targets the $\alpha_5\beta_1$ integrin and achieved increased gene expression in DLD-1 colorectal cancer cells compared to BJ-fibroblast healthy cells *in vitro*. The multi-targeted system was also able to differentiate between cancer cells and healthy cells better than either of the individually targeted systems. In addition, we constructed a novel cancer therapeutic plasmid by cloning a highly potent diphtheria toxin fragment A (DTA) expressing gene under the control of an NF-κB responsive element (pNF-κB-DTA). A dose-dependent reduction of cellular protein expression and increased cytotoxicity in cancer cells was seen when transfected with PR_b functionalized stealth liposomes encapsulating the condensed pNF-κB-DTA plasmid. Our therapeutic delivery system specifically eradicated close to 70% of a variety of cancer cells while minimally affecting healthy cells *in vitro*. Furthermore, the modular nature of the non-viral design allows targeting novel pairs of extracellular receptors and upregulated transcription factors for applications beyond cancer gene therapy.

5.2 Introduction

A major problem facing cancer therapy is non-specific delivery of administered therapeutics. The non-specific accumulation in healthy sites can often result in undesirable toxic side effects, necessitating the development of delivery vectors that can limit off-target cytotoxicity. A significant portion of the delivered therapeutic dose is taken up by the macrophagocytic system (MPS) leading to subsequent accumulation in the liver and the spleen. One strategy to address this issue is the encapsulation of therapeutics in nanoparticles functionalized with a polyethylene glycol (PEG) brush layer, which can help tumor accumulation by increasing circulation lifetime and the enhanced permeation and retention effect.[7,54] In addition, targeting ligands can be incorporated on the nanoparticle surface to bind to extracellular receptors overexpressed in tumor tissue and vasculature[181,196,200,219] thereby facilitating internalization into target cells.[3] While PEGylation and targeting can improve delivery efficiency compared to traditional delivery of free therapeutics, these systems continue to experience significant MPS uptake[29] Also, many widely investigated cancer cell or cancer vasculature receptor targets such as integrins,[30] the endothelial growth factor receptor[31] and fibroblast growth factor receptor [32] are also appreciably expressed in healthy tissues and vasculature.[33–35] These issues can lead to the same non-specific side effects that targeted therapy is striving to avoid, and call for further levels of control to minimize non-specific delivery.[220]

Gene therapy is becoming an increasingly popular form of cancer treatment. One way gene therapy can solve the problem of non-specific delivery is through the addition of transcriptional targeting to the extracellular receptor targeting that is already in place, generating a multi-targeted system for better control of gene expression. Transcriptional targeting has been widely investigated in the past, and has been shown to improve specific delivery to the target tissues.[36,37] Generally, transcriptional targeting involves delivering a gene under the control of a tissue specific promoter – allowing gene expression in target tissues while avoiding healthy areas. Multi-targeting by combining transductional and transcriptional targeting has been shown before to effectively increase the

specificity of a viral gene delivery system,[38–40] however it has not been sufficiently investigated in a non-viral delivery system.[41] Non-viral systems offer several advantages over viral gene delivery vectors – they are tunable, safer, cheaper and easier to build.[6,221] The tunable nature of these systems can facilitate the construction of a modular multi-targeted system.

A second major problem in cancer therapy is the development of resistance to chemo and radiation therapies in cancer cells, rendering these traditional forms of treatment largely ineffective. NF-κB is a well-characterized group of transcription factors that are upregulated in a variety of diseases including cancer[42] and is known to mediate resistance to chemotherapy and radiation therapy.[43] Inhibition of NF-κB activity has been shown to improve cancer therapy by reducing NF-κB mediated chemotherapy resistance.[44] However, its transcriptional activity has never been used as a therapeutic target before. Given the central role played by NF-κB as a transcription factor controlling a variety of cancer progression pathways, we postulated that its upregulated activity would be sufficient to mediate a therapeutic response specifically in cancer cells. In addition, targeting the transcriptional activity of a single upregulated transcription factor may offer better control and outcome predictability compared to conventional transcriptional targeting using entire promoter sequences of upregulated genes.

In this paper, we took advantage of the versatility of gene therapy and developed a multi-functional therapeutic system. As a delivery vehicle we chose PR_b functionalized stealth liposomes encapsulating branched polyethyleneimine (bPEI) condensed plasmid DNA (pDNA), a non-viral gene delivery vehicle recently development in our group to specifically transfect $\alpha_5\beta_1$ integrin bearing cells.[202] The PR_b targeting ligand used in this system is a fibronectin mimetic peptide developed by our group to preferentially bind $\alpha_5\beta_1$ integrin with an affinity of 76.3±6.3 nM,[17,195] and has since been used to improve nanoparticle delivery to $\alpha_5\beta_1$ integrin bearing cells for a variety of applications.[19,21,185,203,204,222] PR_b functionalized nanoparticles can outperform other RGD based peptide functionalized nanoparticles, and can distinguish between cells with differential

expression levels of $\alpha_5\beta_1$ integrin.[20,186] $\alpha_5\beta_1$ integrin is a widely accepted and well-investigated cancer surface marker.[14] It is highly expressed on embryonic cell types but it is downregulated during development.[16] It is also highly upregulated in tumor vasculature and in tumor cells of breast and prostate cancer and, central to this work, colorectal cancer.[14,15] However, $\alpha_5\beta_1$ integrin is also present in normal tissues such as hepatic sinusoids, endothelial venules of lymph nodes, pancreatic ducts and intestinal smooth muscle, even though most of these healthy sites are not accessible from the bloodstream.[33] For example, intravenously injected anti-$\alpha_5\beta_1$ antibody examined the amount and distribution of the integrin present *in vivo* and this study revealed that the injected antibody strongly labeled tumor vessels but did not label most normal blood vessels and did not access pancreatic ducts or intestinal smooth muscle.[33] However, hepatic sinusoids and lymph nodes remain vulnerable to non-specific transfection.[33]

We hypothesized that by adding a second level of control to PR_b functionalized stealth liposomes via transcriptional targeting, we can improve the specificity of cancer cell transfection while minimizing off-target effects. We therefore targeted the upregulated transcriptional activity of NF-κB as a new form of transcriptional targeting, and showed increased cancer specificity. In addition, to address the problem of low gene expression mediated by most transcriptional targeting, we chose the highly potent diphtheria toxin fragment-A (DTA) as the protein product of gene expression. DTA consists of only the catalytic fragment of diphtheria toxin and lacks a cell-penetrating domain, which can minimize any bystander cell killing effect at off-target sites. A few molecules of DTA can be enough to result in cell death through inhibition of protein expression[45] and DTA-encoding plasmids have been previously used to successfully kill cancer cells.[36,46] Moreover, some healthy cell lines have been previously shown to be resistant to DTA activity,[45] which further augments the potential cytotoxic specificity of our design. Thus, by delivering a DTA gene under the regulation of a NF-κB responsive element, we showed that the high transcriptional activity of NF-κB in cancer cells can mediate specific cytotoxicity in a variety of cancer cells compared to healthy cells *in vitro*.

By combining the targeting of two well-recognized cancer markers, $\alpha_5\beta_1$ integrin and upregulated NF-κB transcriptional activity, we created a general, modular platform for cancer-specific transfection agents. This multifunctional design may also offer a solution to NF-κB mediated cancer resistance to chemotherapy and radiation therapy, and can be a useful adjuvant to increase the efficiencies of these traditional forms of cancer treatment.

5.3 Materials and Methods

5.3.1 pNF-κB-DTA construction

pNF-κB-Luc (Agilent, Santa Clara, CA) was sequenced at the University of Minnesota Genomics Center (UMGC) with a Luc-B1 primer according to the manufacturer's instructions. We verified the presence of the NF-κB binding domain, 10 bp tandem repeats of GGGGACTTTC, and identified the region of interest between the promoter and the transcription start site to help determine an insertion site for the diphtheria toxin fragment A (DTA) gene. The gene sequence coding for DTA [223] was designed and manufactured in GeneArt (Life technologies, Grand Island, NY). In order to keep the NF-κB responsiveness of the plasmid the same, the DTA gene (Life Technologies, Grand Island, NY) was inserted exactly in place of the luciferase gene, maintaining the minimal promoter region. DTA was cloned into the pNF-κB-Luc plasmid using an In-Fusion HD cloning kit according to the manufacturer's protocol (Clontech, Mountain View, CA). We first PCR-amplified the DTA gene with primer overhangs complementary to the 16 bp region on either side of the corresponding insertion sites on the pNF-κB-Luc plasmid. Forward primer (ATGGAAGCTCGAATTCCAGCTTGGCA) and reverse primer (TTGTAACA ATATCGATTCATCTCCGCACTCTGTTG) used in this experiment were manufactured at UMGC. The PCR amplified product was verified using gel electrophoresis and sequencing at the UMGC facilities. EcoRI and ClaI restriction enzymes (Invitrogen supply cabinet, University of Minnesota) were used to linearize the pNF-κB-Luc plasmid following the New England Biolabs (Ipswich, MA) protocols. The linearization process was verified using gel electrophoresis. DTA insert was ligated with the linearized pNF-κB-Luc plasmid using the In-

Fusion HD cloning kit according to the manufacturer's instructions. The reaction products were transformed into a Top10 Ecoli strain (Invitrogen, Grand Island, NY) and plated on LB-Amp media. Colony PCR was performed on the bacterial colonies the next day with primers NF-κBDTA-F GGCAGCAGCAGCGTGGAGTA and NF-κBDTA-R CAGGCCTGGGCCATATATCGT (UMGC) against the DTA gene. Out of the eight colonies tested, one appeared to have a plasmid bearing the DTA gene. The colony was amplified and the plasmid harvested using a Plasmid Miniprep kit (Qiagen, Valencia, CA). Presence of DTA gene in the plasmid in the correct position and orientation was verified at the UMGC DNA sequencing facilities.

5.3.2 Liposome synthesis

1,2-Dipalmitoyl-sn-glycero-3-phosphocholine (DPPC), 1,2-dipalmitoyl-sn-glycero-3-phosphoethanol amine-N-[methoxy(polyethylene glycol)-2000] (ammonium salt) (DPPE-PEG2000), and cholesterol were purchased from Avanti Polar Lipids, Inc (Alabaster, AL). PR_b peptide was purchased from UMGC and amphiphiles were synthesized as previously described.[17] PR_b functionalized or non-targeted stealth liposomes were made using a thin film lipid hydration method. Briefly, a mixture of lipids containing x mol % PR_b peptide-amphiphiles, 5 mol % DPPE-PEG2000, (60-x) mol % DPPC and 35 mol % cholesterol were deposited in a round bottom flask and dried under a stream of argon (x =0 for non-targeted stealth liposomes and 5 for PR_b functionalized stealth liposomes). Plasmid DNA was condensed with branched polyethylenemine (bPEI) as previously described (section 4.3.1), and used to hydrate the lipid film for 2 h in a water bath held at 45 ^{o}C. The hydrated liposomes were then extruded through 400nm polycarbonate membranes in a hand held extruder (Avestin, Ontario, CA). Extruded liposomes were dialyzed against water for 24 h in a 1000 kDa MWCO dialysis membrane (Spectrum Labs, Rancho Dominguez, CA) with frequent water changes. pDNA concentration in the liposomes was then measured using a cy5 DNA quantification assay (Mirus Biosciences, Madison, WI) as described previously (Section 3.3.3).

5.3.3 Flow cytometry to detect $\alpha_5\beta_1$ integrin

DLD-1 human colorectal cancer cells and human BJ fibroblasts (ATCC, Manassas, VA) were cultured in T75 flasks in Dulbecco's Modified Eagle Medium (DMEM) supplemented with 10% fetal bovine serum and 10% of a 10,000 units/ml penicillin – 10 mg/ml streptomycin solution (Sigma Aldrich, St Louis, MO), at 37 °C and 5% CO_2 to 70-80% confluence. Cells were harvested and resuspended at $1x10^6$ cells/ml in 500 µl of 4 °C fluorescent buffered saline (FBS, 2 w/v% BSA in PBS buffer), and incubated with 10 µg MAb1969 (Millipore, Billerica, MA) mouse anti-human $\alpha_5\beta_1$ antibody or 5 µg 119K7690 (Sigma-Aldrich, Saint Louis, MO) mouse isotype control for 30 min at 4 °C on a rotary shaker. Cells were pelleted by centrifugation and washed twice with 1 ml of 4°C FBS and incubated with 40 µg of AP124F (Millipore, Billerica, MA) goat anti-mouse fluorescent secondary antibody for 30 min at 4 °C on a rotary shaker. Following incubation, cells were pelleted by centrifugation, washed twice with 4 °C FBS and analyzed immediately on a FACScalibur flow cytometer (Masonic cancer center, University of Minnesota).

5.3.4 RT-PCR for NF-κB mRNA

DLD-1, BJ fibroblasts, or HEK293T cells (gift from Prof. McIvor, University of Minnesota, uninduced or induced with 20 ng/ml TNF-α) were grown on DMEM at 37 °C and 5% CO_2 to 70-80% confluence in a 6 well plate. Manufacturer's protocols were followed for mRNA harvest using an RNeasy extraction kit (Qiagen, Valencia, CA) for cDNA generation using RNA to cDNA ecodry premix (Clontech, Mountain View, CA), and for running PCR on a Stratagene MX3000P using SYBR advantage PCR kit (Clontech, Mountain View, CA). The following PCR primer pairs were identified in NCBI primer blast, manufactured at UMGC and used for the detection of different NF-κB proteins: h-NF-κB1-F GTGCAGAGGAAAC GTCAGAAGC, h-NF-κB1-R CCGCCACTACCAAACATGCC, h-NF-κB2-F AGACAACCTCACCCAGTGGC, h-NF-κB2-R CTCGGGTTTCTGGACCCCTC, h-cRel-F CTCCGGTGCGTATAACCCGT, h-cRel-R CTGTGCTCCCCTGGAATGCT, h-RelA-F AAGAGCAGCGTGGGGACTAC, h-RelA-R

CAGTGTTGGGGGCACGATTG, h-RelB-F CCTCGCGAC CATGACAGCTA, h-RelB-R CCAGGATGGCCGGCTTTTTC. Human β-actin was used as a housekeeping gene control with primers h-Actin-F TGAGACCTTCAACACCCCAG and h-Actin-R AGATGGGCACAGTGTGGGT. The relative amount of NF-κB mRNA was calculated relative to the geometric mean of the cycle thresholds of the housekeeping gene β-actin using the $2^{-\Delta\Delta Ct}$ method.[224]

5.3.5 Luciferase transfection and luminescence measurement

DLD-1 colorectal cancer cells and BJ fibroblast skin cells were plated at 5000 cells per well in a clear 96 well plate in 200 µl of DMEM. Medium was replenished the next day and cells transfected with 100 to 250 ng of pDNA encapsulated in different liposomes. The liposome formulations tested were PR_b functionalized stealth liposomes encapsulating either pNF-κB-DTA plasmid or the pT2/Cal plasmid, and non-targeted stealth liposomes encapsulating pNF-κB-DTA. Liposomes were incubated with the cells for a period of 72 h in an incubator at 37 ^{o}C and 5% CO_2. Cells were then washed in PBS buffer, media was replenished and the WST-1 assay (Promega, Madison, WI) was used to measure cell viability according to the manufacturer's protocol. Cell viability is reported as a percentage of untransfected cells. For experiments demonstrating the versatility of the pNF-κB-DTA plasmid, MCA38 murine colon cancer cells, MCF7 human breast cancer cells and TNF-α induced HEK293T human embryonic kidney cells were similarly transfected with 100 ng pNF-κB-DTA in PR_b functionalized stealth liposomes with pmaxGFP as the control. For experiments investigating the effect of DTA dosage on cell viability, different concentrations of pNF-κB-DTA in PR_b functionalized stealth liposomes were delivered to DLD-1 cells, with pMaxGFP as the control. Cell incubation and cell viability measurements were carried out as described above.

5.3.6 RT-PCR for DTA mRNA

DLD-1 cells were seeded in a 6 well plate at $1x10^5$ cells/well in 1ml DMEM media and cultured at 37 °C and 5% CO_2. 24 h later, medium was replenished and pNF-κB-DTA encapsulated in PR_b functionalized or non-targeted stealth

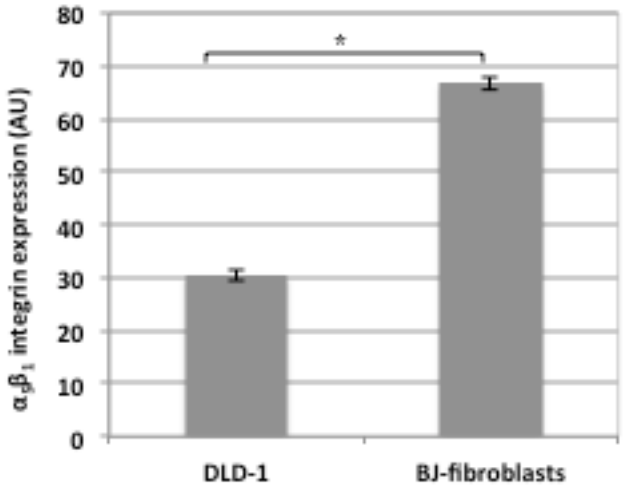

Figure 27. Relative levels of $\alpha_5\beta_1$ integrin expression in DLD-1 cells and BJ-fibroblasts.
Cells were incubated with a mouse anti-human $\alpha_5\beta_1$ integrin antibody, followed by incubation with a FITC labeled goat anti mouse antibody. Cells were then sorted for FITC label on flow cytometry. Data present mean ± standard error for three independent experiments (n=3), done in triplicate. Students t-test statistical analysis was performed, * indicates $p<0.001$.

liposomes was used to transfect the cells at 1 µg/well. Following incubation for 24 h more, manufacturer's protocol was followed for mRNA harvest using an RNeasy extraction kit (Qiagen, Valencia, CA), for cDNA generation using RNA to cDNA ecodry premix (Clontech, Mountain View, CA), and for running PCR on a Stratagene MX3000P using SYBR advantage PCR kit (Clontech, Mountain View, CA). The following PCR primer pairs were manufactured at UMGC and used for the detection of DTA mRNA: NF-κB-DTA-F GGCAGCAGCAGCGTGGAGTA and NF-κB-DTA-R CAGGCCTGGGCCATATATCGT. Human β-actin was used as a housekeeping gene control with primers h-Actin-F TGAGACCTTCAACACCCCAG and h-Actin-R AGATGGGCACAGTGTGGGT. The relative amount of DTA mRNA was calculated relative to the geometric mean of the cycle thresholds of the housekeeping gene β-actin using the $2^{-\Delta\Delta Ct}$ method.[224]

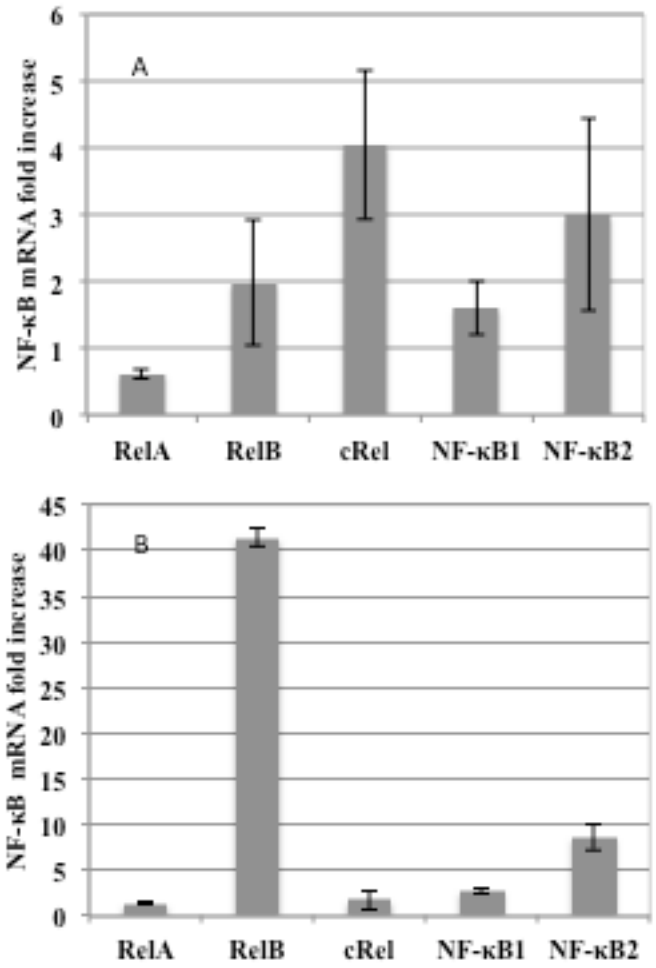

Figure 28. NFκB mRNA levels in (A) DLD-1 cells relative to BJ-fibroblasts and (B) TNF-α induced versus uninduced HEK293 cells.
mRNA harvested from cells was probed for the presence of RelA, RelB, cRel, NF-κB1 and NF-κB2 using RT-PCR, with beta-actin mRNA as a housekeeping gene control. Data presented as mean ± standard error for nine independent experiments (n=9), done in triplicate.

5.4 Results

5.4.1 Expression of $\alpha_5\beta_1$ integrin and NF-κB in cancer cells compared to healthy cells

We hypothesized that in situations where a cancer-related extracellular target receptor is also overexpressed in healthy cell lines, further levels of control would be needed for cancer specific gene delivery. For that we used DLD-1 colorectal

cancer cells and BJ fibroblast that express the $\alpha_5\beta_1$ integrin at a higher level than DLD-1 cancer cells (Fig. 27). BJ fibroblasts are primary fibroblasts from the foreskin of a newborn and $\alpha_5\beta_1$ is highly expressed in embryonic cell types while it is downregulated during development in adult tissues. While this primary cell line is not likely to be encountered by gene delivery vehicles administered in vivo in an adult, it serves as a useful model for healthy cells expressing the receptor of choice. The relative expression levels demonstrate a scenario where the first level of extracellular receptor targeting by itself would be unable to differentiate between healthy cells and cancer cells, leading to undesirable side effects in off target cells. To identify a model for the second level of intracellular targeting that would increase specificity of gene delivery to cancer cells, we chose to investigate the transcription factor NF-κB that is strongly implicated in the development and progression of cancer. NF-κB can exist in several different forms in cells – as homo or heterodimers of RelA, RelB, cRel, NF-κB1 or NF-κB2.[42] mRNA levels of NF-κB in DLD-1 cells and BJ fibroblasts were measured using RT-PCR and four out of the five NF-κB proteins tested were seen to be upregulated in DLD-1 colorectal cancer cells compared to the healthy BJ fibroblasts (Fig. 28A). To further validate the differential NF-κB expression in healthy versus cancer or NF-κB-induced cells, NF-κB expression levels were investigated in normal or TNF-α induced human embryonic kidney HEK293T cells, as TNF-α inflames HEK293T cells and induces NF-κB activation. NF-κB levels were also seen to be upregulated in induced HEK293T cells compared to uninduced cells (Fig. 28B). In some of our subsequent experiments normal or TNF-α induced HEK293T cells were used as a supplementary model to further demonstrate NF- κB mediated gene expression. Thus NF-κB is an intracellular target that could be utilized successfully to differentiate between healthy and diseased cells and in particular the DLD-1 cells and BJ fibroblasts that are used here as a cancer and healthy cell model for therapeutic delivery.

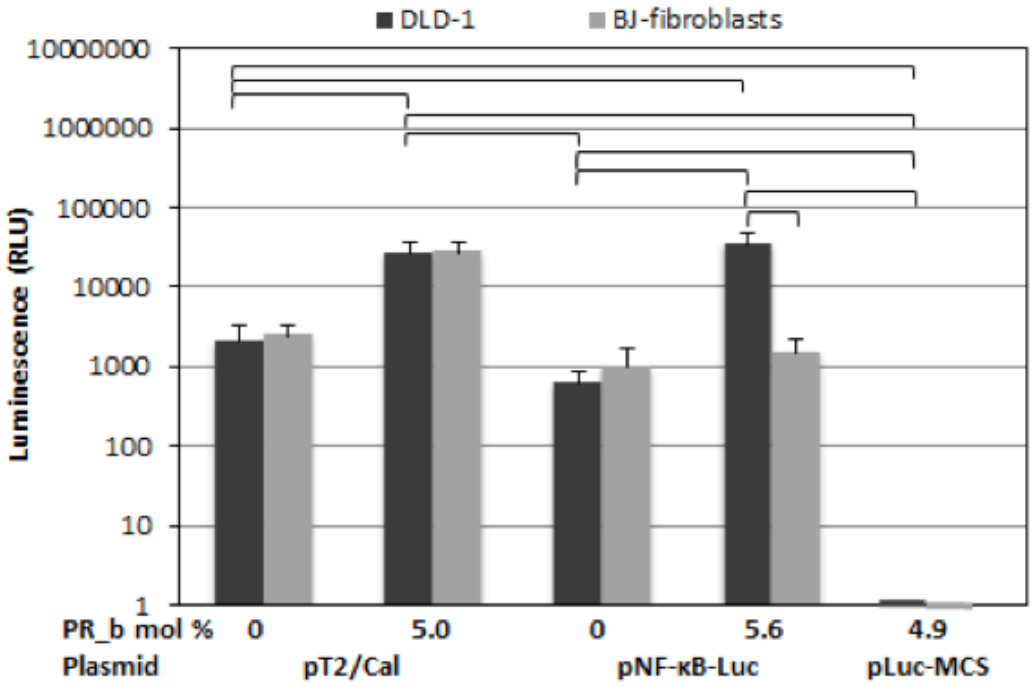

Figure 29. Luciferase expression in DLD-1 cells or BJ fibroblasts.
PR_b functionalized stealth liposomes or stealth liposomes were used to transfect pT2/Cal plasmid (luciferase under a constitutive CAGS promoter), pNF-κB-Luc (luciferase under NF-κB responsive element) or pLucMCS (promoterless luciferase plasmid) in DLD-1 cells or BJ fibroblasts, and luminescence from luciferase expression measured after a 48 h incubation at 37°C. Data presented as mean ± standard error from three independent experiments (n=3), done in triplicate. Students t-test statistical analysis was performed, bracketed data indicates $p<0.05$; absence of brackets for $p>0.05$.

5.4.2 Multi-targeting increases specificity of luciferase gene expression in cancer cells compared to healthy cells

To demonstrate increased specificity with the multi-targeting approach DLD-1 cells and BJ fibroblasts were transfected with two different plasmids – pT2/Cal, that constitutes the luciferase gene under the control of a CAGS constitutive promoter,[187] or pNF-κB-Luc, where the luciferase gene is controlled by an NF-κB responsive element. The plasmids were condensed with bPEI and encapsulated in either PR_b functionalized or non-targeted stealth liposomes. In both cases, non-targeted stealth liposomes resulted in low transfection levels, demonstrating the effectiveness of the first level of extracellular targeting (Fig. 29). When pT2/Cal was delivered to these cells using PR_b functionalized stealth

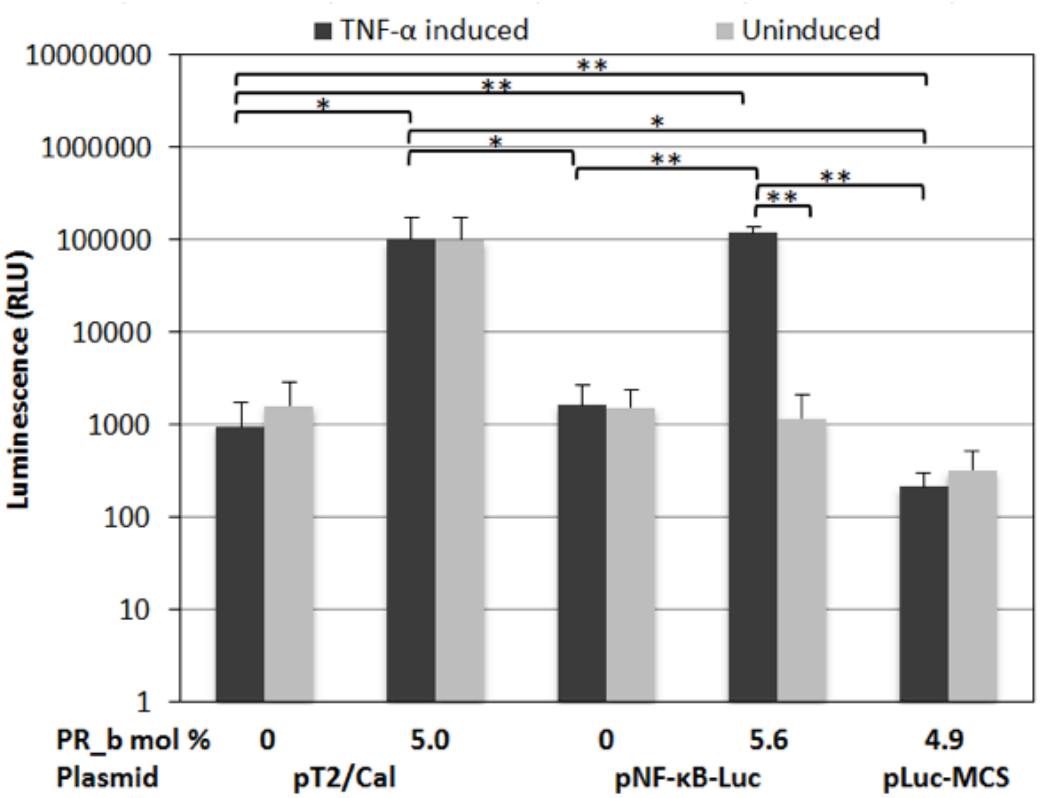

Figure 30. Luciferase expression in TNF-α induced or uninduced HEK293T cells. Cells were transfected with 100ng of pT2/Cal plasmid (luciferase under a constitutive CAGS promoter), pNFκB-Luc (luciferase under NFκB responsive element) or pLucMCS (promoterless luciferase plasmid) encapsulated in PR_b functionalized stealth liposomes or stealth liposomes, and luminescence from luciferase expression measured after a 48hour incubation at 37°C. Data presented as mean ± standard error from three independent experiments (n=3), done in triplicate. Students t-test statistical analysis was performed, * indicates $p<0.05$, ** $p<0.005$, absence of brackets for $p>0.05$.

liposomes, both DLD-1 and BJ-fibroblasts expressed the luciferase gene at very similar levels. This demonstrates a crucial element of our hypothesis – namely the inability to differentiate between cancer cells and healthy cells with a single level of extracellular targeting in situations where the extracellular receptor is upregulated in off-target tissues. These results also show similar transfection efficiencies between these two cell lines, thereby justifying a fair comparison. In contrast, when pNF-κB-Luc was delivered to these cells with PR_b functionalized stealth liposomes, DLD-1 cells maintained similar levels of luciferase expression compared to pT2/Cal transfection, while expression in healthy BJ fibroblasts dropped to control levels as seen in the case where plasmids were delivered

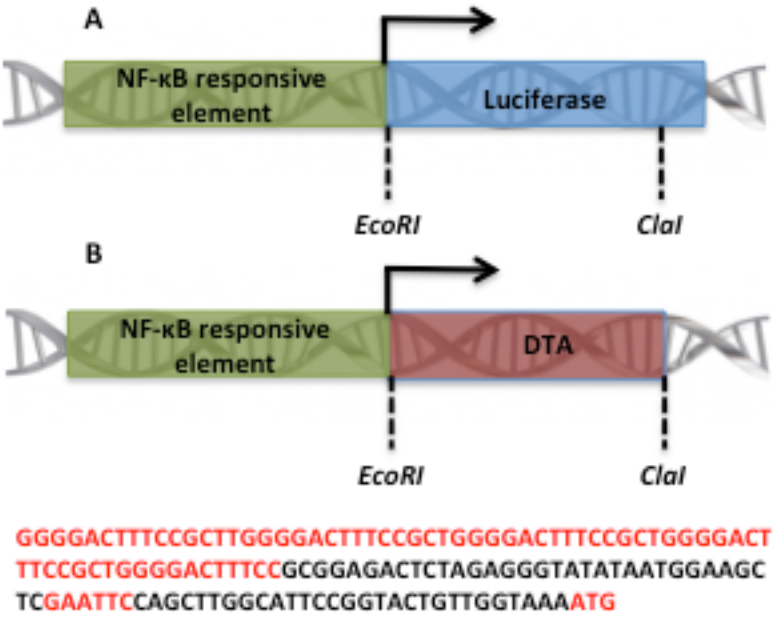

Figure 31. Schematic of A) pNF-κB-Luc and B) pNF-κB-DTA
The common DNA sequence showing the promoter region and transcription start site for A) and B) is presented below. 5 tandem repeats of a 10 bp NF-κB responsive element, EcoRI restriction site, and transcription start site are shown in red. pNF-κB-DTA was constructed by cloning the DTA gene between the EcoRI and ClaI sites in pNF-κB-Luc.

using non-targeted stealth liposomes. Therefore, introducing a second level of intracellular targeting significantly increased specificity of gene expression in cancer cells. To further prove that the luciferase expression seen after transfection with pNF-κB-Luc was due to the activity of NF-κB, the pLuc-MCS plasmid was used as a control, which is the same plasmid lacking the NF-κB responsive element. Luciferase expression was not detectable in either cell line, relating any measurable expression to NF-κB transcriptional activity. With almost two orders of magnitude difference between the levels of gene expression in DLD-1 cells versus BJ fibroblasts, we concluded that using a multi-targeted approach holds promise for cancer-specific gene therapy. In addition, this experiment was repeated using HEK293T cells in their uninduced and induced forms to demonstrate that multi-targeting can increase specificity in other diseases where NF-κB levels are upregulated. Gene expression trends were similar (Fig. 30).

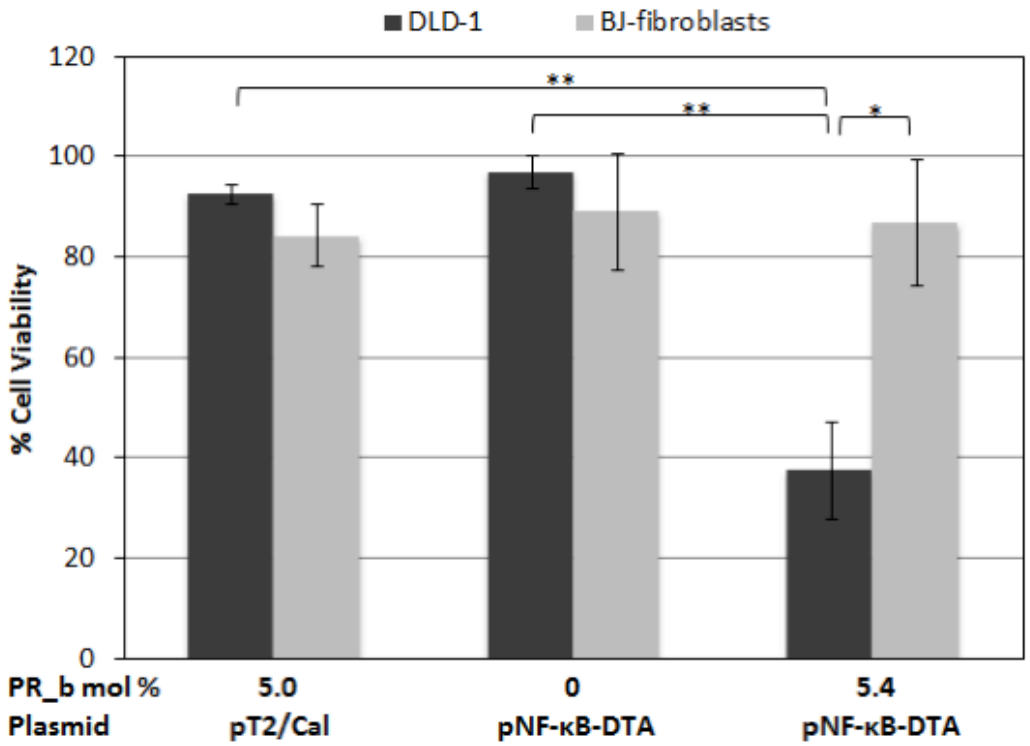

Figure 32. DTA mediated cytotoxicity in DLD-1 cells and BJ fibroblasts.
250 ng of bPEI condensed pNF-κB-DTA or pT2/Cal encapsulated in PR_b functionalized or non-targeted stealth liposomes were used to transfect cells for 72 h at 37 °C, followed by measuring cell viability using a WST-1 metabolic assay and shown as a percentage of untreated samples. Data presented as average ± standard error of three independent experiments (n=3), done in triplicate. Student's t-test statistical analysis was performed, * indicates $p<0.05$, ** $p<0.005$, absence of brackets for $p>0.05$.

5.4.3 Multi-targeting can specifically eradicate cancer cells while sparing healthy cells

To investigate the therapeutic potential of the multi-targeted gene delivery system, we designed a cancer specific suicide gene therapy regime. As a cytotoxic gene of interest we chose the DTA encoding gene, which has been previously shown to effectively kill cancer cells.[225,226] pNF-κB-DTA (Fig. 31) was created by cloning in the DTA gene in the place of the luciferase gene in pNF-κB-Luc. To show cancer specific therapy, pNF-κB-DTA was delivered into DLD-1 cells and BJ-fibroblasts with PR_b functionalized or non-targeted stealth liposomes (Fig. 32). As a control, these cells were transfected with pT2/Cal in PR_b functionalized stealth liposomes. Successful cytotoxic therapy was

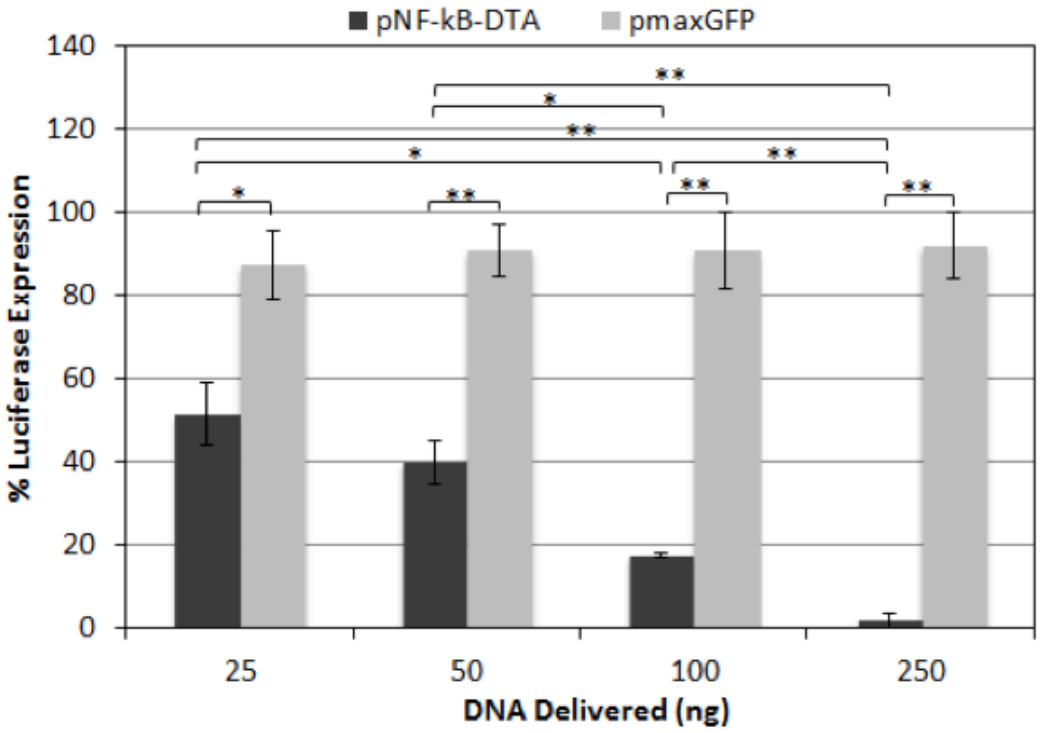

Figure 33. DTA mediated inhibition of protein expression in DLD-1 cells.
5 mol % PR_b functionalized stealth liposomes were used to transfect cells with 100 ng of pT2/Cal plasmid and different amounts of pNF-κB-DTA or pmaxGFP for 48 h at 37 °C. Luminescence was measured with a luciferase expression assay kit and reported as a percentage of expression from control cells that received only the pT2/Cal plasmid. Data presented as average ± standard error of three independent experiments (n=3), done in triplicate. Student's t-test statistical analysis was performed, * indicates $p<0.05$, ** $p<0.005$, absence of brackets for $p>0.05$.

observed only when PR_b functionalized stealth liposomes were used to transfect pNF-κB-DTA in DLD-1 colorectal cancer cells, that is when both levels of targeting were used and both targets were upregulated in the cells. While more than 60% of cancer cells were killed, on average only 15% of the healthy cells were affected. This low level of non-specific cell cytoxicity is thought to be a result of a combination of DTA expression from background NF-κB activity and cytotoxicity from the bPEI used to condense the pDNA.

5.4.4 Further characterization of DTA activity

To relate the cytotoxic effect seen in the cancer cells to DTA production, we further investigated the effect of delivering pNF-κB-DTA to DLD-1 cancer cells

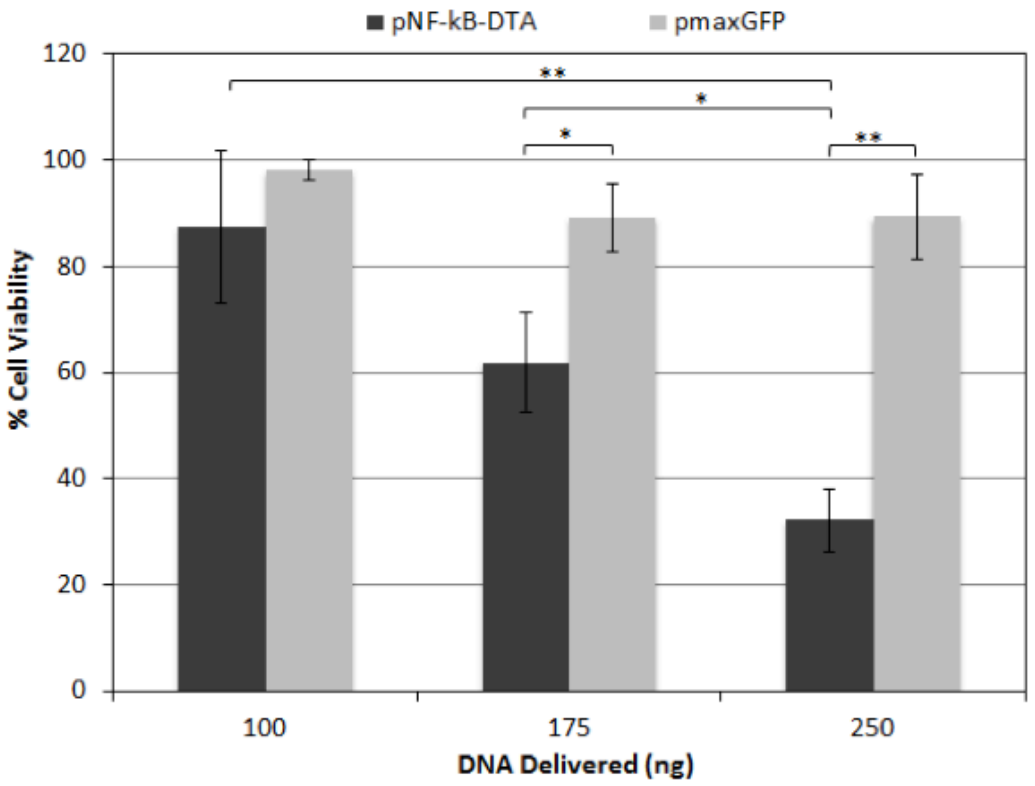

Figure 34. Cytotoxic dose response to increasing pNFκB-DTA delivery. DLD-1 cells were transfected with different amounts of pNF-κB-DTA or pmaxGFP encapsulated in 5 mol% PR_b functionalized stealth liposomes for 72 h at 37 °C. Cell viability was measured using WST-1 metabolic assay and reported as a percentage of the viability of untreated cells. Data presented is average ± standard error of four independent experiments (n=4), done in triplicate. Student's t-test statistical analysis was performed, * indicates $p<0.05$, ** $p<0.005$, absence of brackets for $p>0.05$.

using several different techniques. First, RT-PCR was used to measure the amount of DTA mRNA produced in DLD-1 cells after transfection with pNF-κB-DTA using PR_b functionalized or non-targeted stealth liposomes. DTA mRNA was detected in transfected cells and the levels were 4.5 ± 0.6 times (Ave ± SD from n=3, done in triplicate) higher when PR_b functionalized stealth liposomes were used versus non-targeted stealth liposomes. This explains the low level of cytotoxicity seen when DLD-1 cells are transfected with pNF-κB-DTA encapsulated in non-targeted stealth liposomes, and shows the control over gene expression exerted by the first level of our multi-targeting approach – targeting the extracellular $\alpha_5\beta_1$ integrin.

Second, to investigate the mode of action of DTA in killing cells we measured protein expression after transfecting DLD-1 cells with pNF-κB-DTA encapsulated in PR_b functionalized stealth liposomes. DTA is thought to cause cell death by inhibiting protein expression.[227] DLD-1 cells were co-transfected with pT2/Cal and pNF-κB-DTA and luciferase expression was measured relative to cells that received only pT2/Cal (Fig. 33). Co-transfection with pmaxGFP, a GFP expressing plasmid, was used as a control. A dose dependent reduction in luciferase expression was seen with the delivery of increasing amounts of pNF-κB-DTA. A substantial level of protein inhibition was observed even at 25 ng of pNF-κB-DTA delivered, the lowest amount of DNA delivery investigated in the current studies. When 250 ng of pNF-κB-DTA was delivered we observed instances where the level of protein expression went down below detectable levels.

Third, to complement these protein expression inhibition studies we measured the effect of DNA dosage on cytotoxicity in DLD-1 cells. With increasing amounts of pNF-κB-DTA delivered in PR_b functionalized stealth liposomes, increased cytotoxicity was seen (Fig. 34). There was no corresponding trend observed when pmaxGFP was used as a control, showing on average less than 10% non-specific cytoxicity at all pDNA concentrations delivered. Interestingly, cytotoxicity was not observed in DLD-1 cells at 100 ng of pNF-κB-DTA delivered, an amount which resulted in 82.5±0.5% protein inhibition (Fig. 33). Our results therefore suggest that protein production may need to be completely halted before cytotoxicity results in DLD-1 cancer cells.

5.4.5 pNF-κB-DTA is a versatile plasmid capable of killing a variety of cancer types

We also wanted to investigate the versatility of the pNF-κB-DTA plasmid in killing different types of cancer and diseased cells. To this end, pNF-κB-DTA encapsulated in PR_b functionalized stealth liposomes was delivered to MCA38 murine colon cancer cells, MCF7 human breast cancer cells, and TNF-α induced HEK293T human embryonic kidney cells while using pmaxGFP as a control. In all these cell lines, a high level of cytotoxicity was observed after transfection with

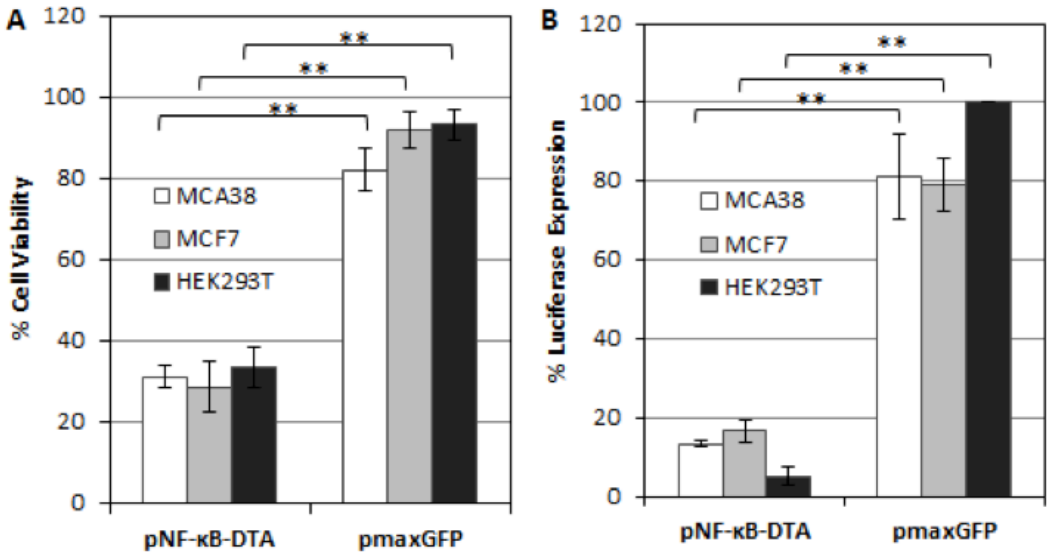

Figure 35. Demonstrating versatility of pNF-κB-DTA
A) DTA mediated cytotoxicity in MCA38 murine colon cancer cells, MCF7 human breast cancer cells and TNF-α induced HEK293T human embryonic kidney cells. 100 ng of pNF-κB-DTA or pmaxGFP encapsulated in 5 mol% PR_b functionalized stealth liposomes were used to transfect cells for 72 h at 37 °C, followed by measuring cell viability using a WST-1 metabolic assay as a percentage of untreated samples. B) DTA mediated inhibition of protein expression in MCA38 cells, MCF7 cells and TNF-α induced HEK293T cells. 5 mol% PR_b functionalized stealth liposomes were used to transfect cells with 100 ng of pT2/Cal plasmid and 100 ng of pNF-κB-DTA or pmaxGFP for 48 h at 37 °C. Luminescence was measured with a luciferase expression assay kit and reported as a percentage of expression from control cells that received only the pT2/Cal plasmid. Data presented is average ± standard error of three independent experiments (n=3), done in triplicate. Student's t-test statistical analysis was performed, ** indicates $p<0.005$.

pNF-κB-DTA compared to the control (Fig. 35A). Furthermore, for each of the cell lines tested DTA was shown to inhibit protein production (Fig. 35B). Taken together, these results demonstrate the versatility of pNF-κB-DTA in killing cancer cells and TNF-α induced HEK293T cells. Also, pNF-κB-DTA was able to kill MCA38, MCF7 and HEK293T induced cells effectively at only 100 ng delivery, in contrast to the higher amounts required for DLD-1 cells. This is likely due to differences in transfection efficiency and differential effectiveness of DTA in different cell lines.[45]

5.5 Discussion

In this paper we focused on the problem of specific delivery of non-viral gene delivery vehicles to cancer cells versus healthy cells *in vitro*. However, the same

problem of off target extracellular receptor expression is prevalent in other therapeutic strategies. For example, an exciting new development in gene therapy is reengineered T cells that can be specifically activated upon interaction with the CD19 receptor found on B cell lymphomas.[228] Unfortunately, CD19 is also expressed on normal B cells.[229] Similarly, myelodysplastic syndrome associated stem cells that progress into amyeloid leukemia offer no distinguishing extracellular receptors compared to normal cells.[230] In situations like these, a multi-targeted therapeutic system could aid recognition of and therapeutic delivery into target cells and subsequently transcriptionally control the expression of a desired gene therapy product.

The regulation of gene expression in mammalian cells however is a complex process. Tumor specific promoters may be regulated by many different transcriptional components. For example, tumor specific promoters previously used in transcriptional targeting such as survivin and H19 [86,231] are regulated by the SP1, E2F, and C/EBP families of transcription factors and their cofactors.[232,233] The involvement of multiple transcription factors and regulatory components may substantially increase the noise in gene expression.[234] While noise in gene expression can be useful in regulatory events in the cell, it can also lead to unpredictable heterogeneous outcomes following uniform inputs.[235] Therefore, the simplicity of a design where gene expression is mediated by a single upregulated transcription factor may be attractive for building more controllable and predictable gene delivery vectors. A similar effect can be obtained by trimming full promoters of upregulated genes to the bare minimum essential for transcription, as was done for HIF-1α.[236] In our design, expression of DTA is regulated by five tandem repeats of a 10 bp NF-κB responsive element (Fig. 31).

We developed a multi-targeted gene delivery system combining extracellular receptor targeting and transcriptional targeting and showed improved specificity of gene expression in cancer cells compared to healthy cells *in vitro*. The PR_b peptide targets the $\alpha_5\beta_1$ integrin receptor and allows for subsequent internalization of the nanoparticles and release of the payload by cells that

overexpress the integrin compared to non-targeted stealth liposomes (Figs. 29 and 32). Previous work in our group showed that PR_b functionalized nanoparticles bind with high specificity to $\alpha_5\beta_1$ and internalization of PR_b functionalized vesicles was absent on cells where the integrin was minimally expressed.[186,204] We further showed that the strategy of using a second level of control for gene expression can successfully relieve the problems of non-specificity faced by current extracellular receptor targeted gene delivery vectors. The increased transcriptional activity of NF-κB in cancer cells versus healthy cells (Fig. 28A) resulted in a twenty-fold increase in luciferase expression (Fig. 29) and substantial cytotoxicity in DLD-1 colorectal cancer cells compared to healthy BJ fibroblast cells (Figs. 32 and 34). Furthermore, the lack of detectable gene expression in the absence of this NF-κB binding element demonstrates the strict control over gene expression exerted by a single transcription factor (Fig 29). The versatility of the constructed pNF-κB-DTA plasmid was demonstrated by successfully inhibiting protein expression and inducing apoptosis in DLD-1 human colorectal cancer cells, MCA38 murine colon cancer cells, MCF7 human breast cancer cells and TNF-α induced HEK293T human embryonic kidney cells (Fig. 35). While the inhibition of protein expression seemed to be similarly effective in all cell lines tested (Figs. 33 and 35B), DLD-1 cells seemed to require a higher dose of pNF-κB-DTA for a cytotoxic effect (Fig. 34). This may be an indication of differential activity of DTA in different cancer or diseased cell lines.[45] We also noticed a low background level of cytotoxicity (Fig. 32) that could be generated by a combination of DTA expression from background NF-κB activity and from the bPEI used to condense the pDNA.

Upregulated NF-κB can be responsible for chemoresistance in cancer.[43] Some successful cancer therapy strategies involve administering NF-κB inhibitors in conjunction to chemotherapy,[44,237] where the reduction in cancer chemoresistance leads to better treatment outcomes. In contrast, our approach uses NF-κB itself to drive therapy in cancer cells and turns cancer cell strength into a weakness. For example, in cases where inhibiting NF-κB activity is ineffective in promoting cancer therapy,[238] targeting NF-κB activity itself to drive

therapy can be a potential solution. MCF7 breast cancer cells, one of the cell lines that failed to respond to chemotherapy after NF-κB inhibition [238], were eradicated with pNF-κB-DTA. This form of NF-κB mediated cancer therapy may also have the potential to be an adjuvant to current chemo- and radiation therapies. In fact, by identifying and killing NF-κB overexpressing, potentially chemoresistant cancer cells, NF-κB mediated therapy may reduce chemo- and radiation therapy dosage - thereby alleviating undesirable side effects of these traditional forms of therapy.

Our results demonstrate the potential of driving therapeutic gene expression where both with the $\alpha_5\beta_1$ integrin and a single transcription factor, NF-κB, are upregulated and warrants further investigation of our design as a new form of cancer multi-targeting. One drawback of the current target pair though is that they may both be expressed in non-cancerous inflamed tissues, and can therefore limit the application of our current delivery system when inflammatory diseases (such as rheumatoid arthritis or asthma) and cancer are both present.[239,240] However, with recent advances in high throughput screening and the ability to determine cell phenotypes quickly, other cancer specific pairs of extracellular receptors and transcriptional targets can be identified.

5.6 Conclusion

We designed a modular non-viral multi-targeted gene delivery platform, and applied it in the construction of a model system for specific delivery to cancer by targeting the overexpressed cancer surface marker $\alpha_5\beta_1$ integrin and the upregulated transcriptional activity of NF-κB. We delivered a cytotoxic DTA gene using our gene delivery platform and demonstrated specific cytotoxicity in several different cancer cell lines while generating minimal non-specific cytotoxicity in healthy cells. Our multifunctional design therefore has the potential to simultaneously address two major problems facing cancer therapy, namely non-specificity of gene expression and NF-κB mediated cancer resistance. The transcriptional activity of NF-κB warrants further investigation as a therapeutic target. Moreover, the versatility of the gene delivery platform developed here can facilitate its use in applications beyond cancer.

Chapter 6. Concluding remarks and future directions

This thesis brings together two separate technologies, self-assembly of biomimetic amphiphiles and genetics, and applies them to cancer therapy. The observations and conclusions presented here can be used as a guide for future work to further advance cancer-specific gene therapy. Through the course of this chapter, several modifications to the current design are suggested to improve efficiency of gene delivery. Some immediate next steps are outlined, and possible long-term future directions are discussed.

6.1 General contributions to the field

When seeking receptor targets for gene therapy, the current prevalent requirement is overexpression on target tissues. However, results presented in Chapter 4 indicate that for successful targeted gene therapy, the optimal receptors should possess several other criteria beyond this sole requirement of overexpression. Receptors that have fast internalization kinetics and are taken up in routes conducive to gene expression are optimal. Adding these criteria to the list of optimum receptor properties may lead to the design of more efficient transfection agents. In Chapter 4, $\alpha_5\beta_1$ integrin is linked to caveolae-mediated endocytosis and a semi-quantitative measure of its internalization kinetics is presented for DLD-1 colorectal cancer cells. A collection of similar sets of data, for other extracellular receptors in different cell lines, can help in selecting appropriate target receptors suited to the application at hand.

Chapter 4 showed that PR_b functionalized stealth liposomes were internalized partially by caveolae-mediated endocytosis, which in turn has previously been shown to be involved with transcytosis in endothelial cells in vivo.[241–243] It may be worth investigating if there is a direct link between $\alpha_5\beta_1$ integrin mediated internalization of PR_b functionalized nanoparticles and transcytosis. Many in vitro models for investigating transcytosis have been extensively reviewed by Tuma and Hubbard,[244] and one such experimental model can be adapted to

study the uptake of PR_b functionalized vectors. Transcytosing delivery systems can be used to treat tumors at their earlier stages, even before they develop the extensive, irregular vasculature that is currently essential for the EPR effect. Catching and treating cancer early can greatly improve treatment outcome.

6.2 Design improvements for PR_b functionalized transfection agent

PR_b functionalized stealth liposome have many strengths as a cancer specific gene delivery vehicle. Chapter 3 presents its specificity for $\alpha_5\beta_1$ integrin bearing cells through in vitro and in vivo experiments; chapter 4 illustrates its high stability, fast internalization kinetics, and discusses the benefits it experiences from caveolar mediated endocytosis. Unfortunately, this system lacks efficient endosomal escape properties, most likely due to ineffective proton sponge effect mediated by bPEI. Thus, identifying a cationic polymer that has better endosomal release properties can benefit the current design. High throughput screening can be used on large combinatorial libraries of polymers with unique properties to identify the most desirable candidates.[245]

The incorporation of PEG has been previously shown to reduce transfection efficiency. However, PEG imparts essential stability to transfection agents, and it may be indispensible in an in vivo application. One suggested solution to this is the incorporation of PEG on the nanoparticle surface through acid labile linkages that are disrupted in the acidic tumor microenvironment. Such acid labile linkages can include vinyl ether, orthoester, diorthoester, phosphoramidate, hydrazone and β-thiopropionate. Upon losing the PEG layer, the particle surface is exposed, thereby increasing the chances of the targeting ligand finding its receptor. In addition, once internalized the particle can interact more effectively with the endosomal membrane thereby facilitating endosomal release.

In Chapter 3, the challenges of encapsulating DNA polyplexes in liposomes were discussed. While a formulation process to address these challenges was outlined, there remains room for improvement. Currently, the average encapsulation yield is approximately 40% based on concentration, and 25%

based on mass. This is sufficient for the in vitro and the initial in vivo experiments presented here, but the inefficiencies can be considerable upon scaling up for larger in vivo experiments. Therefore, it may be worth revisiting condensation variables in an effort to make polyplexes smaller to improve encapsulation. Yet another option may be to replace large plasmid DNA with smaller genetic loads. Plasmid DNA, as discussed in Section 2.2.2, often has components not essential to therapy, thereby making it larger than necessary. Minicircles and siRNA are two other options that have been shown to achieve effective gene therapy.[246,247] Minicircles are minimal expression cassettes, derived from plasmid DNA, that lack antibiotic resistance genes, origin of replication and bacterial inflammatory sequences; siRNA are 21-23 nucleotide duplexes that can regulate protein production by interacting with mRNA in a sequence specific manner and hindering translation. Minicircles and siRNA are both are much smaller than plasmid DNA, and this can significantly improve liposome encapsulation yields. Many of the techniques developed in formulating and characterizing plasmid DNA encapsulated liposomes presented in Chapters 3 and 4 can be readily applied to the encapsulation of minicircles and siRNA.

6.3 Further in vivo investigation of PR_b functionalized transfection agent

The ultimate objective of developing tumor specific gene delivery systems is to achieve target specific gene delivery in an in vivo setting. Qualitative biodistribution data from in vivo experiments presented in Chapter 3 show that PR_b functionalized stealth liposomes are a promising non-viral gene delivery vehicle. After incorporation of the design improvements suggested above, the system should be further investigated in vivo to generate quantitative time-dependent biodistribution data for nanoparticle localization as well as gene expression. Further modifications to the design may be necessary to improve cancer specific distribution in an in vivo setting. In particular, PEG length and surface concentration, and the inclusion of acid-labile linkages may be some of the parameters worth testing.

Following in vivo administration of PR_b functionalized nanoparticles, immunohistochemistry of organs can yield further information on particle distribution at the tissue level. For example, such experiments can be used to investigate the depth of tumor penetration. Tumor penetration is a major problem in the delivery of therapeutics to tumors.[248] In most cases, therapeutics delivered within nanoparticles are only able to migrate a certain distance after extravasation before being absorbed by the surrounding tissue. This means any therapeutic effect is felt within a certain maximum radial distance from the supplying blood vessel, and tumor tissue further away receive no treatment. PR_b functionalized nanoparticles can be optimized to perform better in vivo by characterizing and understanding the barriers faced in tumor penetration.

6.4 Further investigation of NF-κB transcriptional targeting

Chapter 5 presents a form of transcriptional targeting not previously investigated. Instead of selecting a promoter based on the level of expression of its downstream gene, a minimal promoter was chosen based on the level of activation of the single transcription factor it binds. Therefore, for the first time, the transcriptional activity of a single upregulated transcription factor was used to drive therapeutic gene expression specifically in cancer cells. This approach to transcriptional targeting adds a useful new tool to the field of gene therapy.

Chapter 5 also hypothesized several advantages of targeting the activity of a single transcription factor, supported by evidence from literature. Experimental investigations of these hypotheses may be useful. Specifically, a minimal promoter, such as the NF-κB responsive element used in Chapter 5, should be compared to a full promoter also responsive to NF- κB for noise level and controllability in gene expression. To generalize trends, the comparative investigation can be carried out for different transcription factors, regulating minimal or full promoters, in a variety of different cell lines.

The multi-targeted gene delivery system developed in Chapter 5 could effectively differentiate between cancer cells and healthy cells bearing the same extracellular surface marker, and mediate target specific gene expression.

However, a major problem in in vivo administration of nanoparticle delivery systems is uptake by the MPS as discussed throughout this thesis. Macrophages take up nanoparticles irrespective of the targeting ligand on their surface, so it falls to the second level of targeting, i.e. the transcriptional activity of NF-κB in this case, to ensure therapeutic genes are not expressed in these cells. It would therefore be useful to investigate the expression levels and transcriptional activity of NF-κB in an initial in vitro model of macrophages.

After further optimization of the PR_b functionalized transfection agent in vitro and in vivo as described above, the NF-κB regulated plasmid DNA (or minicircle) can be encapsulated to generate an optimized multi-targeted gene delivery system for in vivo animal model experiments. The optimal dosing regimen, in terms of amount of DNA delivered and frequency of administration should be determined for efficient therapy indicated by reduction in tumor growth rate and tumor size. Furthermore, the levels and cancer specificity of gene expression should be compared between PR_b functionalized stealth liposome encapsulating therapeutic genes, such as DTA, under the control of either an NF-κB responsive element or a constitutive promoter. In vitro, the NF-κB responsive element was shown to mediate the same level of gene expression in DLD-1 cancer cells as a strong constitutive promoter (Fig. 29). It would be interesting to see if the effect is maintained in an in vivo setting.

6.5 Modularity of design

NF-κB and $\alpha_5\beta_1$ integrin were chosen as cancer-specific targets here as they are both well-established markers of cancer. Experiments presented in Chapter 5 demonstrate the viability of a multi-targeted gene delivery concept in an in vitro setting. The two major building blocks in this design, biomimetic peptide amphiphiles and genetics, are both tunable technologies. With advances in screening and generating peptide libraries, and our increased understanding of self-assembly processes, the biomimetic peptide amphiphiles can be tuned for diverse applications. Researchers in the life sciences are standardizing genetics and genetic manipulation methods, and they have set up a genetic parts registry (http://parts.igem.org) that allows mixing and matching of components to create

robust gene networks with novel functionalities. The possible modular combinations of our two tunable technologies may become virtually limitless as these fields continue to advance. Thus, moving forward, the modularity of the platform assembled here should allow the targeting of different pairs of overexpressed extracellular receptors and upregulated transcription factors, in applications medically relevant and otherwise.

6.6 Final words

Self-assembled biomimetic amphiphiles and genetics are tunable, flexible and modular technologies– and their combinations can result in robust therapeutic strategies. This notion is demonstrated here through the development of a novel cancer-targeting therapeutic strategy. Biomimimetic peptide amphiphiles were combined with transcriptional targeting to create a multi-functional gene delivery vehicle that compact and protect DNA, evade the MPS, specifically bind and internalize into $\alpha_5\beta_1$ integrin bearing cells, and mediate NF-κB regulated gene expression. Genetics and gene delivery may be the keys to the future of healthcare. The findings and ideas reported here will be a sturdy foothold from which interested researchers can further develop these technologies.

References

(1) Henley, S. H.; King, J. B.; German, R. R.; Richardson, L. C.; Plescia, M. Surveillance of Screening-Detected Cancers (Colon and Rectum, Breast, and Cervix) --- United States, 2004--2006. *Morb. Mortal. Wkly. Rep.* **2010**, *59*, 1–25.

(2) Taplin, S. H.; Ichikawa, L.; Yood, M. U.; Manos, M. M.; Geiger, A. M.; Weinmann, S.; Gilbert, J.; Mouchawar, J.; Leyden, W. A.; Altaras, R.; Beverly, R. K.; Casso, D.; Westbrook, E. O.; Bischoff, K.; Zapka, J. G.; Barlow, W. E. Reason for late-stage breast cancer: absence of screening or detection, or breakdown in follow-up? *J. Natl. Cancer Inst.* **2004**, *96*, 1518–1527.

(3) Guo, X.; Huang, L. Recent advances in nonviral vectors for gene delivery. *Acc. Chem. Res.* **2011**, *45*, 971–979.

(4) Giacca, M.; Zacchigna, S. Virus-mediated gene delivery for human gene therapy. *J. Control. Release* **2012**, *161*, 377–388.

(5) Li, S.-D.; Huang, L. Non-viral is superior to viral gene delivery. *J. Control. Release* **2007**, *123*, 181–183.

(6) Mintzer, M. A.; Simanek, E. E. Nonviral Vectors for Gene Delivery. *Chem. Rev.* **2009**, *109*, 259–302.

(7) Drummond, D. C.; Meyer, O.; Hong, K.; Kirpotin, D. B.; Papahadjopoulos, D. Optimizing Liposomes for Delivery of Chemotherapeutic Agents to Solid Tumors. *Pharmacol. Rev.* **1999**, *51*, 691–743.

(8) Liu, M.; Li, C.; Pazgier, M.; Li, C.; Mao, Y.; Lv, Y.; Gu, B.; Wei, G.; Yuan, W.; Zhan, C.; Lu, W.-Y.; Lu, W. D-peptide inhibitors of the p53-MDM2 interaction for targeted molecular therapy of malignant neoplasms. *Proc. Natl. Acad. Sci. U. S. A.* **2010**, *107*, 14321–14326.

(9) Schiffelers, R. M.; Koning, G. A.; Ten Hagen, T. L. M.; Fens, M. H. A. M.; Schraa, A. J.; Janssen, A. P. C. A.; Kok, R. J.; Molema, G.; Storm, G. Anti-tumor efficacy of tumor vasculature-targeted liposomal doxorubicin. *J. Control. Release* **2003**, *91*, 115–122.

(10) Pangburn, T. O.; Petersen, M. A.; Waybrant, B.; Adil, M. M.; Kokkoli, E. Peptide- and aptamer-functionalized nanovectors for targeted delivery of therapeutics. *J. Biomech. Eng.* **2009**, *131*, 074005.

(11) Fens, M. H. A. M.; Hill, K. J.; Issa, J.; Ashton, S. E.; Westwood, F. R.; Blakey, D. C.; Storm, G.; Ryan, a J.; Schiffelers, R. M. Liposomal encapsulation enhances the antitumour efficacy of the vascular disrupting agent ZD6126 in murine B16.F10 melanoma. *Br. J. Cancer* **2008**, *99*, 1256–1264.

(12) Jiang, J.; Yang, S.-J.; Wang, J.-C.; Yang, L.-J.; Xu, Z.-Z.; Yang, T.; Liu, X.-Y.; Zhang, Q. Sequential treatment of drug-resistant tumors with RGD-modified liposomes containing

siRNA or doxorubicin. *Eur. J. Pharm. Biopharm. Off. J. Arbeitsgemeinschaft fur Pharm. Verfahrenstechnik eV* **2010**, *76*, 170–178.

(13) Dubey, P. K.; Mishra, V.; Jain, S.; Mahor, S.; Vyas, S. P. Liposomes modified with cyclic RGD peptide for tumor targeting. *J. Drug Target.* **2004**, *12*, 257–264.

(14) Gong, J.; Wang, D.; Sun, L.; Zborowska, E.; Willson, J. K. V; Brattain, M. G. Role of α5β1 Integrin in Determining Malignant Properties of Colon Carcinoma Cells. *Cell Growth Differ.* **1997**, *8*, 83–90.

(15) Jayne, D. G.; Heath, R. M.; Dewhurst, O.; Scott, N.; Guillou, P. J. Extracellular matrix proteins and chemoradiotherapy: alpha5beta1 integrin as a predictive marker in rectal cancer. *Eur. J. Surg. Oncol.* **2002**, *28*, 30–36.

(16) Darribère, T.; Skalski, M.; Cousin, H. L.; Gaultier, A.; Montmory, C.; Alfandari, D. Integrins: regulators of embryogenesis. *Biol. cell* **2000**, *92*, 5–25.

(17) Mardilovich, A.; Craig, J. A.; McCammon, M. Q.; Garg, A.; Kokkoli, E. Design of a novel fibronectin-mimetic peptide-amphiphile for functionalized biomaterials. *Langmuir* **2006**, *22*, 3259–3264.

(18) Craig, J. A.; Rexeisen, E. L.; Mardilovich, A.; Shroff, K.; Kokkoli, E. Effect of linker and spacer on the design of a fibronectin-mimetic peptide evaluated via cell studies and AFM adhesion forces. *Langmuir* **2008**, *24*, 10282–10292.

(19) Garg, A.; Tisdale, A. W.; Haidari, E.; Kokkoli, E. Targeting colon cancer cells using PEGylated liposomes modified with a fibronectin-mimetic peptide. *Int. J. Pharm.* **2009**, *366*, 201–210.

(20) Demirgöz, D.; Garg, A.; Kokkoli, E. PR_b-targeted PEGylated liposomes for prostate cancer therapy. *Langmuir* **2008**, *24*, 13518–13524.

(21) Atchison, N. A.; Fan, W.; Papas, K. K.; Hering, B. J.; Tsapatsis, M.; Kokkoli, E. Binding of the fibronectin-mimetic peptide, PR_b, to alpha5beta1 on pig islet cells increases fibronectin production and facilitates internalization of PR_b functionalized liposomes. *Langmuir* **2010**, *26*, 14081–14088.

(22) Payne, C. K.; Jones, S. A.; Chen, C.; Zhuang, X. Internalization and trafficking of cell surface proteoglycans and proteoglycan-binding ligands. *Traffic* **2007**, *8*, 389–401.

(23) Colin, M.; Maurice, M.; Trugnan, G.; Kornprobst, M.; Harbottle, R. P.; Knight, A.; Cooper, R. G.; Miller, A. D.; Capeau, J.; Coutelle, C.; Brahimi-Horn, M. C. Cell delivery , intracellular trafficking and expression of an integrin-mediated gene transfer vector in tracheal epithelial cells. *Gene Ther.* **2000**, *7*, 139–152.

(24) El-Sayed, A.; Harashima, H. Endocytosis of Gene Delivery Vectors: From Clathrin-dependent to Lipid Raft-mediated Endocytosis. *Mol. Ther.* **2013**, *21*, 1118–1130.

(25) Ur Rehman, Z.; Hoekstra, D.; Zuhorn, I. S. Protein kinase A inhibition modulates the intracellular routing of gene delivery vehicles in HeLa cells, leading to productive transfection. *J. Control. Release* **2011**, *156*, 76–84.

(26) Zhang, X.-X.; Allen, P. G.; Grinstaff, M. Macropinocytosis is the major pathway responsible for DNA transfection in CHO cells by a charge-reversal amphiphile. *Mol. Pharm.* **2011**, *8*, 758–766.

(27) Rejman, J.; Bragonzi, A.; Conese, M. Role of clathrin- and caveolae-mediated endocytosis in gene transfer mediated by lipo- and polyplexes. *Mol. Ther.* **2005**, *12*, 468–474.

(28) Sarkar, K.; Kruhlak, M. J.; Erlandsen, S. L.; Shaw, S. Selective inhibition by rottlerin of macropinocytosis in monocyte-derived dendritic cells. *Immunology* **2005**, *116*, 513–524.

(29) Moghimi, S. M.; Szebeni, J. Stealth liposomes and long circulating nanoparticles: critical issues in pharmacokinetics, opsonization and protein-binding properties. *Prog. Lipid Res.* **2003**, *42*, 463–478.

(30) Juliano, R. L.; Ming, X.; Nakagawa, O.; Xu, R.; Yoo, H. Integrin Targeted Delivery of Gene Therapeutics. *Theranostics* **2011**, *1*, 211–219.

(31) Ciardiello, F. EGFR Antagonists in Cancer Treatment. *N. Engl. J. Med.* **2008**, *358*, 1160–1174.

(32) Wesche, J.; Haglund, K.; Haugsten, E. M. Fibroblast growth factors and their receptors in cancer. *Biochem. J.* **2011**, *437*, 199–213.

(33) Parsons-Wingerter, P.; Kasman, I. M.; Norberg, S.; Magnussen, A.; Zanivan, S.; Rissone, A.; Baluk, P.; Favre, C. J.; Jeffry, U.; Murray, R.; McDonald, D. M. Uniform Overexpression and Rapid Accessibility of α5β1 Integrin on Blood Vessels in Tumors. *Am. J. Pathol.* **2005**, *167*, 193–211.

(34) Koretz, K.; Schlag, P.; Möller, P. Expression of epidermal growth factor receptor in normal colorectal mucosa, adenoma, and carcinoma. *Virchows Arch. A. Pathol. Anat. Histopathol.* **1990**, *416*, 343–349.

(35) Hughes, S. E. Differential Expression of the Fibroblast Growth Factor Receptor (FGFR) Multigene Family in Normal Human Adult Tissues. *J. Histochem. Cytochem.* **1997**, *45*, 1005–1019.

(36) Hine, C. M.; Seluanov, A.; Gorbunova, V. Use of the Rad51 promoter for targeted anti-cancer therapy. *Proc. Natl. Acad. Sci. U. S. A.* **2008**, *105*, 20810–20815.

(37) Gu, J.; Kagawa, S.; Takakura, M.; Kyo, S.; Inoue, M.; Roth, J. A.; Fang, B. Tumor-specific transgene expression from the human telomerase reverse transcriptase promoter enables targeting of the therapeutic effects of the Bax gene to cancers. *Cancer Res.* **2000**, *60*, 5359–5364.

(38) Barnett, B. G.; Tillman, B. W.; Curiel, D. T.; Douglas, J. T. Dual targeting of adenoviral vectors at the levels of transduction and transcription enhances the specificity of gene expression in cancer cells. *Mol. Ther.* **2002**, *6*, 377–385.

(39) Barker, S. D.; Dmitriev, I. P.; Nettelbeck, D. M.; Liu, B.; Rivera, A. A.; Alvarez, R. D.; Curiel, D. T.; Hemminki, A. Combined transcriptional and transductional targeting improves the specificity and efficacy of adenoviral gene delivery to ovarian carcinoma. *Gene Ther.* **2003**, *10*, 1198–1204.

(40) Müller, O. J.; Leuchs, B.; Pleger, S. T.; Grimm, D.; Franz, W.-M.; Katus, H. A.; Kleinschmidt, J. A. Improved cardiac gene transfer by transcriptional and transductional targeting of adeno-associated viral vectors. *Cardiovasc. Res.* **2006**, *70*, 70–78.

(41) Nahde, T.; Müller, K.; Fahr, A.; Müller, R.; Brüsselbach, S. Combined transductional and transcriptional targeting of melanoma cells by artificial virus-like particles. *J. Gene Med.* **2001**, *3*, 353–361.

(42) Karin, M.; Cao, Y.; Greten, F. R.; Li, Z.-W. NF-kappaB in cancer: from innocent bystander to major culprit. *Nat. Rev. Cancer* **2002**, *2*, 301–310.

(43) Baldwin, A. S. Control of oncogenesis and cancer therapy resistance by the transcription factor NF-κB. *J. Clin. Invest.* **2001**, *107*, 241–246.

(44) Bivona, T. G.; Hieronymus, H.; Parker, J.; Chang, K.; Taron, M.; Rosell, R.; Moonsamy, P.; Dahlman, K.; Miller, V. a; Costa, C.; Hannon, G.; Sawyers, C. L. FAS and NF-κB signalling modulate dependence of lung cancers on mutant EGFR. *Nature* **2011**, *471*, 523–526.

(45) Zhang, Y.; Schulte, W.; Pink, D.; Phipps, K.; Zijlstra, A.; Lewis, J. D.; Waisman, D. M. Sensitivity of cancer cells to truncated diphtheria toxin. *PLoS One* **2010**, *5*, e10498.

(46) Huang, Y.-H.; Zugates, G. T.; Peng, W.; Holtz, D.; Dunton, C.; Green, J. J.; Hossain, N.; Chernick, M. R.; Padera, R. F.; Langer, R.; Anderson, D. G.; Sawicki, J. a Nanoparticle-Delivered Suicide Gene Therapy Effectively Reduces Ovarian Tumor Burden in Mice. *Cancer Res.* **2009**, *69*, 6184–6191.

(47) Bangham, A. D.; Horne, R. W. Negative staining of phospholipids and their structural modification by surface-active agents as observed in the electron microscope. *J. Mol. Biol.* **1964**, *8*, 660–IN10.

(48) Legha, S. S.; Benjamin, R. S.; Mackay, B.; Ewer, M.; Wallace, S.; Valdivieso, M.; Rasmussen, S. L.; Blumenschein, G. R.; Freireich, E. J. Reduction of doxorubicin cardiotoxicity by prolonged continuous intravenous infusion. *Ann. Intern. Med.* **1982**, *96*, 133–9.

(49) Juliano, R. L.; Stamp, D. Pharmacokinetics of liposome-encapsulated anti-tumor drugs. *Biochem. Pharmacol.* **1978**, *27*, 21–27.

(50) Gabizon, A. A. Liposomal anthracyclines. *Hematol. Oncol. Clin. North Am.* **1994**, *8*, 431–50.

(51) Gabizon, A.; Meshorer, A.; Barenholz, Y. Comparative long-term study of the toxicities of free and liposome-associated doxorubicin in mice after intravenous administration. *J. Natl. Cancer Inst.* **1986**, *77*, 459–69.

(52) Tanford, C. The hydrophobic effect and the organization of living matter. *Science (80-.).* **1978**, *200*, 1012–1018.

(53) Kimelberg, H. K.; Papahadjopoulos, D. Effects of phospholipid acyl chain fluidity, phase transitions, and cholesterol on (Na+ + K+)-stimulated adenosine triphosphatase. *J. Biol. Chem.* **1974**, *249*, 1071–1080.

(54) Liu, D.; Mori, A.; Huang, L. Role of liposome size and RES blockade in controlling biodistribution and tumor uptake of GM1-containing liposomes. *Biochim. Biophys. Acta* **1992**, *1104*, 95–101.

(55) Liu, S.; Ishida, T.; Kiwada, H. Characterization of bovine serum factor triggering the lysis of liposomes via complement activation. *Biol. Pharm. Bull.* **1998**, *21*, 390–7.

(56) Huong, T. M.; Harashima, H.; Kiwada, H. In vivo studies on the role of complement in the clearance of liposomes in rats and guinea pigs. *Biol. Pharm. Bull.* **1999**, *22*, 515–20.

(57) Torchilin, V. P.; Omelyanenko, V. G.; Papisov, M. I.; Bogdanov, A. A.; Trubetskoy, V. S.; Herron, J. N.; Gentry, C. A. Poly(ethylene glycol) on the liposome surface: on the mechanism of polymer-coated liposome longevity. *Biochim. Biophys. Acta* **1994**, *1195*, 11–20.

(58) Woodle, M. C.; Matthay, K. K.; Newman, M. S.; Hidayat, J. E.; Collins, L. R.; Redemann, C.; Martin, F. J.; Papahadjopoulos, D. Versatility in lipid compositions showing prolonged circulation with sterically stabilized liposomes. *Biochim. Biophys. Acta - Biomembr.* **1992**, *1105*, 193–200.

(59) Klibanov, A. L.; Maruyama, K.; Torchilin, V. P.; Huang, L. Amphipathic polyethyleneglycols effectively prolong the circulation time of liposomes. *FEBS Lett.* **1990**, *268*, 235–237.

(60) Senior, J.; Delgado, C.; Fisher, D.; Tilcock, C.; Gregoriadis, G. Influence of surface hydrophilicity of liposomes on their interaction with plasma protein and clearance from the circulation: studies with poly(ethylene glycol)-coated vesicles. *Biochim. Biophys. Acta* **1991**, *1062*, 77–82.

(61) Gabizon, A.; Chemla, M.; Tzemach, D.; Horowitz, A. T.; Goren, D. Liposome longevity and stability in circulation: effects on the in vivo delivery to tumors and therapeutic efficacy of encapsulated anthracyclines. *J. Drug Target.* **1996**, *3*, 391–398.

(62) Webb, M. S.; Harasym, T. O.; Masin, D.; Bally, M. B.; Mayer, L. D. Sphingomyelin-cholesterol liposomes significantly enhance the pharmacokinetic and therapeutic properties of vincristine in murine and human tumour models. *Br. J. Cancer* **1995**, *72*, 896–904.

(63) Jackson, D. V; Bender, R. A. Cytotoxic thresholds of vincristine in a murine and a human leukemia cell line in vitro. *Cancer Res.* **1979**, *39*, 4346–9.

(64) Jain, R. K. Determinants of tumor blood flow: a review. *Cancer Res.* **1988**, *48*, 2641–58.

(65) Yuan, F.; Leunig, M.; Huang, S. K.; Berk, D. A.; Papahadjopoulos, D.; Jam, R. K. Advances in Brief Microvascular Permeability and Interstitial Penetration of Sterically Stabilized (Stealth) Liposomes in a Human Tumor Xenograft. *Cancer Res.* **1994**, *54*, 3352–3356.

(66) Maeda, H.; Wu, J.; Sawa, T.; Matsumura, Y.; Hori, K. Tumor vascular permeability and the EPR effect in macromolecular therapeutics: a review. *J. Control. release* **2000**, *65*, 271–84.

(67) Makrilia, N.; Kollias, A.; Manolopoulos, L.; Syrigos, K. Cell adhesion molecules: role and clinical significance in cancer. *Cancer Invest*. **2009**, *27*, 1023–37.

(68) Frijns, C. J. M. Inflammatory Cell Adhesion Molecules in Ischemic Cerebrovascular Disease. *Stroke* **2002**, *33*, 2115–2122.

(69) Hillis, G. S.; Flapan, A. D. Cell adhesion molecules in cardiovascular disease: a clinical perspective. *Heart* **1998**, *79*, 429–431.

(70) Liu, G.; Jiang, Y.; Wang, P.; Feng, R.; Jiang, N.; Chen, X.; Song, H.; Chen, Z. Cell adhesion molecules contribute to Alzheimer's disease: multiple pathway analyses of two genome-wide association studies. *J. Neurochem*. **2012**, *120*, 190–8.

(71) Hynes, R. O. Integrins: bidirectional, allosteric signaling machines. *Cell* **2002**, *110*, 673–687.

(72) Ruoslahti, E.; Pierschbacher, M. New perspectives in cell adhesion: RGD and integrins. *Science (80-.)*. **1987**, *238*, 491–497.

(73) Sheu, J. R.; Lin, C. H.; Chung, J. L.; Teng, C. M.; Huang, T. F. Triflavin, an Arg-Gly-Asp-containing antiplatelet peptide inhibits cell-substratum adhesion and melanoma cell-induced lung colonization. *Japanese J. cancer Res*. **1992**, *83*, 885–893.

(74) Soszka, T.; Knudsen, K. A.; Beviglia, L.; Rossi, C.; Poggi, A.; Niewiarowski, S. Inhibition of murine melanoma cell-matrix adhesion and experimental metastasis by albolabrin, an RGD-containing peptide isolated from the venom of Trimeresurus albolabris. *Exp. Cell Res*. **1991**, *196*, 6–12.

(75) Fujii, H.; Nishikawa, N.; Komazawa, H.; Orikasa, A.; Ono, M.; Itoh, I.; Murata, J.; Azuma, I.; Saiki, I. Inhibition of tumor invasion and metastasis by peptidic mimetics of Arg-Gly Asp (RGD) derived from the cell recognition site of fibronectin. *Oncol. Res*. **1996**, *8*, 333–342.

(76) Kumagai, H.; Tajima, M.; Ueno, Y.; Giga-Hama, Y.; Ohba, M. Effect of cyclic RGD peptide on cell adhesion and tumor metastasis. *Biochem. Biophys. Res. Commun*. **1991**, *177*, 74–82.

(77) Komazawa, H.; Saiki, I.; Nishikawa, N.; Yoneda, J.; Yoo, Y. C.; Kojima, M.; Ono, M.; Itoh, I.; Nishi, N.; Tokurat, S.; Azuma, I. Inhibition of tumor metastasis by Arg-Gly-Asp-Ser (RGDS) peptide conjugated with sulfated chitin derivative, SCM-chitin-RGDS. *Clin. Exp. Metastasis* **1993**, *11*, 482–491.

(78) Oku, N.; Tokudome, Y.; Koike, C.; Nishikawa, N.; Mori, H.; Saiki, I.; Okada, S. Liposomal Arg-Gly-Asp analogs effectively inhibit metastatic B16 melanoma colonization in murine lungs. *Life Sci*. **1996**, *58*, 2263–70.

(79) Tirrell, M.; Kokkoli, E.; Biesalski, M. The role of surface science in bioengineered materials. *Surf. Sci*. **2002**, *500*, 61–83.

(80) Akiyama, S. K.; Aota, S.; Yamada, K. M. Function and receptor specificity of a minimal 20 kilodalton cell adhesive fragment of fibronectin. *Cell Adhes. Commun*. **1995**, *3*, 13–25.

(81) García, A. J.; Schwarzbauer, J. E.; Boettiger, D. Distinct activation states of alpha5beta1 integrin show differential binding to RGD and synergy domains of fibronectin. *Biochemistry* **2002**, *41*, 9063–9.

(82) Aota, S.; Nomizu, M.; Yamada, K. M. The short amino acid sequence Pro-His-Ser-Arg-Asn in human fibronectin enhances cell-adhesive function. *J. Biol. Chem.* **1994**, *269*, 24756–61.

(83) Mardilovich, A.; Kokkoli, E. Biomimetic peptide-amphiphiles for functional biomaterials: the role of GRGDSP and PHSRN. *Biomacromolecules* **2004**, *5*, 950–957.

(84) Lodish, H.; Berk, A.; Matsudaira, P.; Kaiser, C. A.; Krieger, M.; Scott, M. P. *Molecular Cell Biology*; 5th ed.; W.H. Freeman and Company: New York, 2004.

(85) Robson, T.; Hirst, D. G. Transcriptional Targeting in Cancer Gene Therapy. *J. Biomed. Biotechnol.* **2003**, *2003*, 110–137.

(86) Sidi, A. A.; Ohana, P.; Benjamin, S.; Shalev, M.; Ransom, J. H.; Lamm, D.; Hochberg, A.; Leibovitch, I. Phase I/II marker lesion study of intravesical BC-819 DNA plasmid in H19 over expressing superficial bladder cancer refractory to bacillus Calmette-Guerin. *J. Urol.* **2008**, *180*, 2379–2383.

(87) Dolcet, X.; Llobet, D.; Pallares, J.; Matias-Guiu, X. NF-kB in development and progression of human cancer. *Virchows Arch. an Int. J. Pathol.* **2005**, *446*, 475–482.

(88) Sovak, M. A.; Bellas, R. E.; Kim, D. W.; Zanieski, G. J.; Rogers, A. E.; Traish, A. M. Aberrant Nuclear Factor-kB/Rel Expression and the Pathogenesis of Breast Cancer. *J. Clin. Invest.* **1997**, *100*, 2952–2960.

(89) Zhou, Y.; Eppenberger-Castori, S.; Eppenberger, U.; Benz, C. C. The NFkappaB pathway and endocrine-resistant breast cancer. *Endocrinerelated cancer* **2005**, *12*, S37–S46.

(90) Li, W.; Tan, D.; Zenali, M. J.; Brown, R. E. Constitutive activation of nuclear factor-kappa B (NF-kB) signaling pathway in fibrolamellar hepatocellular carcinoma. *Int. J. Clin. Exp. Pathol.* **2010**, *3*, 238–243.

(91) Hardwick, J. C.; Van Den Brink, G. R.; Offerhaus, G. J.; Van Deventer, S. J.; Peppelenbosch, M. P. NF-kappaB, p38 MAPK and JNK are highly expressed and active in the stroma of human colonic adenomatous polyps. *Oncogene* **2001**, *20*, 819–827.

(92) Yu, L.; Yu, H.; Yu, J.; Luo, H.; Xu, X.; Li, J. Nuclear factor-ϰB p65 (RelA) transcription factor is constitutively activated in human colorectal carcinoma tissue. **2004**, *10*, 3255–3260.

(93) Sasaki, N.; Morisaki, T.; Hashizume, K.; Yao, T.; Tsuneyoshi, M.; Noshiro, H.; Nakamura, K.; Yamanaka, T.; Uchiyama, a; Tanaka, M.; Katano, M. Nuclear factor-kappaB p65 (RelA) transcription factor is constitutively activated in human gastric carcinoma tissue. *World J. Gastroenterol.* **2001**, *10*, 3255–3260.

(94) Yang, G.-F.; Deng, C.-S.; Xiong, Y.-Y.; Gong, L.-L.; Wang, B.-C.; Luo, J. Expression of nuclear factor-kappa B and target genes in gastric precancerous lesions and

adenocarcinoma: association with Helicobactor pylori cagA (+) infection. *World J. Gastroenterol.* **2004**, *10*, 491–496.

(95) Tang, X.; Liu, D.; Shishodia, S.; Ozburn, N.; Behrens, C.; Lee, J. J.; Hong, W. K.; Aggarwal, B. B.; Wistuba, I. I. Nuclear factor-kappaB (NF-kappaB) is frequently expressed in lung cancer and preneoplastic lesions. *Cancer* **2006**, *107*, 2637–2646.

(96) Shukla, S.; MacLennan, G. T.; Fu, P.; Patel, J.; Marengo, S. R.; Resnick, M. I.; Gupta, S. Nuclear factor-kappaB/p65 (Rel A) is constitutively activated in human prostate adenocarcinoma and correlates with disease progression. *Neoplasia* **2004**, *6*, 390–400.

(97) Gosselin, K.; Touzet, H.; Abbadie, C. Rel/NF-kappaB target genes.

(98) Kunsch, C.; Ruben, S. M.; Rosen, C. a Selection of optimal kappa B/Rel DNA-binding motifs: interaction of both subunits of NF-kappa B with DNA is required for transcriptional activation. *Mol. Cell. Biol.* **1992**, *12*, 4412–4421.

(99) Fischer, D.; Osburg, B.; Petersen, H.; Kissel, T.; Bickel, U. Effect of poly(ethylene imine) molecular weight and pegylation on organ distribution and pharmacokinetics of polyplexes with oligodeoxynucleotides in mice. *Drug Metab. Dispos. Biol. fate Chem.* **2004**, *32*, 983–992.

(100) Liu, F.; Shollenberger, L. M.; Conwell, C. C.; Yuan, X.; Huang, L. Mechanism of naked DNA clearance after intravenous injection. *J. Gene Med.* **2007**, *9*, 613–9.

(101) Fraley, R.; Subramani, S.; Berg, P.; Papahadjopoulos, D. Introduction of liposome-encapsulated SV40 DNA into cells. *J. Biol. Chem.* **1980**, *255*, 10431–5.

(102) Wong, T. K.; Nicolau, C.; Hofschneider, P. H. Appearance of beta-lactamase activity in animal cells upon liposome-mediated gene transfer. *Gene* **1980**, *10*, 87–94.

(103) Nicolau, C. In vivo Expression of Rat Insulin after Intravenous Administration of the Liposome-Entrapped Gene for Rat Insulin I. *Proc. Natl. Acad. Sci.* **1983**, *80*, 1068–1072.

(104) Soriano, P. Targeted and Nontargeted Liposomes for in Vivo Transfer to Rat Liver Cells of a Plasmid Containing the Preproinsulin I Gene. *Proc. Natl. Acad. Sci.* **1983**, *80*, 7128–7131.

(105) Felgner, P. L.; Gadek, T. R.; Holm, M.; Roman, R.; Chan, H. W.; Wenz, M.; Northrop, J. P.; Ringold, G. M.; Danielsen, M. Lipofection: a highly efficient, lipid-mediated DNA-transfection procedure. *Proc. Natl. Acad. Sci. U. S. A.* **1987**, *84*, 7413–7.

(106) Düzgüneş, N.; Felgner, P. L. Intracellular delivery of nucleic acids and transcription factors by cationic liposomes. *Methods Enzymol.* **1993**, *221*, 303–6.

(107) Logan, J. J.; Bebok, Z.; Walker, L. C.; Peng, S.; Felgner, P. L.; Siegal, G. P.; Frizzell, R. A.; Dong, J.; Howard, M.; Matalon Cationic lipids for reporter gene and CFTR transfer to rat pulmonary epithelium. *Gene Ther.* **1995**, *2*, 38–49.

(108) Hyde, S. C.; Gill, D. R.; Higgins, C. F.; Trezise, A. E.; MacVinish, L. J.; Cuthbert, A. W.; Ratcliff, R.; Evans, M. J.; Colledge, W. H. Correction of the ion transport defect in cystic fibrosis transgenic mice by gene therapy. *Nature* **1993**, *362*, 250–5.

(109) Zhu, N.; Liggitt, D.; Liu, Y.; Debs, R. Systemic gene expression after intravenous DNA delivery into adult mice. *Science (80-.).* **1993**, *261*, 209–211.

(110) Plautz, G. E.; Yang, Z. Y.; Wu, B. Y.; Gao, X.; Huang, L.; Nabel, G. J. Immunotherapy of malignancy by in vivo gene transfer into tumors. *Proc. Natl. Acad. Sci. U. S. A.* **1993**, *90*, 4645–9.

(111) Lai, E.; van Zanten, J. H. Evidence of lipoplex dissociation in liquid formulations. *J. Pharm. Sci.* **2002**, *91*, 1225–32.

(112) Harrison, G. S.; Wang, Y.; Tomczak, J.; Hogan, C.; Shpall, E. J.; Curiel, T. J.; Felgner, P. L. Optimization of gene transfer using cationic lipids in cell lines and primary human CD4+ and CD34+ hematopoietic cells. *Biotechniques* **1995**, *19*, 816–23.

(113) Li, S.; Huang, L. In vivo gene transfer via intravenous administration of cationic lipid-protamine-DNA (LPD) complexes. *Gene Ther.* **1997**, *4*, 891–900.

(114) Ginn, S. L.; Alexander, I. E.; Edelstein, M. L.; Abedi, M. R.; Wixon, J. Gene therapy clinical trials worldwide to 2012 - an update. *J. Gene Med.* **2013**, *15*, 65–77.

(115) Vijayanathan, V.; Thomas, T.; Thomas, T. J. DNA nanoparticles and development of DNA delivery vehicles for gene therapy. *Biochemistry* **2002**, *41*, 14085–14094.

(116) Bloomfield, V. A. DNA condensation by multivalent cations. *Biopolymers* **1997**, *44*, 269–282.

(117) Boussif, O.; Lezoualc'h, F.; Zanta, M. a; Mergny, M. D.; Scherman, D.; Demeneix, B.; Behr, J. P. A versatile vector for gene and oligonucleotide transfer into cells in culture and in vivo: polyethylenimine. *Proc. Natl. Acad. Sci. U. S. A.* **1995**, *92*, 7297–7301.

(118) Behr, J.-P. The Proton Sponge: a Trick to Enter Cells the Viruses Did Not Exploit. *Chimia (Aarau).* **1997**, *51*, 34–36.

(119) Balazs, D. A.; Godbey, W. Liposomes for Use in Gene Delivery. *J. Drug Deliv.* **2011**, *2011*, 326497.

(120) Boussif, O.; Zanta, M. A.; Behr, J. P. Optimized galenics improve in vitro gene transfer with cationic molecules up to 1000-fold. *Gene Ther.* **1996**, *3*, 1074–1080.

(121) Koltover, I. An Inverted Hexagonal Phase of Cationic Liposome-DNA Complexes Related to DNA Release and Delivery. *Science (80-.).* **1998**, *281*, 78–81.

(122) Juliano, R. L.; Ming, X.; Nakagawa, O.; Xu, R.; Yoo, H. Integrin Targeted Delivery of Gene Therapeutics. *Theranostics* **2011**, *1*, 211–219.

(123) Godbey, W. T.; Wu, K. K.; Mikos, A. G. Poly (ethylenimine)-mediated gene delivery affects endothelial cell function and viability. *Biomaterials* **2001**, *22*, 471–480.

(124) Filion, M. C.; Phillips, N. C. Toxicity and immunomodulatory activity of liposomal vectors formulated with cationic lipids toward immune effector cells. *Biochim. Biophys. Acta* **1997**, *1329*, 345–56.

(125) Hong, S.; Leroueil, P. R.; Janus, E. K.; Peters, J. L.; Kober, M.-M.; Islam, M. T.; Orr, B. G.; Baker, J. R.; Banaszak Holl, M. M. Interaction of polycationic polymers with supported lipid bilayers and cells: nanoscale hole formation and enhanced membrane permeability. *Bioconjug. Chem.* **2006**, *17*, 728–734.

(126) Fenske, D. B.; MacLachlan, I.; Cullis, P. R. Long-circulating vectors for the systemic delivery of genes. *Curr. Opin. Mol. Ther.* **2001**, *3*, 153–8.

(127) Erbacher, P.; Bettinger, T.; Belguise-Valladier, P.; Zou, S.; Coll, J. L.; Behr, J. P.; Remy, J. S. Transfection and physical properties of various saccharide, poly(ethylene glycol), and antibody-derivatized polyethylenimines (PEI). *J. Gene Med.* **1999**, *1*, 210–222.

(128) Shi, F.; Wasungu, L.; Nomden, A.; Stuart, M. C. A.; Polushkin, E.; Engberts, J. B. F. N.; Hoekstra, D. Interference of poly(ethylene glycol)-lipid analogues with cationic-lipid-mediated delivery of oligonucleotides; role of lipid exchangeability and non-lamellar transitions. *Biochem. J.* **2002**, *366*, 333–341.

(129) Wang, X.-L.; Xu, R.; Wu, X.; Gillespie, D.; Jensen, R.; Lu, Z.-R. Targeted systemic delivery of a therapeutic siRNA with a multifunctional carrier controls tumor proliferation in mice. *Mol. Pharm.* **2009**, *6*, 738–746.

(130) Ko, Y. T.; Bhattacharya, R.; Bickel, U. Liposome encapsulated polyethylenimine/ODN polyplexes for brain targeting. *J. Control. Release* **2009**, *133*, 230–237.

(131) Von Gersdorff, K.; Sanders, N. N.; Vandenbroucke, R.; De Smedt, S. C.; Wagner, E.; Ogris, M. The internalization route resulting in successful gene expression depends on both cell line and polyethylenimine polyplex type. *Mol. Ther.* **2006**, *14*, 745–753.

(132) Pike, L. J. Rafts defined: a report on the Keystone Symposium on Lipid Rafts and Cell Function. *J. Lipid Res.* **2006**, *47*, 1597–1598.

(133) Gonçalves, C.; Mennesson, E.; Fuchs, R.; Gorvel, J.-P.; Midoux, P.; Pichon, C. Macropinocytosis of polyplexes and recycling of plasmid via the clathrin-dependent pathway impair the transfection efficiency of human hepatocarcinoma cells. *Mol. Ther.* **2004**, *10*, 373–385.

(134) Rejman, J.; Bragonzi, A.; Conese, M. Role of clathrin- and caveolae-mediated endocytosis in gene transfer mediated by lipo- and polyplexes. *Mol. Ther.* **2005**, *12*, 468–474.

(135) Zuhorn, I. S.; Kalicharan, R.; Hoekstra, D. Lipoplex-mediated transfection of mammalian cells occurs through the cholesterol-dependent clathrin-mediated pathway of endocytosis. *J. Biol. Chem.* **2002**, *277*, 18021–8.

(136) MacAllister, S. L.; Young, C.; Guzdek, A.; Zhidkov, N.; O'Brien, P. J. Molecular cytotoxic mechanisms of chlorpromazine in isolated rat hepatocytes. *Can. J. Physiol. Pharmacol.* **2013**, *91*, 56–63.

(137) Murata, T.; Maruoka, N.; Omata, N.; Takashima, Y.; Fujibayashi, Y.; Yonekura, Y.; Wada, Y. A comparative study of the plasma membrane permeabilization and fluidization induced by antipsychotic drugs in the rat brain. *Int. J. Neuropsychopharmacol.* **2007**, *10*, 683–689.

(138) Rabinovitch, M. Professional and non-professional phagocytes: an introduction. *Trends Cell Biol.* **1995**, *5*, 85–7.

(139) Macia, E.; Ehrlich, M.; Massol, R.; Boucrot, E.; Brunner, C.; Kirchhausen, T. Dynasore, a cell-permeable inhibitor of dynamin. *Dev. Cell* **2006**, *10*, 839–50.

(140) Hillaireau, H.; Couvreur, P. Nanocarriers' entry into the cell: relevance to drug delivery. *Cell. Mol. Life Sci.* **2009**, *66*, 2873–96.

(141) Lim, J. P.; Gleeson, P. A. Macropinocytosis: an endocytic pathway for internalising large gulps. *Immunol. Cell Biol.* **2011**, *89*, 836–43.

(142) Pelkmans, L.; Helenius, A. Insider information: what viruses tell us about endocytosis. *Curr. Opin. Cell Biol.* **2003**, *15*, 414–22.

(143) Cardarelli, F.; Pozzi, D.; Bifone, A.; Marchini, C.; Caracciolo, G. Cholesterol-dependent macropinocytosis and endosomal escape control the transfection efficiency of lipoplexes in CHO living cells. *Mol. Pharm.* **2012**, *9*, 334–40.

(144) Sarkar, K.; Kruhlak, M. J.; Erlandsen, S. L.; Shaw, S. Selective inhibition by rottlerin of macropinocytosis in monocyte-derived dendritic cells. *Immunology* **2005**, *116*, 513–524.

(145) Ivanov, A. I. Pharmacological inhibition of endocytic pathways: is it specific enough to be useful? *Methods Mol. Biol.* **2008**, *440*, 15–33.

(146) Wong, A. W.; Scales, S. J.; Reilly, D. E. DNA internalized via caveolae requires microtubule-dependent, Rab7-independent transport to the late endocytic pathway for delivery to the nucleus. *J. Biol. Chem.* **2007**, *282*, 22953–63.

(147) Perumal, O. P.; Inapagolla, R.; Kannan, S.; Kannan, R. M. The effect of surface functionality on cellular trafficking of dendrimers. *Biomaterials 29*, 3469–76.

(148) Chiu, Y.-L.; Ho, Y.-C.; Chen, Y.-M.; Peng, S.-F.; Ke, C.-J.; Chen, K.-J.; Mi, F.-L.; Sung, H.-W. The characteristics, cellular uptake and intracellular trafficking of nanoparticles made of hydrophobically-modified chitosan. *J. Control. release* **2010**, *146*, 152–159.

(149) Billiet, L.; Gomez, J.-P.; Berchel, M.; Jaffrès, P.-A.; Le Gall, T.; Montier, T.; Bertrand, E.; Cheradame, H.; Guégan, P.; Mével, M.; Pitard, B.; Benvegnu, T.; Lehn, P.; Pichon, C.; Midoux, P. Gene transfer by chemical vectors, and endocytosis routes of polyplexes, lipoplexes and lipopolyplexes in a myoblast cell line. *Biomaterials* **2012**, *33*, 2980–90.

(150) Doherty, G. J.; McMahon, H. T. Mechanisms of endocytosis. *Annu. Rev. Biochem.* **2008**, *78*, 857–902.

(151) Niven, R.; Pearlman, R.; Wedeking, T.; Mackeigan, J.; Noker, P.; Simpson-Herren, L.; Smith, J. G. Biodistribution of radiolabeled lipid-DNA complexes and DNA in mice. *J. Pharm. Sci.* **1998**, *87*, 1292–1299.

(152) Kircheis, R.; Schüller, S.; Brunner, S.; Ogris, M.; Heider, K. H.; Zauner, W.; Wagner, E. Polycation-based DNA complexes for tumor-targeted gene delivery in vivo. *J. Gene Med.* **1999**, *1*, 111–120.

(153) Zhao, X. B.; Lee, R. J. Tumor-selective targeted delivery of genes and antisense oligodeoxyribonucleotides via the folate receptor. *Adv. Drug Deliv. Rev.* **2004**, *56*, 1193–1204.

(154) Wang, L.; Su, W.; Liu, Z.; Zhou, M.; Chen, S.; Chen, Y.; Lu, D.; Liu, Y.; Fan, Y.; Zheng, Y.; Han, Z.; Kong, D.; Wu, J. C.; Xiang, R.; Li, Z. CD44 antibody-targeted liposomal nanoparticles for molecular imaging and therapy of hepatocellular carcinoma. *Biomaterials* **2012**, *33*, 5107–5114.

(155) Kunath, K.; Von Harpe, A.; Fischer, D.; Petersen, H.; Bickel, U.; Voigt, K.; Kissel, T. Low-molecular-weight polyethylenimine as a non-viral vector for DNA delivery: comparison of physicochemical properties, transfection efficiency and in vivo distribution with high-molecular-weight polyethylenimine. *J. Control. Release* **2003**, *89*, 113–125.

(156) Fu, C.; Lin, L.; Shi, H.; Zheng, D.; Wang, W.; Gao, S.; Zhao, Y.; Tian, H.; Zhu, X.; Chen, X. Hydrophobic poly (amino acid) modified PEI mediated delivery of rev-casp-3 for cancer therapy. *Biomaterials* **2012**, *33*, 4589–96.

(157) Kim, Y. Il; Ahn, B.-C.; Ronald, J. a; Katzenberg, R.; Singh, A.; Paulmurugan, R.; Ray, S.; Gambhir, S. S.; Hofmann, L. V Intratumoral versus Intravenous Gene Therapy Using a Transcriptionally Targeted Viral Vector in an Orthotopic Hepatocellular Carcinoma Rat Model. *J. Vasc. Interv. Radiol.* **2012**, *23*, 1–8.

(158) Cole, C.; Qiao, J.; Kottke, T.; Diaz, R. M.; Ahmed, A.; Sanchez-Perez, L.; Brunn, G.; Thompson, J.; Chester, J.; Vile, R. G. Tumor-targeted, systemic delivery of therapeutic viral vectors using hitchhiking on antigen-specific T cells. *Nat. Med.* **2005**, *11*, 1073–1081.

(159) De Smedt, S. C.; Demeester, J.; Hennink, W. E. Cationic polymer based gene delivery systems. *Pharm. Res.* **2000**, *17*, 113–26.

(160) Yue, Y.; Jin, F.; Deng, R.; Cai, J.; Dai, Z.; Lin, M. C. M.; Kung, H.-F.; Mattebjerg, M. a; Andresen, T. L.; Wu, C. Revisit complexation between DNA and polyethylenimine--effect of length of free polycationic chains on gene transfection. *J. Control. Release* **2011**, *152*, 143–151.

(161) Hsu, C. Y. M.; Uludağ, H. Effects of size and topology of DNA molecules on intracellular delivery with non-viral gene carriers. *BMC Biotechnol.* **2008**, *8*, 23.

(162) Männistö, M.; Reinisalo, M.; Ruponen, M.; Honkakoski, P.; Tammi, M.; Urtti, A. Polyplex-mediated gene transfer and cell cycle: effect of carrier on cellular uptake and intracellular kinetics, and significance of glycosaminoglycans. *J. Gene Med.* **2007**, *9*, 479–487.

(163) Boussif, O.; Lezoualc'h, F.; Zanta, M. a; Mergny, M. D.; Scherman, D.; Demeneix, B.; Behr, J. P. A versatile vector for gene and oligonucleotide transfer into cells in culture and in vivo: polyethylenimine. *Proc. Natl. Acad. Sci. U. S. A.* **1995**, *92*, 7297–7301.

(164) Akinc, A.; Thomas, M.; Klibanov, A. M.; Langer, R. Exploring polyethylenimine-mediated DNA transfection and the proton sponge hypothesis. *J. Gene Med.* **2005**, *7*, 657–663.

(165) Chen, D.; Ping, Y.; Tang, G.; Li, J. Polyethyleneimine-grafted poly(N-3-hydroxypropyl)aspartamide as a biodegradable gene vector for efficient gene transfection. *Soft Matter* **2010**, *6*, 955.

(166) Chen, L.; Chen, J.; Chen, X. Multi-armed poly (L -glutamic acid) -graft-oligoethylenimine copolymers as efficient nonviral gene delivery vectors. **2010**, 64–76.

(167) Sun, Y.-X.; Xiao, W.; Cheng, S.-X.; Zhang, X.-Z.; Zhuo, R.-X. Synthesis of (Dex-HMDI)-g-PEIs as effective and low cytotoxic nonviral gene vectors. *J. Control. release* **2008**, *128*, 171–178.

(168) Wang, C.-F.; Lin, Y.-X.; Jiang, T.; He, F.; Zhuo, R.-X. Polyethylenimine-grafted polycarbonates as biodegradable polycations for gene delivery. *Biomaterials* **2009**, *30*, 4824–32.

(169) Deng, R.; Yue, Y.; Jin, F.; Chen, Y.; Kung, H.-F.; Lin, M. C. M.; Wu, C. Revisit the complexation of PEI and DNA - how to make low cytotoxic and highly efficient PEI gene transfection non-viral vectors with a controllable chain length and structure? *J. Control. release* **2009**, *140*, 40–46.

(170) Kim, Y. H.; Park, J. H.; Lee, M.; Kim, Y.-H.; Park, T. G.; Kim, S. W. Polyethylenimine with acid-labile linkages as a biodegradable gene carrier. *J. Control. release* **2005**, *103*, 209–219.

(171) Cheng, H.; Zhu, J.; Zeng, X.; Jing, Y.; Zhang, X.; Zhuo, R. Targeted Gene Delivery Mediated by Folate-polyethylenimine-block-poly (ethylene glycol) with Receptor Selectivity. *Bioconjug. Chem.* **2009**, *20*, 481–487.

(172) Nie, Y.; Schaffert, D.; Rödl, W.; Ogris, M.; Wagner, E.; Günther, M. Dual-targeted polyplexes: one step towards a synthetic virus for cancer gene therapy. *J. Control. Release* **2011**, *152*, 127–134.

(173) Yamano, S.; Dai, J.; Yuvienco, C.; Khapli, S.; Moursi, A. M.; Montclare, J. K. Modified Tat peptide with cationic lipids enhances gene transfection efficiency via temperature-dependent and caveolae-mediated endocytosis. *J. Control. release* **2011**, *152*, 278–85.

(174) García, L.; Buñuales, M.; Düzgüneş, N.; Tros De Ilarduya, C. Serum-resistant lipopolyplexes for gene delivery to liver tumour cells. *Eur. J. Pharm. Biopharm.* **2007**, *67*, 58–66.

(175) Lee, C.-H.; Ni, Y.-H.; Chen, C.-C.; Chou, C. K.; Chang, F.-H. Synergistic effect of polyethylenimine and cationic liposomes in nucleic acid delivery to human cancer cells. *Biochim. Biophys. Acta* **2003**, *1611*, 55–62.

(176) Pelisek, J.; Gaedtke, L.; DeRouchey, J.; Walker, G. F.; Nikol, S.; Wagner, E. Optimized lipopolyplex formulations for gene transfer to human colon carcinoma cells under in vitro conditions. *J. Gene Med.* **2006**, *8*, 186–197.

(177) Schäfer, J.; Höbel, S.; Bakowsky, U.; Aigner, A. Liposome-polyethylenimine complexes for enhanced DNA and siRNA delivery. *Biomaterials* **2010**, *31*, 6892–6900.

(178) Litzinger, D. C.; Huang, L. Amphipathic poly (ethylene glycol) 5000-stabilized dioleoylphosphatidylethanolamine liposomes accumulate in spleen. *Biochim. Biophys. Acta* **1992**, *1127*, 249–254.

(179) Ahl, P. L.; Bhatia, S. K.; Meers, P.; Roberts, P.; Stevens, R.; Dause, R.; Perkins, W. R.; Janoff, A. S. Enhancement of the in vivo circulation lifetime of L-alpha-distearoylphosphatidylcholine liposomes: importance of liposomal aggregation versus complement opsonization. *Biochim. Biophys. Acta* **1997**, *1329*, 370–82.

(180) Ahmad, I.; Allen, T. M. Antibody-mediated specific binding and cytotoxicity of liposome-entrapped doxorubicin to lung cancer cells in vitro. *Cancer Res.* **1992**, *52*, 4817–4820.

(181) Pangburn, T. O.; Petersen, M. A.; Waybrant, B.; Adil, M. M.; Kokkoli, E. Peptide- and aptamer-functionalized nanovectors for targeted delivery of therapeutics. *J. Biomech. Eng.* **2009**, *131*, 074005.

(182) Jia, Y.; Zeng, Z.; Markwart, S. M.; Rockwood, K. F.; Ignatoski, K. M. W.; Ethier, S. P.; Livant, D. L. Integrin Fibronectin Receptors in Matrix Metalloproteinase-1 – Dependent Invasion by Breast Cancer and Mammary Epithelial Cells Integrin Fibronectin Receptors in Matrix Metalloproteinase-1 – Dependent Invasion by Breast Cancer and Mammary Epithelial Cells. *Cancer Res.* **2004**, *64*, 8674–8681.

(183) Maglott, A.; Bartik, P.; Cosgun, S.; Klotz, P.; Rondé, P.; Fuhrmann, G.; Takeda, K.; Martin, S.; Dontenwill, M. The small alpha5beta1 integrin antagonist, SJ749, reduces proliferation and clonogenicity of human astrocytoma cells. *Cancer Res.* **2006**, *66*.

(184) Dingemans, A.-M. C.; van den Boogaart, V.; Vosse, B. A.; van Suylen, R.-J.; Griffioen, A. W.; Thijssen, V. L. Integrin expression profiling identifies integrin alpha5 and beta1 as prognostic factors in early stage non-small cell lung cancer. *Mol. Cancer* **2010**, *9*, 152.

(185) Garg, A.; Kokkoli, E. pH-Sensitive PEGylated liposomes functionalized with a fibronectin-mimetic peptide show enhanced intracellular delivery to colon cancer cell. *Curr. Pharm. Biotechnol.* **2011**, *12*, 1135–1143.

(186) Pangburn, T. O.; Bates, F. S.; Kokkoli, E. Polymersomes functionalized via "' click '" chemistry with the fibronectin mimetic peptides PR _ b and GRGDSP for targeted delivery to cells with different levels of $\alpha 5\beta 1$ expression. *Soft Matter* **2012**, *8*, 4449–4461.

(187) Belur, L. R.; McIvor, R. S.; Wilber, A. Liver-directed gene therapy using the sleeping beauty transposon system. *Methods Mol. Biol.* **2008**, *434*, 267–276.

(188) Lucas, B.; Remaut, K.; Sanders, N. N.; Braeckmans, K.; De Smedt, S. C.; Demeester, J. Studying the intracellular dissociation of polymer-oligonucleotide complexes by dual color fluorescence fluctuation spectroscopy and confocal imaging. *Biochemistry* **2005**, *44*, 9905–9912.

(189) Berndt, P.; Fields, G. B.; Tirrell, M. Synthetic lipidation of peptides and amino acids: monolayer structure and properties. *J. Am. Chem. Soc.* **1995**, *117*, 9515–9522.

(190) Szoka, F.; Papahadjopoulos, D. Comparative properties and methods of preparation of lipid vesicles (liposomes). *Annu. Rev. Biophys. Bioeng.* **1980**, *9*, 467–508.

(191) Fiske, C. H.; Subbarow, Y. The colorimetric determination of phosphorus. *J. Biol. Chem.* **1925**, *66*, 375–400.

(192) Ikonen, M.; Murtomäki, L.; Kontturi, K. Controlled complexation of plasmid DNA with cationic polymers: effect of surfactant on the complexation and stability of the complexes. *Colloids surfaces B Biointerfaces* **2008**, *66*, 77–83.

(193) Tarwadi; Jazayeri, J. a; Prankerd, R. J.; Pouton, C. W. Preparation and in vitro evaluation of novel lipopeptide transfection agents for efficient gene delivery. *Bioconjug. Chem.* **2008**, *19*, 940–950.

(194) Mardilovich, A.; Kokkoli, E. Patterned biomimetic membranes: effect of concentration and pH. *Langmuir* **2005**, *21*, 7468–7475.

(195) Shroff, K.; Pearce, T. R.; Kokkoli, E. Enhanced integrin mediated signaling and cell cycle progression on fibronectin mimetic peptide amphiphile monolayers. *Langmuir* **2012**, *28*, 1858–1865.

(196) Pearce, T. R.; Shroff, K.; Kokkoli, E. Peptide targeted lipid nanoparticles for anticancer drug delivery. *Adv. Mater.* **2012**, *24*, 3803–3822.

(197) Harrison, J. K.; Jiang, Y.; Chen, S.; Xia, Y.; Maciejewski, D.; Mcnamara, R. K.; Streit, W. J.; Salafranca, M. N.; Adhikari, S.; Thomson, D. A.; Botti, P.; Bacon, K. B.; Feng, L.; Jiang, Y. A. N.; Chens, S.; Xiat, Y.; Salafranca, M. D. T. Role for neuronally derived frac talkine in mediating interactions between neurons and CX3CR1-e : xpressing microglia. **2009**, *95*, 10896–10901.

(198) Belur, L. R.; Podetz-Pedersen, K. M.; Sorenson, B. S.; Hsu, A. H.; Parker, J. B.; Carlson, C. S.; Saltzman, D. a; Ramakrishnan, S.; McIvor, R. S. Inhibition of angiogenesis and suppression of colorectal cancer metastatic to the liver using the Sleeping Beauty Transposon System. *Mol. Cancer* **2011**, *10*, 14.

(199) Gong, C.; Li, X.; Xu, L.; Zhang, Y.-H. Target delivery of a gene into the brain using the RVG29-oligoarginine peptide. *Biomaterials* **2012**, *33*, 3456–63.

(200) Levine, R. M.; Scott, C. M.; Kokkoli, E. Peptide functionalized nanoparticles for nonviral gene delivery. *Soft Matter* **2013**, *9*, 985–1004.

(201) Doyle, S. R.; Chan, C. K. Differential intracellular distribution of DNA complexed with polyethylenimine (PEI) and PEI-polyarginine PTD influences exogenous gene expression within live COS-7 cells. *Genet. Vaccines Ther.* **2007**, *5*, 11.

(202) Adil, M.; Belur, L.; Pearce, T. R.; Levine, R. M.; Tisdale, A. W.; Sorenson, B. S.; McIvor, R. S.; Kokkoli, E. PR_b functionalized stealth liposomes for targeted delivery to metastatic colon cancer. *Biomater. Sci.* **2013**, *1*, 393–401.

(203) Pangburn, T. O.; Georgiou, K.; Bates, F. S.; Kokkoli, E. Targeted polymersome delivery of siRNA induces cell death of breast cancer cells dependent upon Orai3 protein expression. *Langmuir* **2012**, *28*, 12816–12830.

(204) Petersen, M. A.; Hillmyer, M. A.; Kokkoli, E. Bioresorbable polymersomes for targeted delivery of Cisplatin. *Bioconjug. Chem.* **2013**, *24*, 533–543.

(205) Levine, R. M.; Pearce, T. R.; Adil, M.; Kokkoli, E. Preparation and Characterization of Liposome-Encapsulated Plasmid DNA for Gene Delivery. *Langmuir* **2013**, *29*, 9208–9215.

(206) Akita, H.; Ito, R.; Khalil, I. A.; Futaki, S.; Harashima, H. Quantitative three-dimensional analysis of the intracellular trafficking of plasmid DNA transfected by a nonviral gene delivery system using confocal laser scanning microscopy. *Mol. Ther.* **2004**, *9*, 443–451.

(207) Vercauteren, D.; Vandenbroucke, R. E.; Jones, A. T.; Rejman, J.; Demeester, J.; De Smedt, S. C.; Sanders, N. N.; Braeckmans, K. The Use of Inhibitors to Study Endocytic Pathways of Gene Carriers: Optimization and Pitfalls. *Mol. Ther.* **2010**, *18*, 561–569.

(208) Forrest, M. L.; Pack, D. W. On the kinetics of polyplex endocytic trafficking: implications for gene delivery vector design. *Mol. Ther.* **2002**, *6*, 57–66.

(209) Gabrielson, N. P.; Pack, D. W. Acetylation of polyethylenimine enhances gene delivery via weakened polymer/DNA interactions. *Biomacromolecules* **2006**, *7*, 2427–2435.

(210) Benjaminsen, R. V; Mattebjerg, M. a; Henriksen, J. R.; Moghimi, S. M.; Andresen, T. L. The possible "proton sponge " effect of polyethylenimine (PEI) does not include change in lysosomal pH. *Mol. Ther.* **2013**, *21*, 149–57.

(211) Khalil, I. A.; Kogure, K.; Futaki, S.; Harashima, H. High density of octaarginine stimulates macropinocytosis leading to efficient intracellular trafficking for gene expression. *J. Biol. Chem.* **2006**, *281*, 3544–3551.

(212) Wadia, J. S.; Stan, R. V; Dowdy, S. F. Transducible TAT-HA fusogenic peptide enhances escape of TAT-fusion proteins after lipid raft macropinocytosis. *Nat. Med.* **2004**, *10*, 310–315.

(213) Kerr, M. C.; Lindsay, M. R.; Luetterforst, R.; Hamilton, N.; Simpson, F.; Parton, R. G.; Gleeson, P. A.; Teasdale, R. D. Visualisation of macropinosome maturation by the recruitment of sorting nexins. *J. Cell Sci.* **2006**, *119*, 3967–3980.

(214) Racoosin, E. L.; Swanson, J. A. Macropinosome maturation and fusion with tubular lysosomes in macrophages. *J. Cell Biol.* **1993**, *121*, 1011–1020.

(215) Oba, M.; Aoyagi, K.; Miyata, K.; Matsumoto, Y.; Itaka, K.; Nishiyama, N.; Yamasaki, Y.; Koyama, H.; Kataoka, K. Polyplex micelles with cyclic RGD peptide ligands and disulfide cross-links directing to the enhanced transfection via controlled intracellular trafficking. *Mol. Pharm.* **2008**, *5*, 1080–1092.

(216) Pelkmans, L.; Kartenbeck, J.; Helenius, A. Caveolar endocytosis of simian virus 40 reveals a new two-step vesicular-transport pathway to the ER. *Nat. Cell Biol.* **2001**, *3*, 473–483.

(217) Hayer, A.; Stoeber, M.; Ritz, D.; Engel, S.; Meyer, H. H.; Helenius, A. Caveolin-1 is ubiquitinated and targeted to intralumenal vesicles in endolysosomes for degradation. *J. Cell Biol.* **2010**, *191*, 615–629.

(218) Shi, F.; Sottile, J. Caveolin-1-dependent beta1 integrin endocytosis is a critical regulator of fibronectin turnover. *J. Cell Sci.* **2008**, *121*, 2360–2371.

(219) Ogris, M.; Wagner, E. To be targeted: is the magic bullet concept a viable option for synthetic nucleic acid therapeutics? *Hum. Gene Ther.* **2011**, *22*, 799–807.

(220) Parodi, A.; Quattrocchi, N.; van de Ven, A. L.; Chiappini, C.; Evangelopoulos, M.; Martinez, J. O.; Brown, B. S.; Khaled, S. Z.; Yazdi, I. K.; Enzo, M. V.; Isenhart, L.; Ferrari, M.; Tasciotti, E. Synthetic nanoparticles functionalized with biomimetic leukocyte membranes possess cell-like functions. *Nat. Nanotechnol.* **2013**, *8*, 61–68.

(221) Li, S.-D.; Huang, L. Non-viral is superior to viral gene delivery. *J. Control. Release* **2007**, *123*, 181–183.

(222) Demirgöz, D.; Pangburn, T. O.; Davis, K. P.; Lee, S.; Bates, F. S.; Kokkoli, E. PR_b-targeted delivery of tumor necrosis factor-α by polymersomes for the treatment of prostate cancer. *Soft Matter* **2009**, *5*, 2011–2019.

(223) Greenfield, L.; Bjorn, M. J.; Horn, G.; Fong, D.; Buck, G. a; Collier, R. J.; Kaplan, D. a Nucleotide sequence of the structural gene for diphtheria toxin carried by corynebacteriophage beta. *Proc. Natl. Acad. Sci. U. S. A.* **1983**, *80*, 6853–6857.

(224) Livak, K. J.; Schmittgen, T. D. Analysis of relative gene expression data using real-time quantitative PCR and the 2-ΔΔCt Method. *Methods* **2001**, *25*, 402–408.

(225) Hine, C. M.; Seluanov, A.; Gorbunova, V. Rad51 Promoter-Targeted Gene Therapy Is Effective for In Vivo Visualization and Treatment of Cancer. *Mol. Ther.* **2011**, *20*, 347–355.

(226) Pang, S. Targeting and eradicating cancer cells by a prostate-specific vector carrying the diphtheria toxin A gene. *Cancer Gene Ther.* **2000**, *7*, 991–996.

(227) Morimoto, H.; Bonavida, B. Diptheria Toxin - and Pseudomonas A Toxin-Mediated Apoptosis ADP Ribosylation of Elongation Factor-2 Is Required for DNA Fragmentation and Cell Lysis and Synergy with Tumor Necrosis Factor-a. *J. Immunol.* **1992**, *149*, 2089–2094.

(228) Porter, D. L.; Kalos, M.; Zheng, Z.; Levine, B.; June, C. Chimeric Antigen Receptor Therapy for B-cell Malignancies. *J. Cancer* **2011**, *2*, 331–332.

(229) Wang, K.; Wei, G.; Liu, D. CD19: a biomarker for B cell development, lymphoma diagnosis and therapy. *Exp. Hematol. Oncol.* **2012**, *1*, 36–43.

(230) Xie, W.; Wang, X.; Du, W.; Liu, W.; Qin, X.; Huang, S. Detection of molecular targets on the surface of CD34+CD38- bone marrow cells in myelodysplastic syndromes. *Cytometry* **2010**, *77*, 840–848.

(231) Zhu, Z. B.; Makhija, S. K.; Lu, B.; Wang, M.; Kaliberova, L.; Liu, B.; Rivera, A. A.; Nettelbeck, D. M.; Mahasreshti, P. J.; Leath, C. a; Barker, S.; Yamaoto, M.; Li, F.; Alvarez, R. D.; Curiel, D. T. Transcriptional targeting of tumors with a novel tumor-specific survivin promoter. *Cancer Gene Ther*. **2004**, *11*, 256–262.

(232) Li, F.; Altieri, D. C. Transcriptional analysis of human survivin gene expression. *Biochem. J*. **1999**, *344*, 305–311.

(233) Banet, G.; Bibi, O.; Matouk, I.; Ayesh, S.; Laster, M.; Kimber, K. M.; Tykocinski, M.; de Groot, N.; Hochberg, A.; Ohana, P. Characterization of human and mouse H19 regulatory sequences. *Mol. Biol. Rep*. **2000**, *27*, 157–165.

(234) Tkacik, G.; Gregor, T.; Bialek, W. The role of input noise in transcriptional regulation. *PLoS One* **2008**, *3*, e2774.

(235) Chalancon, G.; Ravarani, C. N. J.; Balaji, S.; Martinez-Arias, A.; Aravind, L.; Jothi, R.; Babu, M. M. Interplay between gene expression noise and regulatory network architecture. *Trends Genet*. **2012**, *28*, 221–232.

(236) Liu, Y.; Cox, S. R.; Morita, T.; Kourembanas, S. Hypoxia Regulates Vascular Endothelial Growth Factor Gene Expression in Endothelial Cells : Identification of a 5' Enhancer. *Circ. Res*. **1995**, *77*, 638–643.

(237) Wang, C. Y.; Cusack, J. C.; Liu, R.; Baldwin, A. S. Control of inducible chemoresistance: enhanced anti-tumor therapy through increased apoptosis by inhibition of NF-κB. *Nat. Med*. **1999**, *5*, 412–417.

(238) Bentires-Alj, M.; Hellin, A. C.; Ameyar, M.; Chouaib, S.; Merville, M. P.; Bours, V. Stable inhibition of NF-κB in cancer cells does not increase sensitivity to cytotoxic drugs. *Cancer Res*. **1999**, *59*, 811–815.

(239) Makarov, S. NF-kappaB in rheumatoid arthritis: a pivotal regulator of inflammation, hyperplasia, and tissue destruction. *Arthritis Res*. **2001**, *3*, 200–206.

(240) Gagliardo, R.; Chanez, P.; Mathieu, M.; Bruno, A.; Costanzo, G.; Gougat, C.; Vachier, I.; Bousquet, J.; Bonsignore, G.; Vignola, A. M. Persistent activation of nuclear factor-kappaB signaling pathway in severe uncontrolled asthma. *Am. J. Respir. Crit. Care Med*. **2003**, *168*, 1190–1198.

(241) Desai, N.; Trieu, V.; Yao, Z.; Louie, L.; Ci, S.; Yang, A.; Tao, C.; De, T.; Beals, B.; Dykes, D.; Noker, P.; Yao, R.; Labao, E.; Hawkins, M.; Soon-Shiong, P. Increased antitumor activity, intratumor paclitaxel concentrations, and endothelial cell transport of cremophor-free, albumin-bound paclitaxel, ABI-007, compared with cremophor-based paclitaxel. *Clin. Cancer Res*. **2006**, *12*, 1317–1324.

(242) Roger, E.; Lagarce, F.; Garcion, E.; Benoit, J.-P. Lipid nanocarriers improve paclitaxel transport throughout human intestinal epithelial cells by using vesicle-mediated transcytosis. *J. Control. Release* **2009**, *140*, 174–181.

(243) Ke, W.; Shao, K.; Huang, R.; Han, L.; Liu, Y.; Li, J.; Kuang, Y.; Ye, L.; Lou, J.; Jiang, C. Gene delivery targeted to the brain using an Angiopep-conjugated polyethyleneglycol-modified polyamidoamine dendrimer. *Biomaterials* **2009**, *30*, 6976–6985.

(244) Tuma, P. L.; Hubbard, A. L. Transcytosis: crossing cellular barriers. *Physiol. Rev.* **2003**, *83*, 871–932.

(245) Green, J. J.; Langer, R.; Anderson, D. G. A combinatorial polymer library approach yields insight into nonviral gene delivery. *Acc. Chem. Res.* **2008**, *41*, 749–759.

(246) Ryther, R. C. C.; Flynt, A. S.; Phillips, J. A.; Patton, J. G. siRNA therapeutics: big potential from small RNAs. *Gene Ther.* **2005**, *12*, 5–11.

(247) Mayrhofer, P.; Schleef, M.; Jechlinger, W. Use of minicircle plasmids for gene therapy. *Methods Mol. Biol.* **2009**, *542*, 87–104.

(248) Tannock, I. F.; Lee, C. M.; Tunggal, J. K.; Cowan, D. S. M.; Egorin, M. J. Limited Penetration of Anticancer Drugs through Tumor Tissue : A Potential Cause of Resistance of Solid Tumors to Chemotherapy Limited Penetration of Anticancer Drugs through Tumor Tissue : A Potential Cause of Resistance of Solid Tumors to Chemotherapy 1. *Clin. Cancer Res.* **2002**, *8*, 878–884.